U.S. Department of the Interior
Mineral Management Service

OCS Study MMS 2010-018

RECOMMENDED PHYSICAL OCEANOGRAPHIC STUDIES IN THE ALASKAN BEAUFORT SEA

Thomas J. Weingartner[1], Robert S. Pickart[2], and Mark A. Johnson[1]

[1]Institute of Marine Science, University of Alaska, Fairbanks, AK 99775
[1]Department of Physical Oceanography, Woods Hole Oceanographic Institution, Woods Hole, MA, 02543

April 2010
Final Report
MMS Contract: M06PC00030

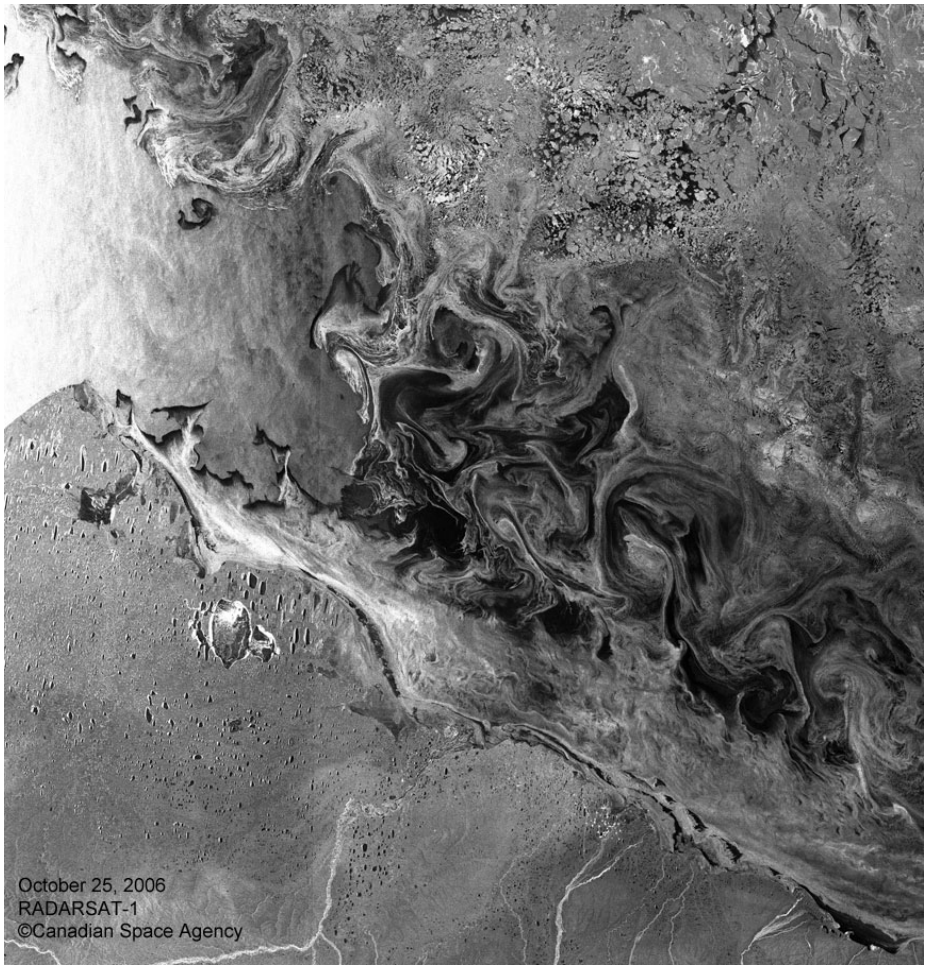

U.S. Department of the Interior
Minerals Management Service
Alaska OCS Region

RECOMMENDED PHYSICAL OCEANOGRAPHIC STUDIES IN THE ALASKAN BEAUFORT SEA

Thomas J. Weingartner[1], Robert S. Pickart[2], and Mark A. Johnson[1]

[1]Institute of Marine Science, University of Alaska, Fairbanks, AK 99775
[1]Department of Physical Oceanography, Woods Hole Oceanographic Institution, Woods Hole, MA, 02543April 2010

This study was funded by the U.S. Department of the Interior, Minerals Management Service (MMS), Alaska Outer Continental Shelf Region, Anchorage Alaska, under Contract No. M06PC00030, as part of the MMS Environmental Studies Program.

Final Report
April 2010

This study was funded by the U.S. Department of the Interior, Minerals Management Service (MMS), Alaska Outer Continental Shelf Region, Anchorage Alaska, under Contract No. M06PC00030, as part of the MMS Environmental Studies Program.

TABLE OF CONTENTS

LIST OF FIGURES

ABSTRACT

This report is an outgrowth of an MMS sponsored workshop on the physical oceanography of the Alaskan Beaufort Sea (ABS) held in Fairbanks in 2003. The ~30 workshop attendees identified a number of broad concerns that they believed were relevant to the MMS's mission in the ABS. The workshop formulated these concerns according to the various factors operating along the "boundaries" of the ABS. The boundaries include the oceanic boundary along the continental slope and shelfbreak, the western boundary and its connection to the Chukchi shelf, the eastern boundary's link to the Mackenzie shelf, the influence of river inflow along the coastal boundary, and the ice thickness distribution (ice topography) at the surface boundary.

Here, we have expanded upon those concerns by describing relatively new, but tested, observational technologies relevant to future studies and reviewing relevant field work conducted since the 2003 workshop. We have also provided a set of recommended observational programs that examine forcing along the boundaries and included the approximate costs associated with the projects. The report concludes with a brief statement of possible collaborators including both private industry and international institutions.

I. INTRODUCTION

In February 2003 the US Minerals Management Service (MMS) held a 2.5 day workshop in Fairbanks, Alaska to identify key issues pertaining to the physical oceanography of the Alaskan Beaufort Sea (hereafter abbreviated as ABS) that were considered essential to MMS management concerns with respect to marine industrial development in the region. Approximately 30 arctic physical oceanographers from the United States, Japan, and Canada participated in the workshop. (The report is available at: http:/www.mms.gov/Alaska/reports/2003rpts/2003-045.pdf.) The MMS subsequently asked the authors to expand upon the workshop report by:

1. Describing recently developed technologies that could be applicable to ABS studies;
2. Providing a status report on projects completed or underway since 2003 that have contributed insights on these issues;
3. Recommending specific studies (including cost estimates) that would address the issues raised during the workshop; and
4. Identifying potential partnerships, such as international collaborators, other agencies, and/or industries.

The results of this effort constitute this report and each of the above issues is addressed sequentially.

The ABS is a relatively narrow (~80 km wide) continental shelf (**Figure 1.1**), extending some 600 km eastward from Pt. Barrow, Alaska to the US-Canada boundary. The shelf grades gradually from the coast to the shelfbreak, which lies at about the 100 m isobath. Isobaths tend to parallel the coast and the shelf bathymetry (although not well-known) is relatively smooth suggesting that bathymetric effects on the circulation are likely small. In contrast, the slope has a more complex bathymetry that includes deep gullies and ridges extending across the slope. Given its relatively small size, apparently gentle bathymetry, and a basic understanding of the regional oceanography, the workshop conferees agreed that an understanding of the ABS required more detailed knowledge of the "boundary" influences that control the fluxes of mass, heat, salt, momentum, nutrients, and dissolved and suspended materials that influence the shelf dynamics and water masses. These boundaries include the:

1. *Western:* Chukchi inflow (yellow arrow; Figure 1)
2. *Eastern*: Mackenzie shelf inflow (blue arrow; Figure 1)
3. *Oceanic*: Shelf-basin exchanges (red arrows; Figure 1)
4. *Coastal*: Rivers (mainly central and eastern North Slope; Figure 1)
5. *Surface*: Sea ice and winds

We have sketched double-headed arrows in **Figure 1.1** to emphasize that the exchanges across the western, eastern, and oceanic boundaries are bilateral, e.g. the ABS receives and delivers waters from and to the Arctic basin, and the Chukchi and Mackenzie shelves.

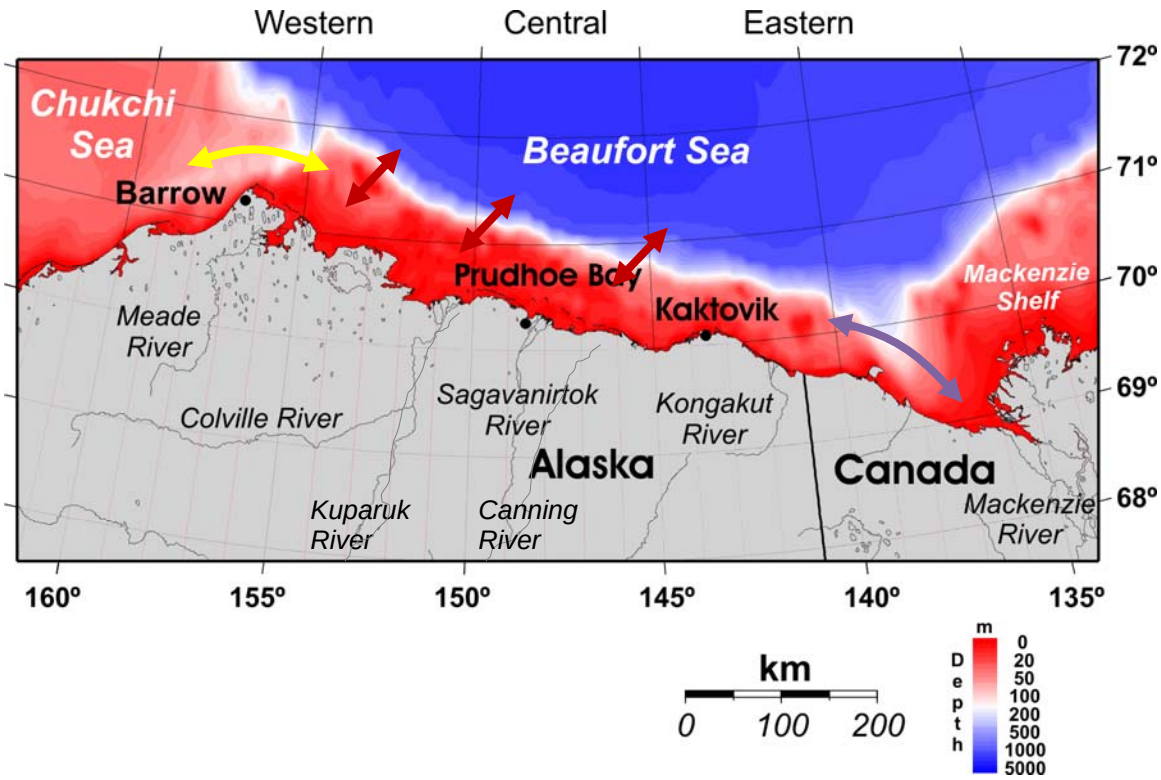

Figure 1.1. Map of the Alaska Beaufort Sea showing major rivers and geographic names. See text for explanation of arrows.

The report proceeds as follows. In Section 2 we discuss recent technologies that are applicable to the ABS (indeed some are essential elements in the recommended studies). In addition to describing the instrument, we comment on its benefits and limitations. Section 3 provides an update on ongoing and recently completed studies in the region that bear on the issues raised at the 2003 workshop. Section 4 outlines the recommended studies. Section 5 discusses potential partnerships and Section 6 summarizes the report.

SECTION 2. APPLICABLE TECHNOLOGIES

2.1 Airborne Microwave Remote Sensing Radiometers for Measuring Salinity

Scientific need

Water density variations on the ABS shelf are primarily influenced by salinity variability due to the generally low temperatures (<5^{o}C) and large range in salinities encountered due to river runoff, ice melt, and oceanic source waters. Hence, the dynamically important density gradients (stratification and fronts) are determined by salinity. Sea surface temperature (SST) maps are easily measured remotely from airborne or satellite platforms but SST features may not be co-located with sea surface salinity (SSS) variations. The ability to map SSS would provide a better broad-scale and dynamical perspective of the ABS.

Description

The physics of microwave remote sensing of sea surface salinity is well known and depends upon measuring the microwave emission (emissivity or brightness temperature) from the sea surface at a variety of wavelengths. Emissivity is a function of salinity (*Klein and Swift*, 1977) and temperature. By measuring microwave emission at several wavelengths (including within the infrared band) the temperature effects on emissivity can be determined and eliminated. High precision, multi-beam passive microwave radiometers capable of remotely sensing SSS exist. Indeed satellite measurements of global salinity are now underway (*Lagerloef et al*., 2008) from the Soil Moisture and Ocean Salinity (SMOS) satellite, but these are unsuitable for use on the ABS because of their coarse horizontal resolution (~50 km) and because clouds interfere with the signals. Airborne microwave multi-channel radiometers provide a potential remote sensing capability of SSS for the ABS. Several of these instruments have been developed and applied successfully in a variety of mid- and low-latitude settings (*Wang et al.,* 2007; *Le Vine et al.,* 1998). Although the accuracy is relatively low (~1 psu), the large range in surface salinities on the ABS in summer (~10 – 30) suggest that the airborne SSS sensor would be a valuable tool in mapping fronts and eddies, especially when used in conjunction with *in-situ* measurements. However, high-latitude tests of the airborne SSS sensors have not been made and the accuracy of the instrument may be lower at the relatively low temperatures (-1 to 5^{o}C) typical of the ABS. We have discussed the potential application of this technology with Derek Barrage of the Naval Research Laboratory who has tested a number of airborne SSS systems. He recommended that additional experimental testing and verification in arctic and sub-arctic settings be undertaken to determine the operational constraints of this sensor in these environments. Assessing the sensor will be expensive because this will require a dedicated technical team and aircraft onto which the sensor is custom-mounted. We therefore do not recommend that SSS-mappers be used in the studies outlined below. Rather we suggest that verification studies be undertaken by either NASA or NSF, possibly in conjunction with any future MMS field programs.

2.2 High-frequency shore-based surface current mapping radars (HFR)

Scientific Need

Shore-based, high frequency, surface current mapping radars (HFR) provide a means for comprehensively mapping the surface velocity field of the ocean over a variety of spatial scales (1 – 6 km resolution and 20 – 170 km range depending upon the radar's operating frequency). The HFR sample roughly the upper 1 m of the water column, which is notoriously difficult and expensive to obtain from oceanographic moorings. Given its broad sampling range and ~hourly sampling, the HFR is an ideal tool for obtaining synoptic-scale measurements of the 2-dimensional surface current field. HFRs deliver data in near real-time and so can be used in programs involving adaptive sampling, data assimilation modeling, oil spill response, and search and rescue applications. In principle, the setup and operation of the instruments is simple and rapid so that the logistics required are minimal. HFRs have been applied in many settings world-wide and may be considered a standard ocean surface current measuring technology. Indeed an extensive network of HFRs operates continuously along the coastline of the contiguous United States [http://cordc.ucsd.edu/projects/mapping/maps/]. Most of these systems, and the ones recommended in the following sections, are manufactured by Coastal Ocean Dynamics Applications Radar (CODAR) Ocean Sensors.

Description

HFR measures surface currents by analyzing and processing the Doppler spectrum of backscattered radar waves (*Barrick et al.*, 1985, see also *Codar Ocean Sensors*, 2003). The cross-spectra of the backscattered radar waves have a characteristic appearance that includes dominant first-order peaks, which are used to calculate the current speeds. These peaks are due to Bragg scattering from ocean waves having half the wavelength of the radar wave. When the appropriate Bragg scattering waves are present, the backscattered signal would appear as delta functions in the spectra with perfect signal processing, no ambient noise, and no ocean currents. Spectral broadening occurs due to currents in the radar field of view, digital signal processing, the presence of breaking waves, and sources of background electrical noise. Bearing and range of the sea echo are part of the normal observables of the radar. A single site HFR obtains radial velocities only, but by combining data from two radar sites, observing the same region, horizontal currents are obtained. CODAR provides software that requires minimal user interaction in generating the surface current field under ice-free conditions.

There have been few HFR applications in partially ice-covered waters, the most recent being the effort by Weingartner and his research group in the nearshore Beaufort Sea in 2005 and 2006 [*Potter and Weingartner,* 2010] and in the Chukchi Sea in fall 2009 (see http://www.chukchicurrents.com). Both programs have been successful although several unique issues present themselves to HFR users operating at high-latitude and/or partially ice-covered settings. First, processing the cross spectra from partially ice-covered waters is more time-consuming because the default parameters normally used in processing are sub-optimal when ice is present. Sea ice can split the first order peak so that the default settings only capture a portion of the first order energy. This leads to an incomplete set of radial currents. The problem is overcome, however, by examining all of the range cells in aggregate to determine where the split peaks occur. Once this is determined the processing settings can be adjusted. Visual inspection of the individual spectrum along with ancillary wind, wave, and ice cover data pertinent to each spectrum assists in adjusting the processing settings. Second, the signal from long-range radars (~4MHz), with a range of ~150 km, can interact with the relatively low altitude of the high-latitude ionosphere and thus contaminate the reflected signal. (Higher frequency HFRs have a shorter range and thus do not interact with the ionosphere.) Our experience in autumn 2009 indicated that this interference was highly variable through time, occurring mostly at night (between about 1100-0500) and in late fall. The interference resulted in a reduction in range so that data was missing in portions of the radar mask. In some cases data gaps may last up to eight hours. While a drawback, the data loss does not negate the utility of the HFR in the ABS where tidal currents are negligible and most of the variability during the ice-free season is at sub-inertial time scales. Third, the most limiting issue for HFR application in the remote coastal settings of Alaska is, in our experience, electric power. Typically, HFRs are connected to shore-based AC power sources, which are widely available along most of the coastline of the 48 contiguous states. AC power sources are few and far between along Alaska's coast, so deployments to date have been restricted to sites with available power. Hence, HFR siting in Alaska has been largely dictated by logistical issues and may not always be optimal in terms of sampling design.

In some of the recommended studies that follow, we suggest that MMS consider HFR deployments at sites without shoreside power and instead rely upon alternate power sources. Weingartner has been funded by the Department of Homeland Security to develop an autonomous power supply that will support remote operation of HFRs. The Remote Power Module (RPM; **Figure 2.1.1**) is a fully–automated, renewable (solar and wind) hybrid power station designed for remote arctic and sub-arctic maritime environments. It includes redundant components to enhance reliability in such settings and utilizes a compact footprint that minimizes permitting constraints in many areas. The RPM includes a climate-controlled shelter that houses the HFR electronics, communications equipment, and the electrical components of the power plant. The RPM mainly uses renewable energy thus reducing operating costs since power derived primarily from fossil fuel generators is very costly due to maintenance, limited life expectancy, logistics, fuel, and permitting issues.

The RPM, which uses off-the-shelf components that have low EM interference, meets the power requirements of a typical CODAR Ocean Sensors Seasonde, a high-speed satellite communications link, a small meteorological station, and power monitoring and control equipment. The total power requirement of the HFR and communication systems is ~11 kwh per day. The RPM is modular and portable so it can be transported and serviced from small cargo planes, boats, four-wheelers (ATVs), or snow machines with trailers.

Figure 2.2.1. The Remote Power Module (RPM) under construction in Fairbanks, winter 2010.

The RPM consists of:

1. a 16’ x 20’ foundation to accommodate uneven surfaces and unstable soils and to inihibit permafrost melting;
2. a 2-room shelter (for electronics and backup generator) using an 8’x12’x10’ walk-in freezer built from 30 foam and aluminum sections secured by cam-locks;
3. 4 600W wind turbines that supply 2.5 KW of power (and all of the power needed in a 10 mph wind);
4. a 3.5 Kilowatt photovoltaic array connected to two solar charge controllers;
5. a Kubota engine that powers a 24VDC alternator with a rated output of 170 amps. This enables rapid, temperature-compensated charging for the battery bank should renewable power fail for extended periods. The generator is remotely configurable, fully automated, and uses diesel or biodiesel fuel to offer flexibility with respect to permitting issues;
6. 3-days of standby power from a 2800 Amp-hour maintenance-free battery bank;
7. a datalogger that collects RPM data on power, voltages, temperatures, wind speed and solar radiation;
8. a Hughes Net satellite communication system for wireless Internet access to HFR and RPM data and to allow configuration changes in the power system.

The development of the RPM is underway and testing of the system will begin in spring and summer 2010, including a long-term system test in Barrow from August through November 2010. The research plan includes operating the system again in Barrow in the summer of 2011. Assuming satisfactory performance of the RPM, we anticipate that it can be applied routinely beginning in 2012. At the end of each open water period in Barrow, the system will be shut down, winterized, and evaluated. Multi-year remote deployments envision many of the bulkiest RPM components remaining on site through winter with only some electronics and antenna components secured in warm storage. This design minimizes logistics costs associated with winterization. The design goals also include the preparation of a trouble-shooting and routine maintenance manual to be used by local residents employed to assist in remote HFR operations. Logistics costs will be minimized by allowing local residents to perform routine maintenance and/or troubleshooting of the HFR and RPM.

Cost

An HFR system costs $300,000 and consists of 2 transmit and receive stations, associated electronics, and central site. The latter consists of the computer hardware and software that merges data from the radars into 2-dimensional surface current vectors. A central site can handle up to 6 different radar sites at one time. Each additional site added to the central site costs $130,000 and consists of a transmit/receive antenna pair and associated electronics. As presently configured the RPM cost is ~$130,000. Future costs may vary depending upon the number of solar panels used and the battery bank size. For example, the RPM allows flexibility in the battery bank size to provide longer (or shorter) operation of the HFR if all other power systems fail. Our tests may indicate that wind power suffices along the North Slope so that solar panels may prove unnecessary in future configurations here resulting in a savings of ~$15,000 per RPM.

2.3 Airborne electromagnetic measurements of sea ice thickness

Scientific Need

The shelf ice environment consists of both drifting ("pack") ice and landfast ice that is immobile (or nearly so). The seasonally varying ice thickness distribution function of the ABS ice environment is poorly known, but fundamentally reflects the ice dynamics of the ABS. Ice experts attending the 2003 workshop agreed that shelf ice dynamics, including the inner shelf and landfast ice zone were not well-known and that constitutive laws applicable to the basin may not apply to the shelf. Ice dynamics on the shelf are pivotal in controlling the transfer of momentum from the atmosphere to the ocean, channeling or blocking the circulation (particularly in the nearshore), and in determining the frictional coupling between the ice and water. In addition, spatial variations in the ice thickness distribution may result in spatial variations in the stress distribution that would then alter both the local, and, through sub-inertial wave generation, the remote response to wind forcing.

Description

Airborne Electromagnetic (EM) measurements provide a direct method to estimate sea ice thickness. EM induction soundings can acquire kilometers-long profiles of ice thickness. A typical electromagnetic induction device such as the EM-BIRD has transmitter and receiver coils separated by ~2.5m and generate (~4Hz) and record (10 Hz) electromagnetic signals. The strength of the secondary (receive) field is proportional to the conductivity of the resistive sea ice and conductive saline sea water. Thickness measurements depend on this high conductivity contrast between sea water and other media, an assumption validated as well in areas of low salinity such as the Baltic Sea. Typical sea ice conductivity is small compared to sea water so the induction in the sea ice can be neglected. Thus, the measured apparent conductivity is related only to the distance and conductivity of the sea water (**Figure 2.3.1**). Over level ice the system has noise of ± 5 cm and an accuracy of ± 10 cm. Sources of error include conductivity variations (bottom melting) and sea ice porosity. Measurements of freeboard height are acquired using a laser/radar mounted to the sensor (**Figure 2.3.1**). Operation height is 10-15 m above surface with a footprint of 40-50m.

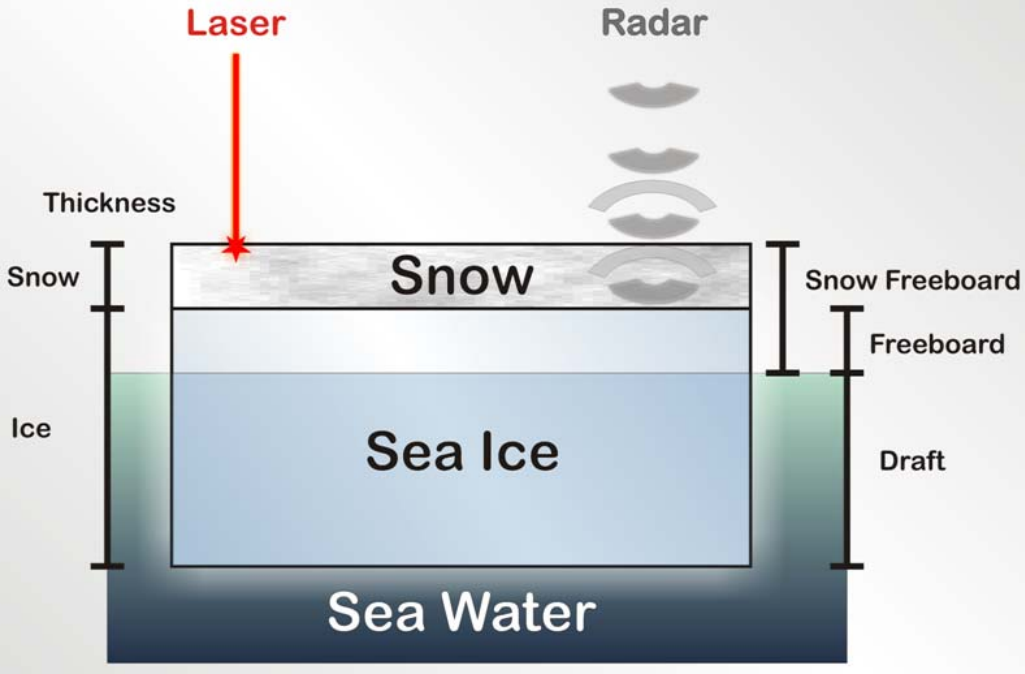

Figure 2.3.1. Sketch showing the operation of the EM ice thickness sensor which detects the conductive sea water beneath the ice and the height of the snow above the ice.

Electromagnetic induction (EM) techniques employing airborne platforms have been widely used by non-US scientists for ice thickness measurements in both polar regions. Two airborne sensors are available. The IcePic is an electromagnetic sensor hard-mounted to the front of a helicopter (**Figure 2.3.2** shows the IcePic mounted to the nose of a Canadian CG Eurocopter105 (BO105) helicopter). The IcePic can operate in a mode where it hovers just above the ice for several seconds, then moves to the next site or the helicopter can sample while flying at nearly cruising speed. The IcePic instrument and associated equipment are light, ~ 50-60 lb. A second

Figure 2.3.2. IcePIC hard-mounted on the front of a helicopter flying over sea ice

option is the EM "Bird", a sensor suspended by cable below a helicopter (**Figure 2.3.3**). It is easier to use when the choice of helicopter is unknown, but is less aerodynamic than the fix-mounted Pic.

Figure 2.3.3. EM Bird on sled behind snowmachine with cable to helicopter.

Example

Both instruments have a thickness measurement accuracy of about 6 cm (**Figure 2.3.4**) and both have been tested under Arctic conditions. The Bird was developed in Germany, and the Pic was developed in Canada.

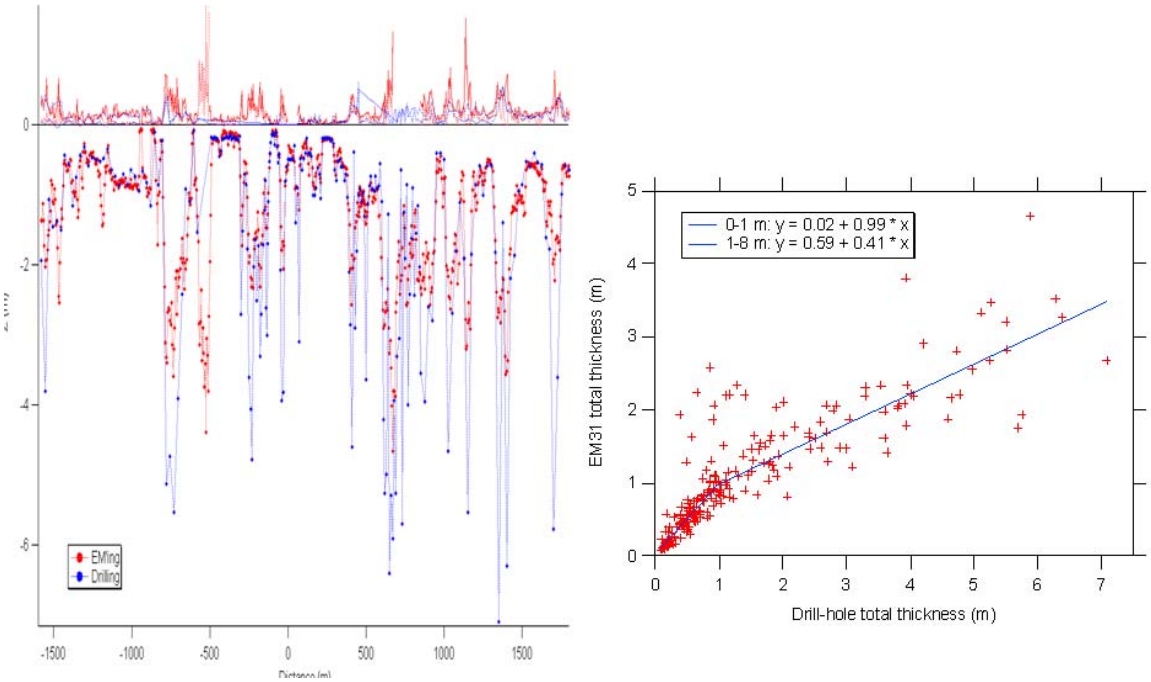

Figure 2.3.4. Left. EM measurements vs. drill holes over ridged, unconsolidated ice in the Baltic Sea. Right: Relationship between EM and measured data. (S. Holladay; pers. comm.)

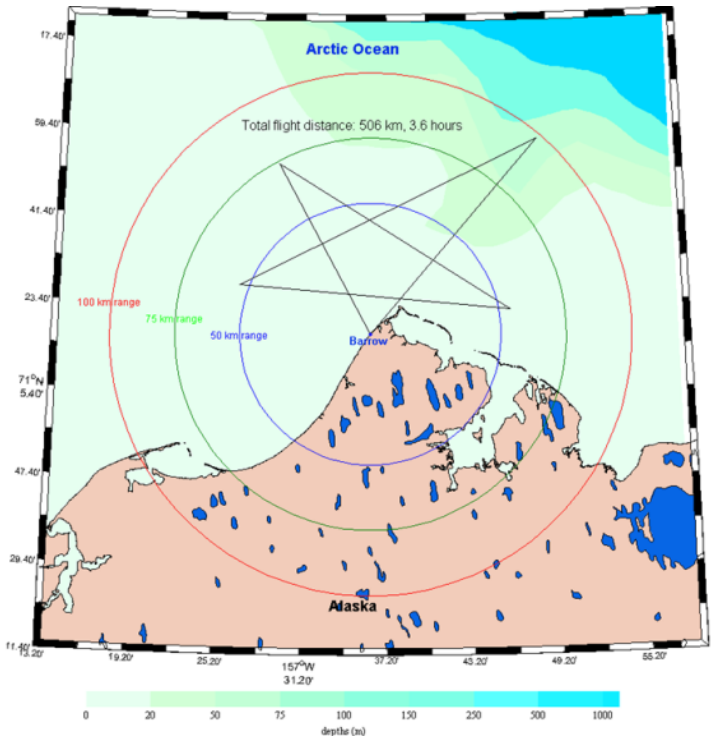

Figure 2.3.5. Star sampling pattern to map sea ice thickness off Barrow (or other regions). Cross-over points provide estimates of precision and can be used for on-ice measurements for EM validation.

Flight lines utilizing either sensor could follow a "star" pattern to optimize the coverage of a continuous flight (**Figure 2.3.5**) with end points optimized for *in-situ* measurements. Depending on weather conditions this flight pattern could be repeated quarterly yielding information on seasonal changes in ice thickness and the distribution and orientation of ridges.

Intensive radial measurements could be made (**Figure 2.3.6**) when a ridge or other ice thickness feature motivates the need for additional spatial information. As with similar studies (NSF SIZONET, PI: H.Eicken, Johnson is a co-investigator) some on-ice measurements are desirable to continue validation of the EM systems. Sampling would include coring and simultaneous measurements of coincident snow cover in order to estimate uncertainties in field programs using the PIC system.

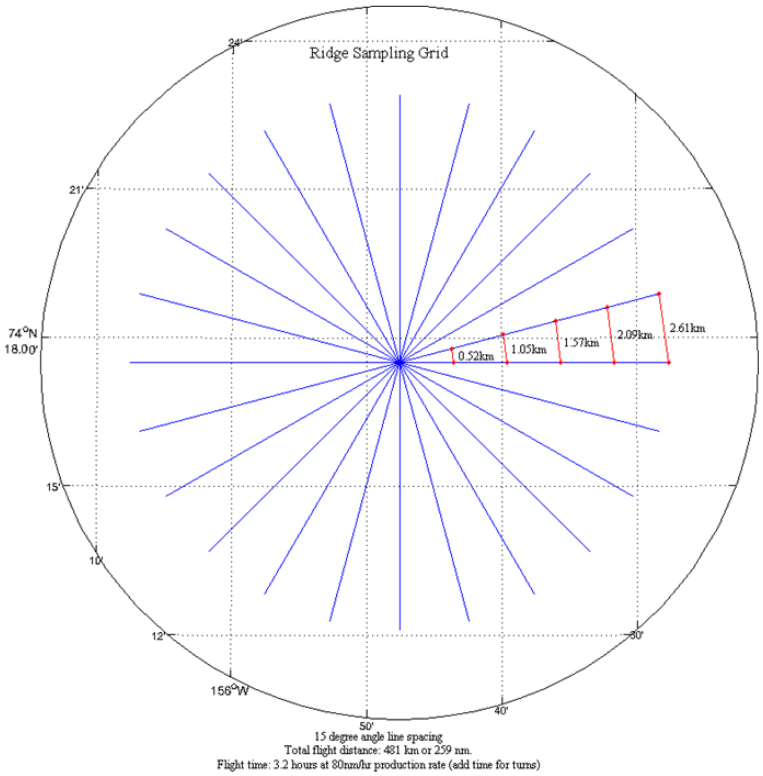

Figure 2.3.6. Example flight pattern with cross-over points for possible on-ice sampling over a ridge. At 90 knots, this pattern will take about 4 hours of flying time, weather permitting.

Cost

The IcePic or Bird EM Ice Measurement device costs $250,000 and includes initial training.

2.4 Coastal Moored Profiler

Scientific Need

The Moored Profiler is a recently-developed technology that is being used extensively within the oceanographic community. Originally developed by the Woods Hole Oceanographic Institution, it is now commercially available from McLane Instruments (called the McLane Moored Profiler, MMP). The MMP provides high-resolution vertical profiles of hydrographic variables—including velocity using an acoustic current meter—capable of sampling to great depth. However, in the coastal environment, where lateral gradients are particularly sharp (e.g. near the shelfbreak), there is a need for a more inexpensive option to allow for a greater number of instruments to be deployed simultaneously. Furthermore, there is no need for acoustic current meters on the shelf and upper slope, since acoustic Doppler current profilers can span the entire water column at these relatively shallow depths.

Description

To address this need, the Coastal Moored Profiler (CMP) was designed and built by the Woods Hole Oceanographic Institution. The instrument contains the same basic components as the MMP, except that it does not measure velocity and its dimensions are smaller. The electronics are contained within a glass ball (**Figure 2.4.1**), with the conductivity/pressure/depth (CTD) sensor oriented just below this. The large fin aligns the unit with the flow. A recent upgrade of the CMP allows for a multi-parameter CTD to be used, which measures pressure, temperature, conductivity (salinity), dissolved oxygen, pH, turbidity, and chlorophyll fluorescence. The vertical resolution of the profile (after data processing) is 1 m (and similar to the resolution obtained from shipboard CTD casts). **Figure 2.4.2** shows a typical mooring configuration containing a CMP that profiles the water column between the top float and just above the bottom. Beneath the lower "bumper stop" of the profiler resides an upward-facing acoustic Doppler current profiler that returns vertical profiles of velocity to compliment the CMP hydrographic profiles.

Example

Coastal Moored Profilers have been used successfully in the ABS in the vicinity of the shelfbreak and on the upper continental slope. Since the instruments are less expensive than MMPs, this allows for better horizontal resolution. Such was the case for the Western Arctic Shelf-Basin Interactions (SBI) experiment that was carried out in 2002-4 across the ABS shelfbreak at 152^{o}W. **Figure 2.4.3** shows a synoptic section of temperature overlaid by density taken during the month of April 2003. A section such as this would take 6-8 hours to occupy on a ship—if the ice conditions were favorable. The section in question was collected in under 45

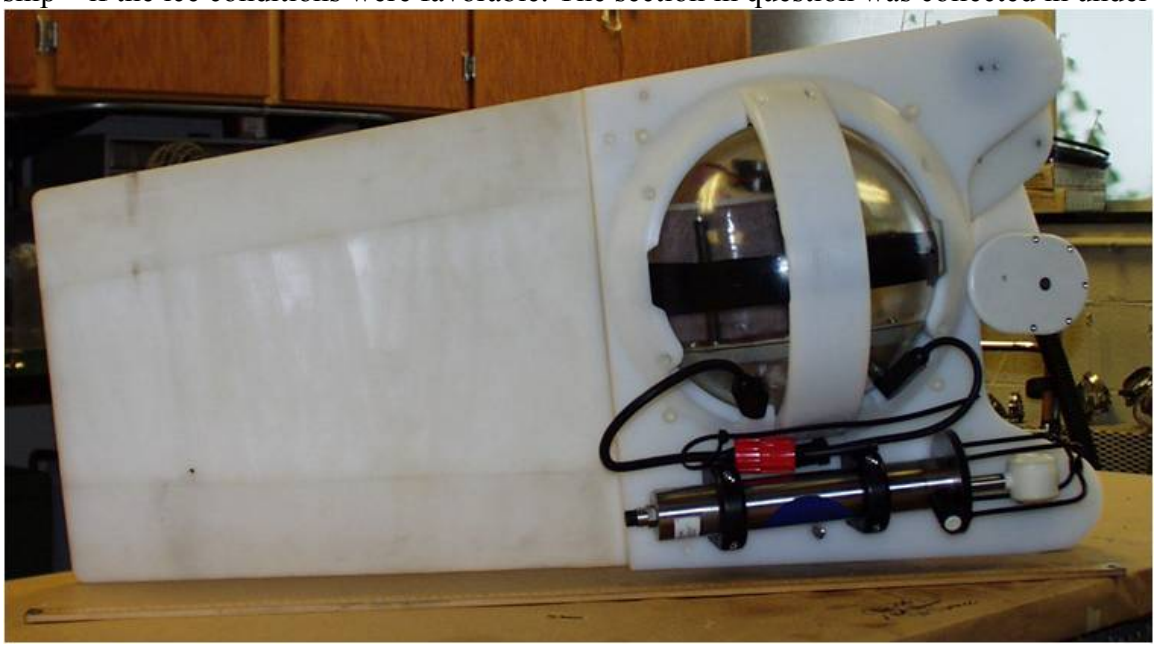

Figure 2.4.1. Coastal Moored Profiler. The electronics are housed in the glass ball, and the sensor suite (in this case a Falmouth Scientific Inc. CTD) is aligned horizontally at the base. The large white fin aligns the CMP with the horizontal flow as it profiles.

minutes. This array of CMPs produced a synoptic vertical section across the shelfbreak every 6 hours for a year. This particular snapshot shows a large lens of weakly stratified Pacific winter water near the freezing point, which causes the deep isopycnals to dive sharply downward

towards the slope. The section demonstrates the remarkably rich structure that can occur on very small lateral scales near the ABS shelfbreak.

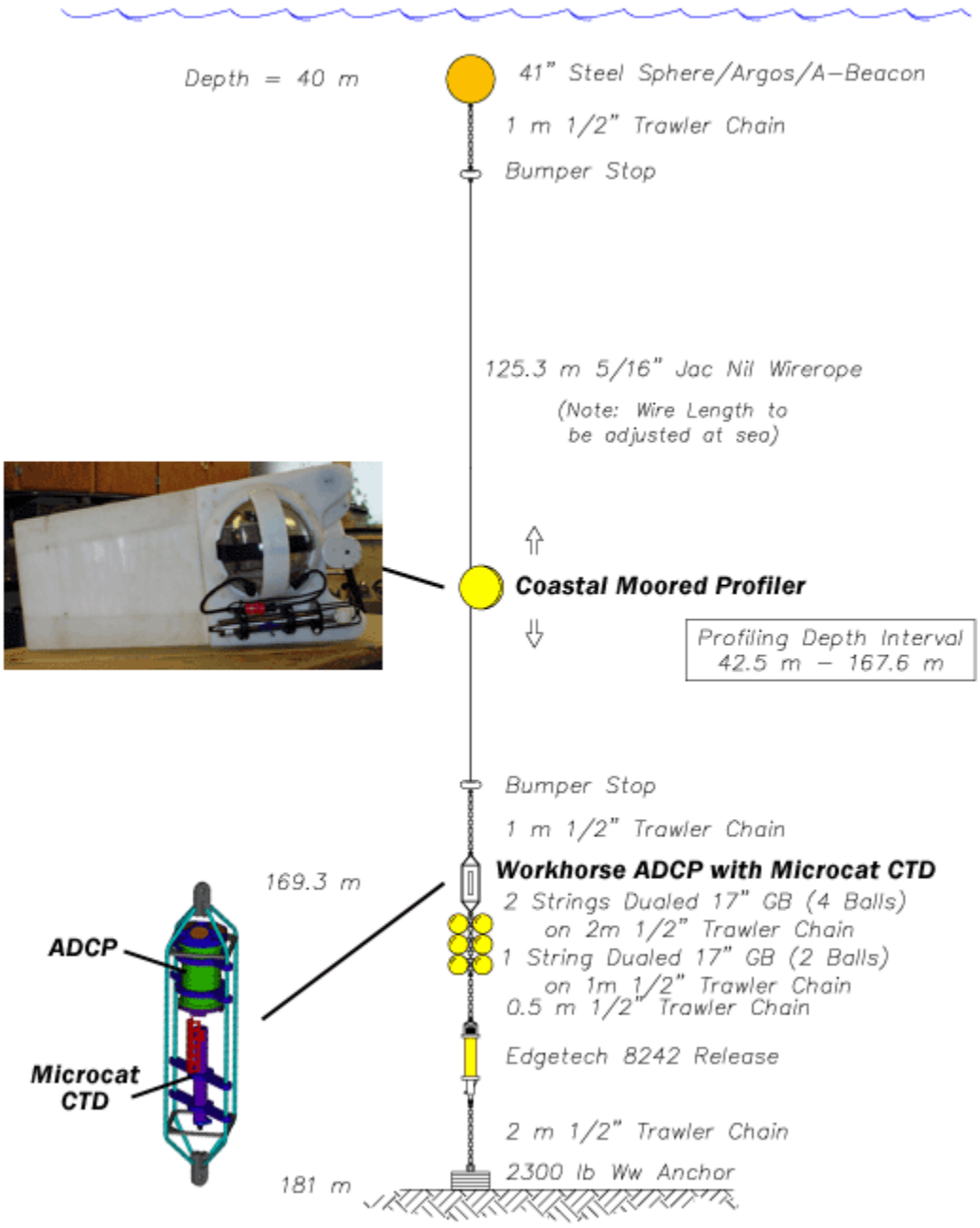

Figure 2.4.2. Mooring diagram showing the configuration of the Coastal Moored Profiler together with an upward-facing Acoustic Doppler current profiler.

Future Enhancements

A new capability presently being added to the Coastal Moored Profiler (funded by the National Science Foundation) is the addition of an ISUS version 3 nitrate sensor. This will be implemented on the multi-disciplinary boundary current mooring at 152°W as part of the Arctic

Observing Network (AON), to be deployed in summer 2010. An additional variable of interest is pCO2. Adding this sensor is technically feasible in terms of weight and power consumption, but the CMP would need to make temporary stops during its ascent, which requires more complex programming.

Cost

For the present configuration of the CMP (i.e. without the nitrate sensor or the pCO2 sensor), the cost is $40,000 per unit. If multiple units are constructed at once the price is reduced.

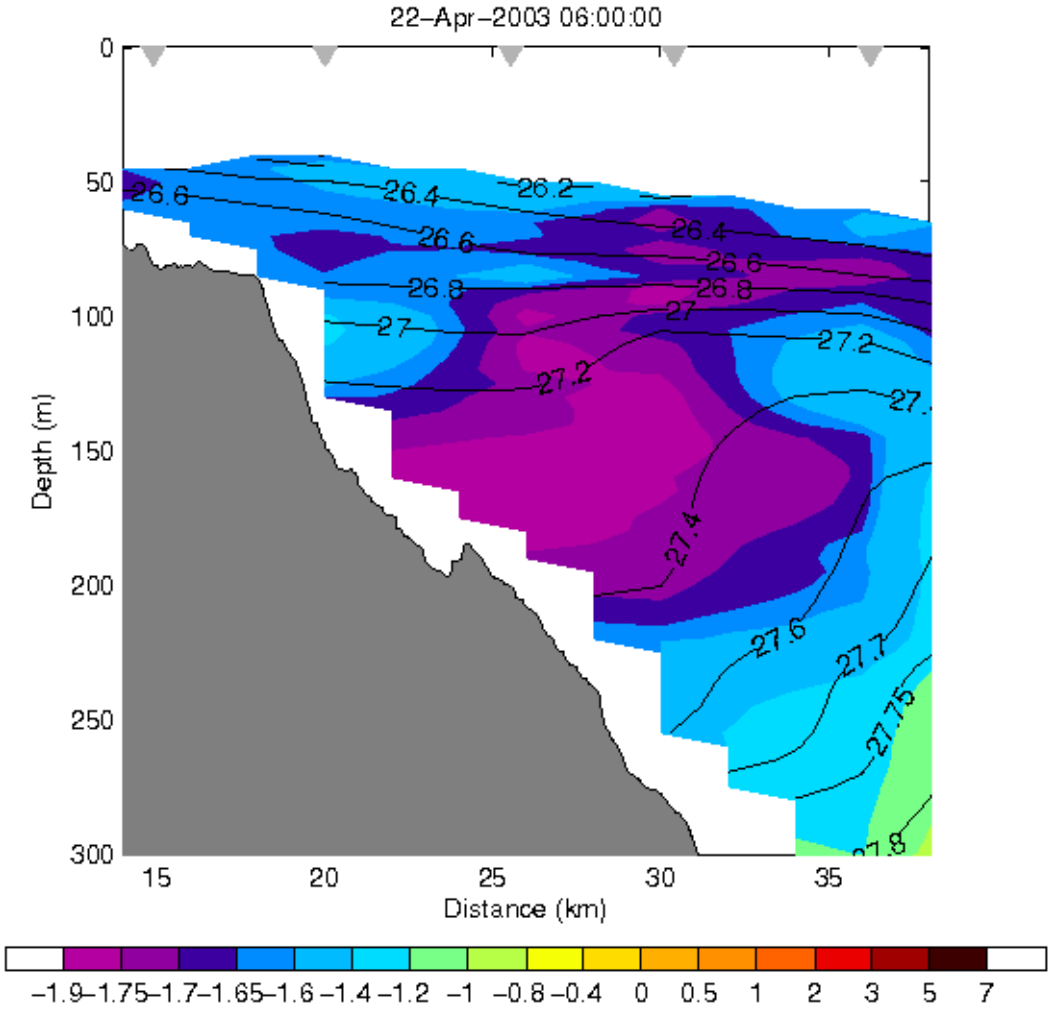

Figure 2.4.3. Synoptic vertical section of potential temperature (^{o}C, color) overlaid by potential density (kg m^{-3}, contours) across the ABS shelfbreak at 152^{o}W, occupied during the SBI experiment. An array of Coastal Moored Profilers produced such a section every 6 hours (each section took less than 45 minutes to occupy).

2.5 The Arctic Winch

Scientific Need

While subsurface moorings have been used extensively in the Arctic Ocean, instruments cannot be placed near the sea surface due to the dangers of ice keels. Typical depths of the top floats on subsurface moorings in the western Arctic are 35-45 m below the surface. Consequently, there is a dearth of understanding of the oceanographic conditions and processes in the upper-part of the water column. While drifting platforms (ice stations, ice-tethered profilers, profiling floats, etc.) provide important information in this part of the water column, these measurements are Lagrangian. Furthermore, such platforms are inappropriate for the shelves. There is a strong need for stationary time series of hydrographic properties of the upper layer in high-gradient regions such as boundary currents and on stratified continental shelves.

Description

To address this need, the Arctic Winch was designed and built by the Woods Hole Oceanographic Institution. The instrument consists of a sensor suite on a buoyant sphere, connected via nylon line to a small winch. The winch and a data logger are attached to the top float of the mooring next to a cradle that houses the buoyant sphere (**Figure 2.5.1**). As specified by the deployment schedule (typically set to once per day for a year-long deployment), the sphere rises to the sea surface or the underside of the pack ice. It is programmed so that once its vertical motion stops, the winch retracts the package back to the tripod. At the conclusion of the profile, the data are transferred inductively to a data logger. This way if the profiler were to be inadvertently snagged by the ice, breaking the nylon line, the data collected up to that point are not lost. The variables measured by the Arctic Winch are pressure, temperature, conductivity (salinity), dissolved oxygen, pH, turbidity, and chlorophyll fluorescence. The vertical resolution of the profile (after data processing) is 1m. An alternative configuration for the Arctic Winch, for applications on the shelf, is to house the instrument in a tripod that sits on the sea floor (**Figure 2.5.2**).

Example

The Arctic Winch has been used successfully in the ABS, both at the shelfbreak and on the shelf. In addition to the basic variables, the high vertical resolution of the profiler allows computation of the stratification, a particularly important variable for understanding the mesoscale to seasonal processes in the ABS. The first-ever time series of buoyancy frequency in the upper part of the water column on the ABS shelfbreak (or anywhere in the Arctic for that matter) is shown in **Figure 2.5.3**. Among the interesting features are the signature of convective events in late-October/early-November (low stratification throughout the water column), and an enhanced seasonal pycnocline (sharp layer of high stratification) from December through January.

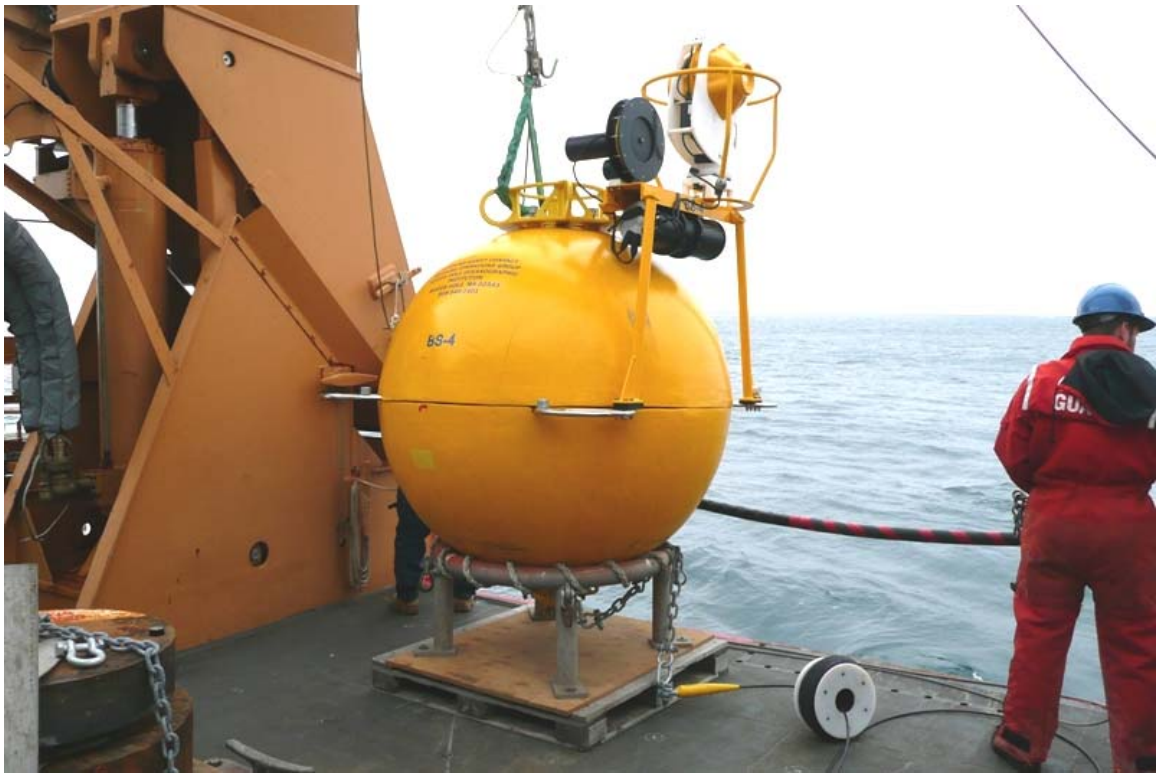

Figure 2.5.1. The Arctic Winch attached to the top float of a subsurface mooring being deployed in the Beaufort Sea. The sensor suite is attached to the small yellow buoyant float which sits in a cradle above the data logger (black cylinder), next to the winch spool and motor (black disk).

Future Enhancements

A new capability presently being added to the Arctic Winch (funded by the National Science Foundation) is the addition of an ISUS version 3 nitrate sensor. This will be implemented on the multi-disciplinary boundary current mooring at 152^{o}W as part of the Arctic Observing Network (AON), to be deployed in summer 2010. An additional variable of interest is pCO2. Adding this sensor is doable in terms of weight and power consumption, but the Arctic Winch would need to make temporary stops during its ascent, which requires more complex programming. The most pressing enhancement to the Arctic Winch is the inclusion of an ice-avoidance system. This would alleviate the need for the instrument to touch the ice, thereby reducing the risk of snagging. Preliminary assessments have indicated that the Arctic Winch could be used successfully with an ice-profiling sonar, such that prior to each ascent the profiling height would be specified to end just beneath the underside of the ice.

Cost

For the present configuration of the Arctic Winch (i.e. without the nitrate sensor or the ice-avoidance system), the cost is $120,000 per unit. If multiple units are constructed at once the price is reduced.

Figure 2.5.2. The Arctic Winch attached to a tripod being lowered to the seafloor on the continental shelf in the Beaufort Sea.

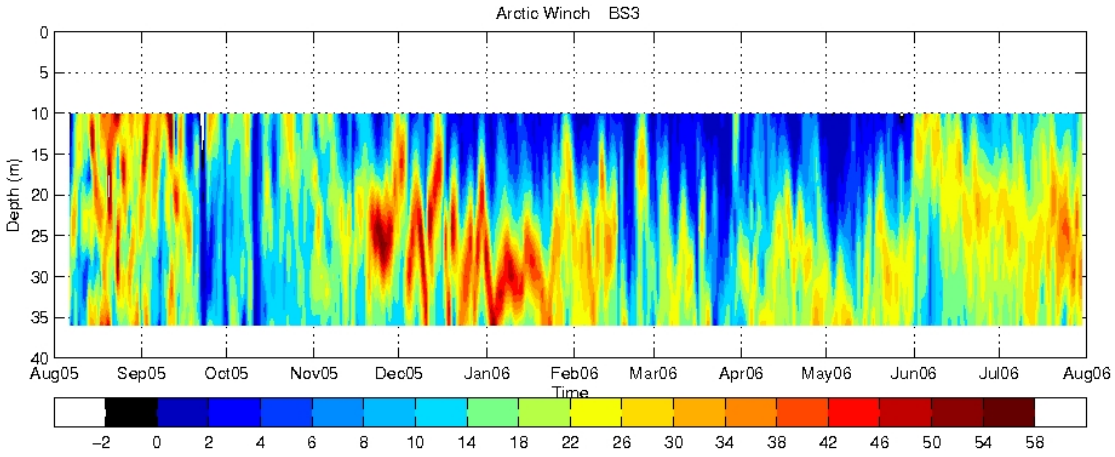

Figure 2.5.3. Year-long time series of buoyancy frequency (cycles per hour; cph) between 10 and 35 m depth collected by an Arctic Winch deployed at the shelfbreak of the ABS (152°W). The instrument was located on the top float of a subsurface mooring situated at the 150 m isobath.

2.6 Autonomous Underwater Vehicles: Gliders

Scientific Need

Autonomous Underwater Vehicles (AUVs) are becoming a convenient and routine tool for hydrographic surveys. These AUVs largely eliminate the need for shipboard measurements of routinely sampled physical variables. While several glider AUVs are available we describe the coastal model of the Webb Slocum Glider for application to the ABS, which is equipped with Seabird sensors for temperature/conductivity (T/C), pressure, and a Wetlabs Triplet ECO Puck to enable sampling for phytoplankton and CDOM (color dissolved organic matter), fluorescence, and optical backscatter data (turbidity). The chief advantage of the gliders is that they can inexpensively (compared to ship costs) and repeatedly sample the water column along pre-programmed transects. Real-time transmission of the measurements also allows the shore-based pilot to modify remotely the mission profiles to focus on evolving features of interest. For example, **Figure 2.6.1** (from *Schofield et al*., 2007) compares the costs of mid-latitude glider surveys with a variety of different sized ocean research vessels as a function of survey time. The figure clearly indicates that glider surveys are cost-effective for routine sampling. They are particularly valuable when combined with other sampling systems such as oceanographic moorings (which collect time series at a location) or HFRs, which collect surface currents over a specified geographic area.

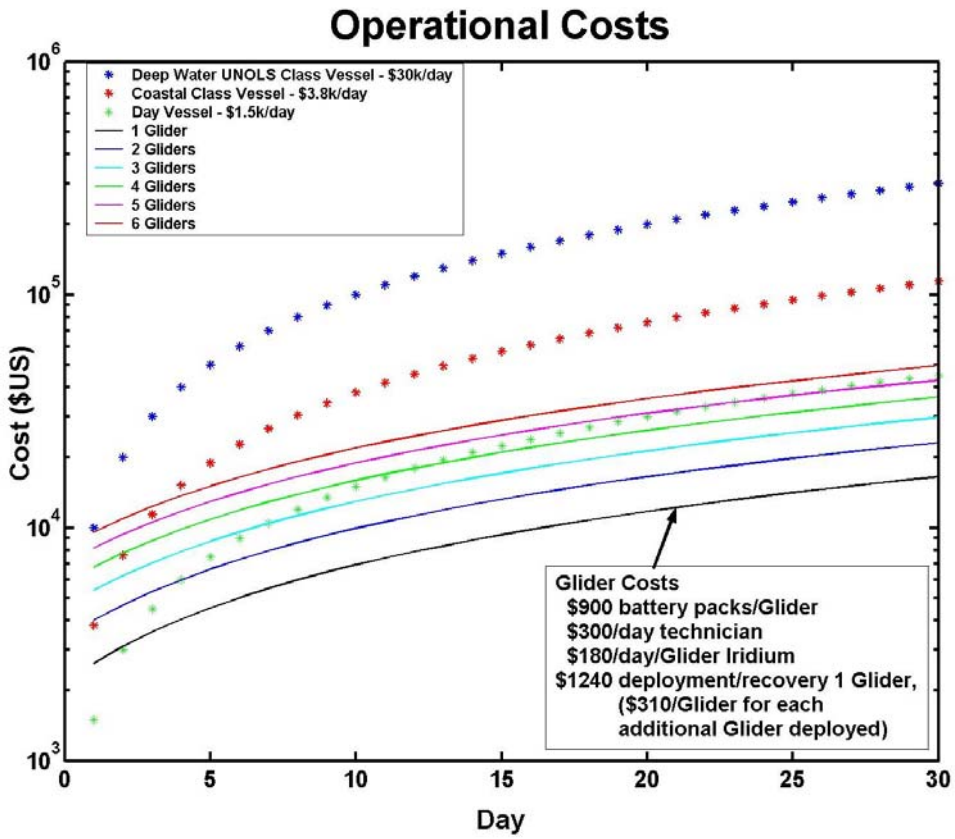

Figure 2.6.1. Comparison of the maintenance costs (vertical axis) as a function of duration at sea (horizontal axis) for one or more gliders (solid curves) versus different classes of oceanographic vessels (From *Schofield et al.,* 2007.)

Description

The Webb Slocum gliders are small, reusable, long-range AUVs that undulate between the ocean surface and bottom while collecting profiles of oceanographic data [e.g., *Eriksen et al.*, 2001]. The glider is a low-power (~ 2 W) high-endurance AUV that is manageable by 1-2 persons for deployment and recovery from a dock or small boat. It weighs 52 kg in air, has a hull diameter of 21.3 cm and is 1.5 m long. It is powered with alkaline or lithium battery packs and glides at a typical horizontal speed of 40 cm s^{-1}, while navigating via GPS, internal dead reckoning, and an altimeter. The communications package includes an RF modem, Iridium and ARGO satellite communication, and a Telesonar modem. In this configuration and with alkaline batteries, the glider has a typical endurance of one month, or ~1100 km of survey tracks, and could make up to 600 dives per day. (Lithium batteries would nearly triple the endurance.) The glider dead reckons to waypoints, following a vertically zigzagging pattern wherein it inflects at set depths and altitudes based on a mission text file. As set by the mission protocol, the glider periodically surfaces to communicate data and instructions (including new waypoints) and to obtain a GPS position fix. Differences between dead reckoning and position are attributed to currents, and that knowledge is used on the subsequent segment. Moreover, depth-integrated, horizontal velocities are estimated by comparing the difference between dead-reckoned and actual displacements.

The data are transmitted via Iridium satellite at pre-programmed time intervals allowing near realtime access to the data. In addition, the shore-based pilot can re-program the glider path and thus allow adaptive sampling based on the data received. For applications in partially ice-covered seas, the ability to alter the glider mission allows the pilot to avoid ice from interfering with glider performance. The MMS, Shell and ConocoPhillips are supporting P. Winsor (U. Alaska) to use these gliders on the Chukchi Sea shelf beginning in August 2010. To our knowledge this will be their first application to an Arctic shelf. We anticipate that the glider operations will not be interrupted under light ice concentrations. The glider moves slowly so it will not be damaged if it surfaces beneath or strikes an ice floe. It will instead change its vertical orientation and continue along its trajectory. Glider operations in partially ice-covered seas will have to be guided with the assistance of Synthetic Aperture Radar imagery that provide detailed views of sea ice conditions and/or other sea ice information. However, we believe that under typical August-September ABS sea ice conditions glider operations will be successful.

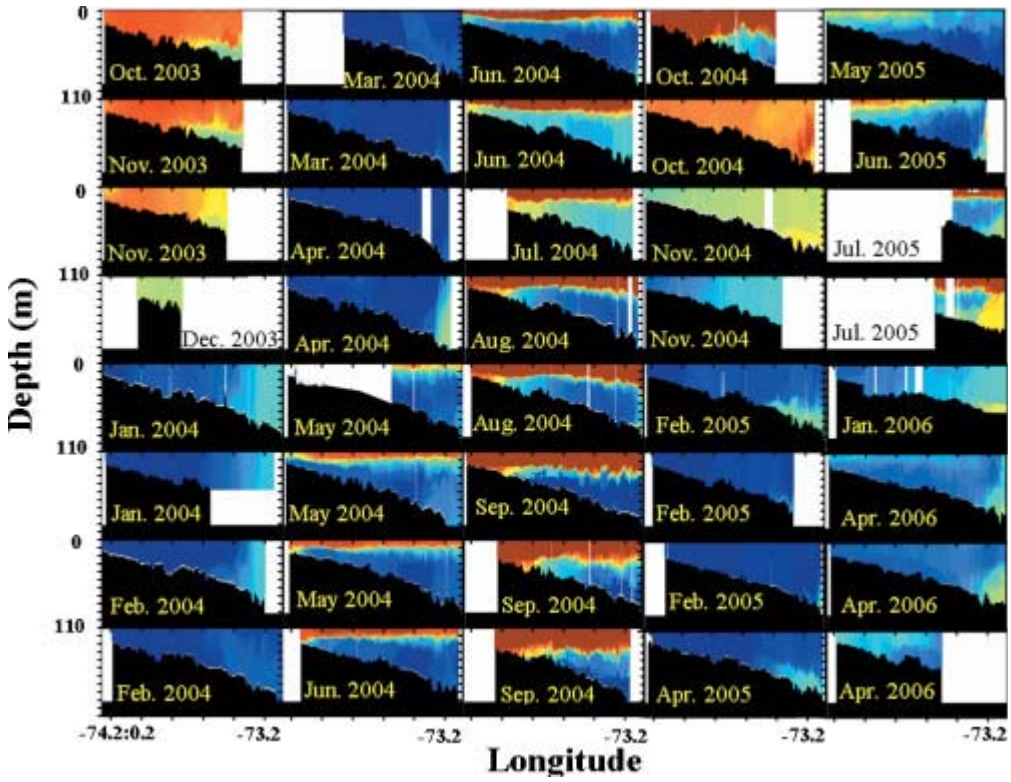

Figure 2.6.2. Time series of the cross-shelf distribution of temperature across the New Jersey continental shelf collected by the Slocum Webb gliders (from *Schofield et al.,* 2007).

Enhancements

Peter Winsor (U. Alaska) has been funded to incorporate and test an ISUS nitrate sensor on a Webb Slocum glider. If successful, the glider's sensor suite would be expanded to sample nitrate continuously along transects.

Cost

The Webb Slocum glider with all sensors (except the nitrate analyzer) costs $130,000.

SECTION 3. RECENT AND ONGOING EFFORTS

Since the 2003 workshop, several measurement programs were undertaken that address some aspects of the issues raised by the workshop participants. Two separate field programs, funded by the National Ocean Partnership Program (NOPP) and the Office of Naval Research (ONR) were co-located in the central ABS and these programs concluded their field measurements in August 2009. (Both programs are sharing data with one another and thus generating unprecedented data on the time-varying circulation and hydrographic structure of the central ABS.) The ONR program (Ice-Covered Ocean Response to Atmospheric Storms [ICORTAS]) focused on storm-generated near-inertial waves along the central ABS continental slope, but also provides information for assessing sub-inertial dynamics. The overall objective of the NOPP effort (Circulation, cross-shelf exchange, sea ice, and marine mammal habitats on the Alaskan

Beaufort Sea shelf) is to understand how the wind-forced response (over both the shelf and shelfbreak) and the cross-shelf exchange of mass, materials, and momentum are influenced by seasonal variations in ice and stratification on the central ABS. Collectively these programs address 2-dimensional (vertical and cross-shore) exchanges between the shelfbreak and mid-shelf and between the mid- and inner shelf. The heart of the program consisted of 9 NOPP and ICORTAS moorings (enclosed by the red oval in **Figure 3.0.1**) that extended from the 13 - 1800 m isobaths. The array included arctic winches, CMPs, and MMPs in depths $\geq$35 m and an additional mooring at the shelfbreak at152^{o}W (blue square; **Figure 3.0.1**). The latter extends a time series at this location that began in 2002 as part of the NSF-SBI program and thus provides a temporal context for examining the measurements in the central ABS. (This mooring has since been extended for another 4 years under the NSF-funded Arctic Observing Network program.) Additional efforts included the deployment of several passive acoustic recorders on the outer shelf and shelfbreak and at 152^{o}W, time series of SAR-derived sea ice deformation fields and early August hydrography.

A second NOPP-supported project was led by C. Ashjian (Woods Hole) and Stephen Okkonen (U. Alaska), entitled "Episodic Upwelling of Zooplankton within a Bowhead Whale Feeding Area near Barrow, AK". This project examined exchanges of Pacific Water and plankton/krill (acoustic backscatter as a zooplankton proxy) between Barrow Canyon and the adjacent Beaufort shelf (yellow square and some moorings in the blue square; **Figure 3.0.1**) over two full years in relation to the feeding of bowhead whales. Physical oceanographic sampling included hydrographic and moored oceanographic instruments (current meters, temperature/salinity recorders, and bottom pressure) during the open water season only. Some of their preliminary results have guided the work recommended with respect to the western boundary as discussed in Section 4.1.

Additional moorings deployed in 2008-09 include a 3-mooring array (black circle; **Figure 3.0.1)** that contained ice profiling sonars (IPS) and moored ADCPs over the middle shelf between 145 and 146^{o}W. This array was maintained by Canadian scientists from the Institute of Ocean Sciences (IOS) of Sydney, BC. Farther east was a broadly spaced IPS and ADCP array deployed on the Mackenzie shelf by IOS scientists with Canadian government support.

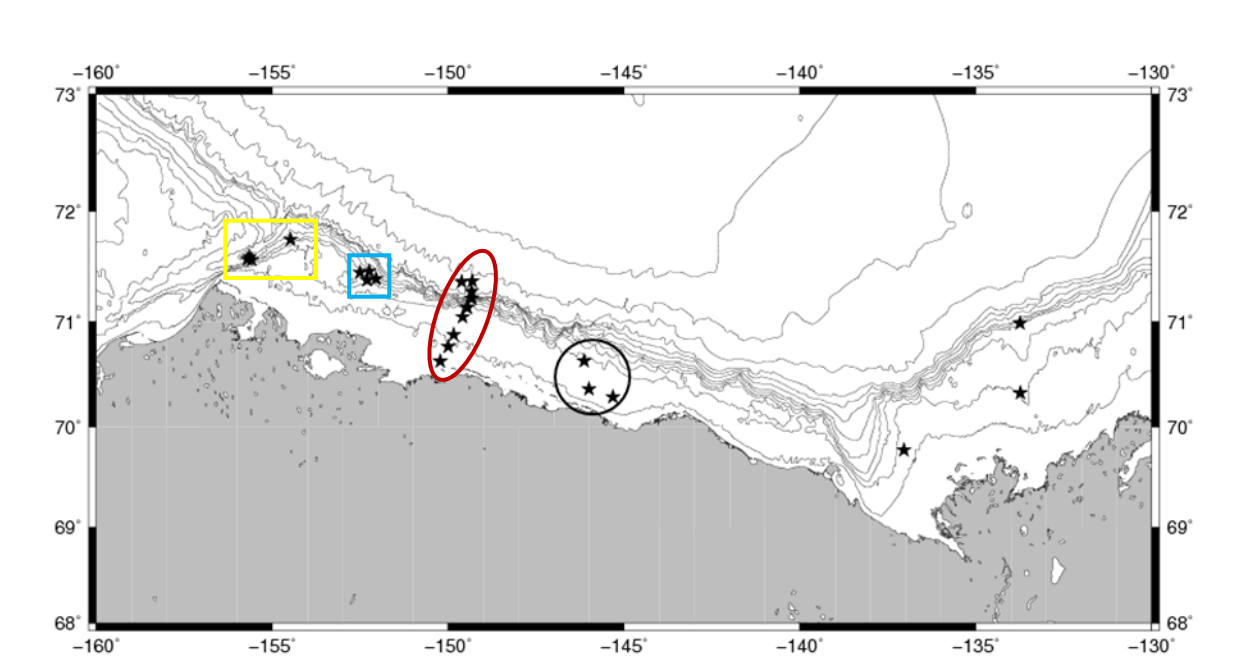

Figure 3.0.1. Oceanographic and passive acoustic recorder moorings deployed in summer/fall 2008 and recovered in summer/fall 2009. The red oval encloses the Weingartner et al. NOPP and ICORTAS moorings along the central ABS. The yellow square encloses the passive acoustic recorders deployed as part of the Ashjian et al. NOPP array. Oceanographic and passive acoustic recorders from both NOPP programs were deployed at the shelfbreak near 152°W (blue square). The black oval encloses moored ADCPs and ice-profiling sonars (IPS) deployed by the oil industry and IOS scientists. The stars on the Mackenzie shelf are ADCP and IPS moorings deployed by IOS scientists with Canadian government support.

While the bulk of these data are being analyzed, some preliminary results from the central ABS NOPP program underscore the hydrographic complexity of the ABS shelf that is tied directly to the forcing along its boundaries. These are evident in **Figure 3.0.2** in which potential temperature (color shading) is overlain by salinity isopleths. The section was constructed from data collected by a REMUS AUV inshore of the 30 m isobath and CTDs from the USCGC *Healy* farther offshore. The data were gathered by both platforms on the same day and so are synoptic. The numbers in the figure denote the location of various water masses:

1. warm, fresh, Colville River plume (*coastal boundary*)
2. mid-shelf cold pool, remnant from winter or from a prior shelfbreak upwelling event (*oceanic boundary*);
3. shelfbreak eddy of cold Chukchi winter water (*oceanic boundary*);
4. Mackenzie River plume filament spreading westward (*eastern boundary*);
5. cold Chukchi winter water (*western boundary joining the oceanic boundary*), and;
6. warmer Chukchi summer water (*western boundary*).

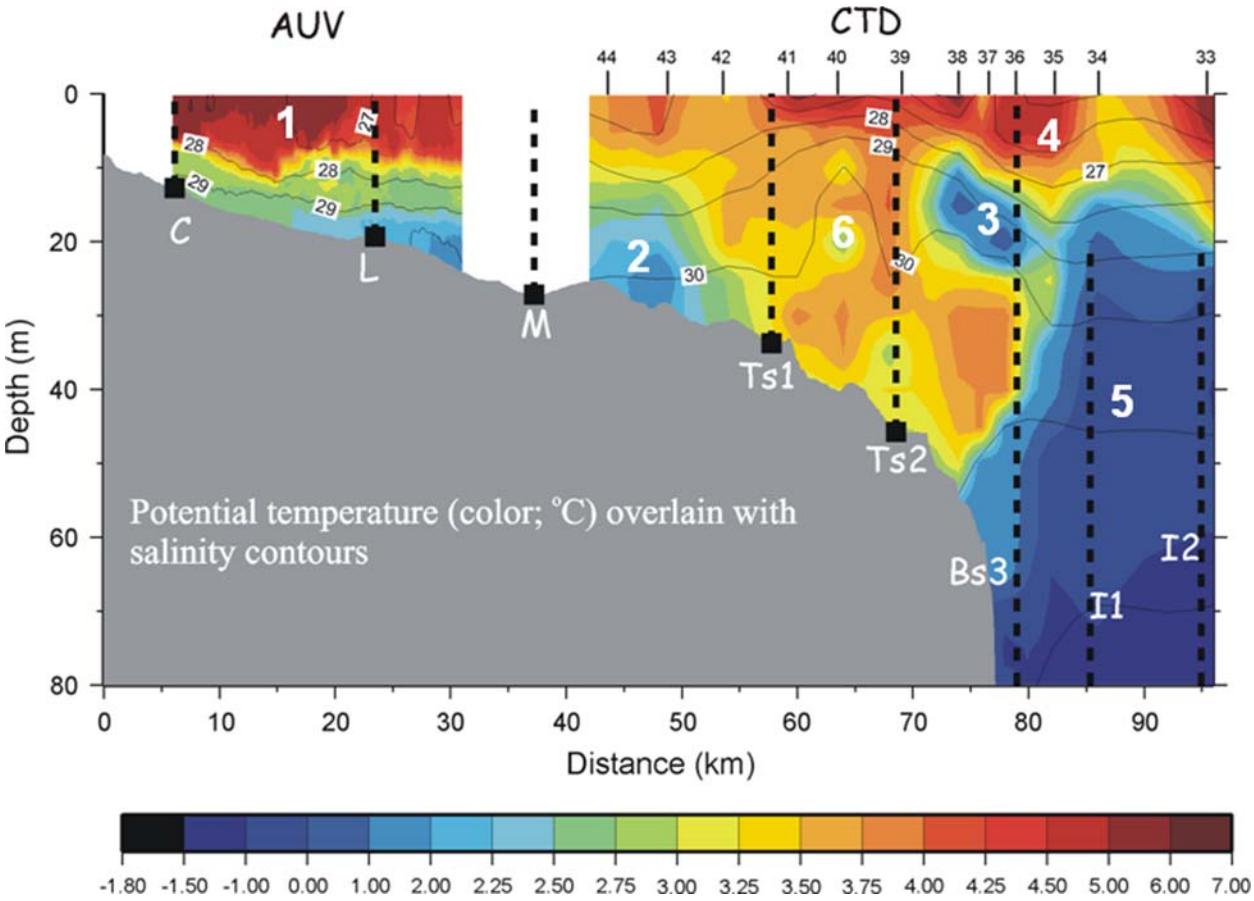

Figure 3.0.2. Synoptic vertical section of potential temperature (color shading) overlain by salinity occupied on August 8, 2008 offshore of the Colville River on the central ABS shelf. The numbers in the figure refer to various water masses discussed in the text. The vertical dashed lines are the locations of 8 of the 9 current meter moorings along the central ABS encircled by the red oval in **Figure 3.0.1**.

Several programs of relevance to this report are in progress. These include a collaborative effort amongst the MMS, Shell and ConocoPhillips in an extensive physical oceanographic research program in the Northeast Chukchi Sea. That effort, which includes HFRs and gliders (during the open water season) and year-round oceanographic moorings, will yield results pertinent to ABS studies. One particularly relevant result will be an improved estimate of the time-varying transport entering upper Barrow Canyon throughout the year. Previous studies (e.g., *Weingartner et al.,* 1998; *Weingartner et al.,* 2005; *Woodgate et al.,* 2005) indicate that the currents here are well-correlated with winds and consequently we expect that the Chukchi studies will establish a firm statistical relationship between winds and transport at the head of Barrow Canyon. That relationship will be useful in understanding exchanges across the western boundary as discussed in Sections 4.1 and 4.2.

The Japan Marine Science and Technology Center (JAMSTEC) has conducted physical oceanographic measurements along the Chukchi continental slope and adjacent basin for the past decade. Their emphasis has largely been on the fate of Pacific Ocean waters (especially those flowing through Barrow Canyon) in the region eastward from the Chukchi Cap and Northwind Ridge to Barrow Canyon. Of relevance to this document is that JAMSTEC has maintained at

least two current meter moorings on the east and west sides of the mouth of Barrow Canyon, and they have indicated that this effort will likely continue for several more years. While the foci of their research is on water masses and flow at the mouth of the canyon, we believe that these measurements can inform shelfbreak processes that control exchanges across the oceanic boundary discussed in Section 4.2.

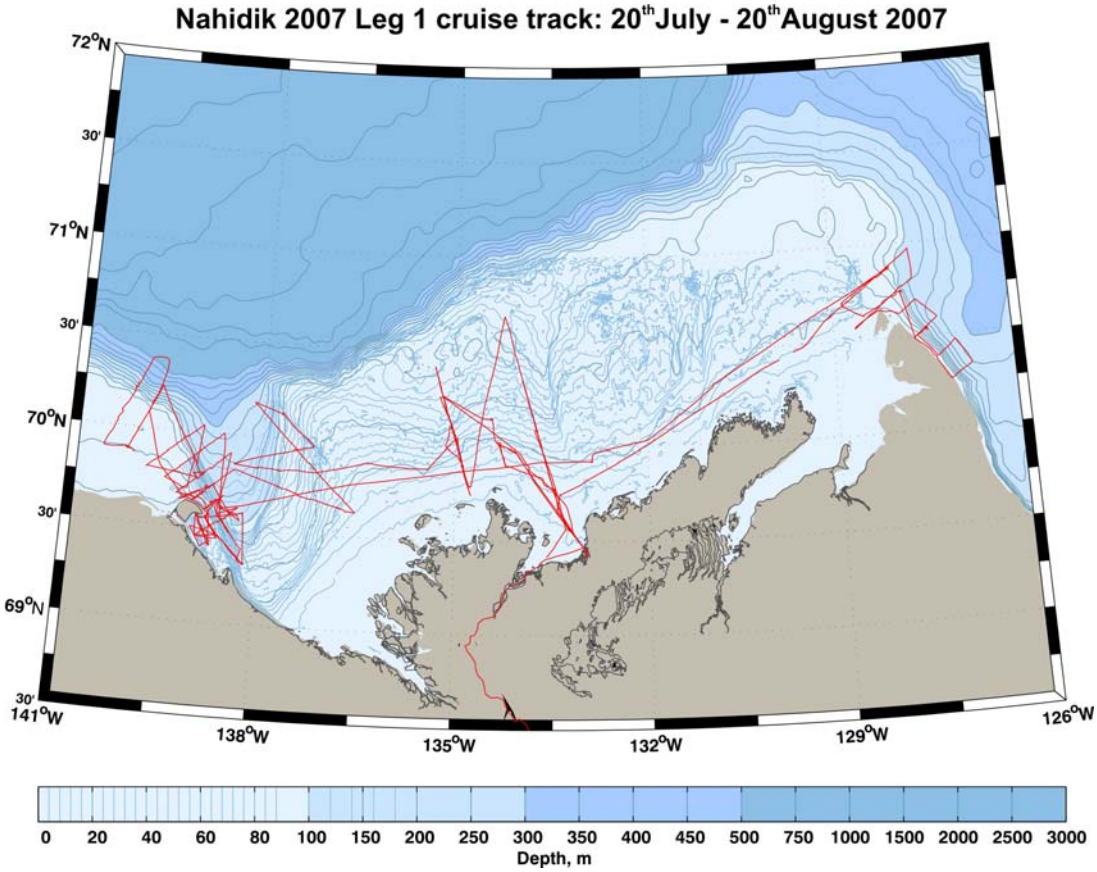

Figure 3.0.3. Example cruise track from July-August 2007 conducted by Canadian scientists on the Mackenzie shelf aboard the CGC *Nahidik*.

The Canadian government is supporting IOS scientists in annual open water studies on the Mackenzie shelf. This interdisciplinary program includes physical and biological oceanography including fish and marine mammals. While the sampling varies from year-to-year, the program encompasses the entire Mackenzie shelf (e.g., **Figure 3.0.3**). Unfortunately, the program is temporarily suspended due to a required re-fit of the vessel dedicated to this work (CCGC *Nahidik*). It remains unclear when this refit will be performed. There is, however, considerable interest on the part of Canadian government scientists in working collaboratively on eastern boundary issues in light of offshore development issues on this shelf. Collaborations are discussed further in section 5.

4.0. RECOMMENDED STUDIES

4.1. THE WESTERN BOUNDARY: exchange with the Chukchi Sea Shelf.

Statement of the Problem

The mean northward flow of approximately 0.8 Sv (1 Sv = 10^6 m^3 s^{-1}) through Bering Strait proceeds northward across the Chukchi Sea shelf along three principal pathways (illustrated schematically in **Figure 4.1.1**): Herald Valley in the western Chukchi, a branch between Herald and Hanna Shoals on the central shelf, and through Barrow Canyon adjacent to the Alaskan coast.

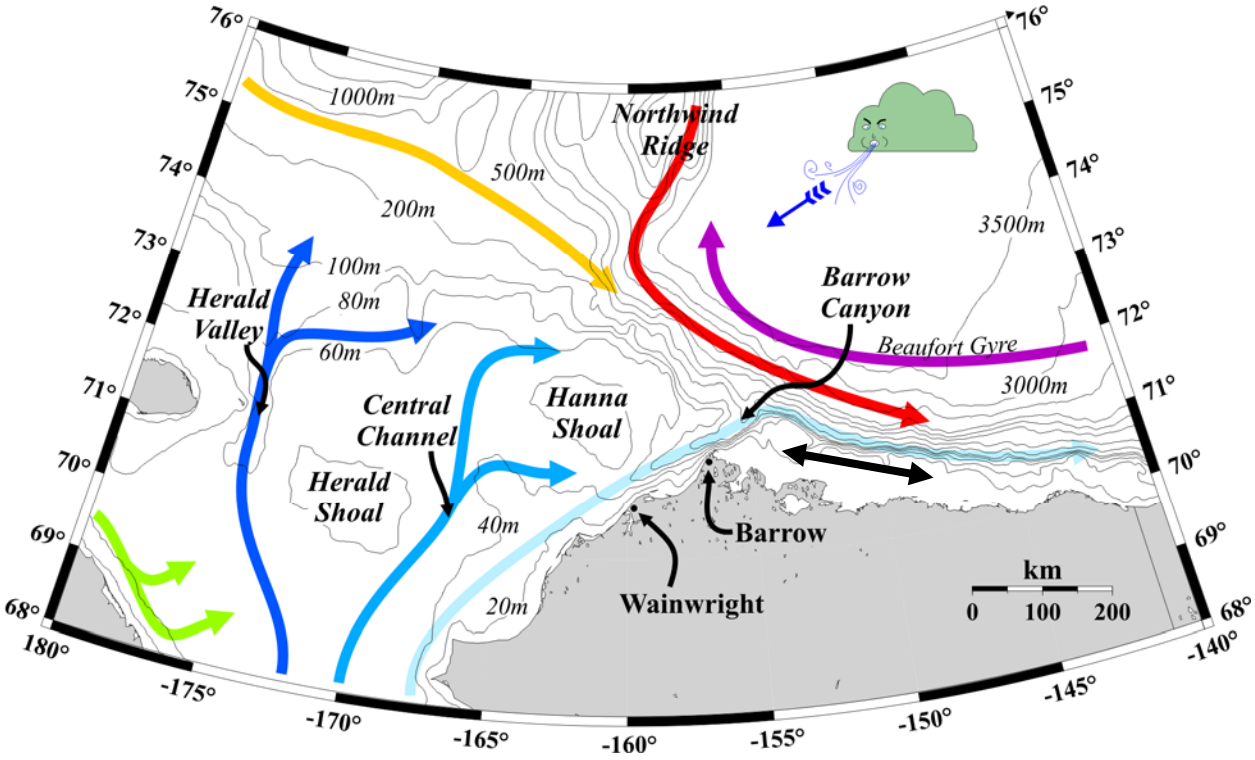

Figure 4.1.1. Schematic of the circulation across the Chukchi and Beaufort seas. The three principal branches flowing northward from Bering Strait are through Herald Valley (dark blue), the central shelf (medium blue), and through Barrow Canyon (cyan). The Barrow Canyon outflow proceeds eastward along the ABS shelfbreak above Atlantic Water (red) and beneath the counterclockwise wind-driven flow of the Beaufort Gyre (magenta). The black double-pronged arrow on the ABS shelf implies variable wind-driven flows.

The transport through each of these branches is only approximately known, with the flow through Barrow Canyon estimated to be ~0.3 Sv on average (*Woodgate et al.*, 2005; *Weingartner*, unpub. data). (Note that moored ocean measurements to be made in the Chukchi Sea beginning fall 2010 will yield more precise estimates of this transport.) The branch through Barrow Canyon is of interest here for it feeds the western boundary of the ABS.

While some of the water entering Barrow Canyon does so within the Alaskan Coastal Current (ACC), other waters entering the Canyon are drawn from the central Chukchi Sea shelf, very likely from the vicinity of the Klondike and Burger oil lease areas. In summer and early fall, canyon waters include warm, relatively fresh Alaskan Coastal Water overlying and/or adjacent to very cold (near-freezing), salty waters formed on the Chukchi shelf the previous winter. In winter and spring the flow consists mainly of winter-formed waters. The canyon outflow is swift ($0.5 – 1$ m s^{-1}) and flows primarily along the eastern wall of the canyon (and so against the prevailing northeasterly winds). The fate of the outflow is not completely known, but appears to be complicated. Some of it proceeds eastward along the shelfbreak and slope, with the depth of this eastward flow varying seasonally (Section 4.2), some may be entrained into eddies formed at the mouth of the canyon, some may drift downwind to the west (both of these features are suggested in **Figures 4.1.2** and **4.1.3**), and some may flow eastward over the inner and mid-shelf of the ABS. The disposition of the outflow likely varies seasonally depending upon the stratification, the winds, and the sea ice. In addition the abrupt changes between the Chukchi and Beaufort shelves in shelf width and coastline orientation, with Barrow Canyon delineating these transitions, is likely to scatter coastal-trapped waves propagating from west to east. For this setting, some of the incoming wave energy would be reflected and some transmitted into both long and short waves. The long waves would propagate along the ABS shelfbreak, whereas the short wave energy would be concentrated at the mouth of Barrow Canyon (*Wilkin and Chapman*, 1987; 1990), possibly resulting in energetic, mesoscale motions.

The canyon outflow appears to be ecologically important. The denser portions of the outflow are enriched in nutrients and carbon, which may support biological production within and downstream of the canyon. *Logerwell et al.* (2009) suggest that adult arctic cod may preferentially inhabit the cold, salty (denser) fraction of the outflow that forms subsurface waters along the shelfbreak. The prevailing northeastward flow appears to be an important advective route by which plankton and fish are carried from the Bering Sea into the ABS. Finally, the canyon itself is an important migratory corridor and habitat (at least seasonally) for a variety of marine mammals. Indeed *Moore et al.* (2000) identify the region to be important for bowhead and beluga feeding and *Ashjian et al.* (2010) describe regional flow scenarios that apparently concentrate euphausiids and thus enhance bowhead whale foraging.

The outflow from Barrow Canyon affects the circulation and temperature and salinity properties of the ABS shelf and slope (or at the very least the "western" portion of the ABS). However, the junction between the Chukchi and Beaufort shelves is likely complex for a number of reasons. For example, it seems likely that some of the canyon outflow rounds Pt. Barrow and spills onto the inner and mid-ABS shelf. If so, then in the mean the flow over the shelf north and northeast of Barrow involves the convergence of the westward wind-driven flow of the ABS with the eastward-trending outflow from Barrow Canyon. The nature of this convergence will vary in response to the strength of the ACC, the stratification, winds and sea ice.

Review of current and previous work

Section 4.2 will outline previous and ongoing efforts associated with the fraction of the canyon outflow transported along the ABS shelbreak and slope. *Okkonen et al.* (2009) examined the fate of Alaskan Coastal Current waters with respect to wind variations from a late summer shipboard hydrographic and ADCP surveys between 2005 and 2007. They inferred that when winds are

weak (regardless of direction), the ACC tends to be relatively strong along the eastern flank of Barrow Canyon and feeds the shelfbreak and a weak onshelf flow. Moderate winds from the east propel inner shelf ABS waters northwestward, which inhibit the inflow of warm, fresh Alaskan Coastal Water onto the inner shelf from Barrow Canyon (**Figures 4.1.2 – 4.1.4**). They also argue that moderate-to-strong winds from the northeast promote separation of the ACC from the eastern flank of Barrow Canyon and establish an up-canyon current along the eastern wall that is fed in part by waters from the western Beaufort shelf. (Similarly, *Weingartner et al.,* [1998] observed that subsurface currents in Barrow Canyon reversed only when northeasterly wind speeds exceeded ~5 m s^{-1}.) Southerly and southwesterly winds appear most effective in causing warm Bering/Chukchi waters from Barrow Canyon to intrude onto the western ABS shelf. The extent of the eastward intrusions will depend upon the magnitude and duration of the winds.

Okkonen (pers. comm.) also had a current meter mooring in the westernmost passage to Elson Lagoon (about ~7 km east of Pt. Barrow) between August and December 2007. He finds that for the open water season moderately strong winds from the east force waters out of the lagoon through this passage (as expected). However, when landfast ice is present, the ice decouples lagoon and nearshore waters from the winds and inflow to the lagoon through the westernmost passage occurs. While the dynamics of the landfast ice wind-current regime are not entirely understood in this setting, these observations imply that ACC waters occasionally penetrate eastward onto the inner shelf in winter.

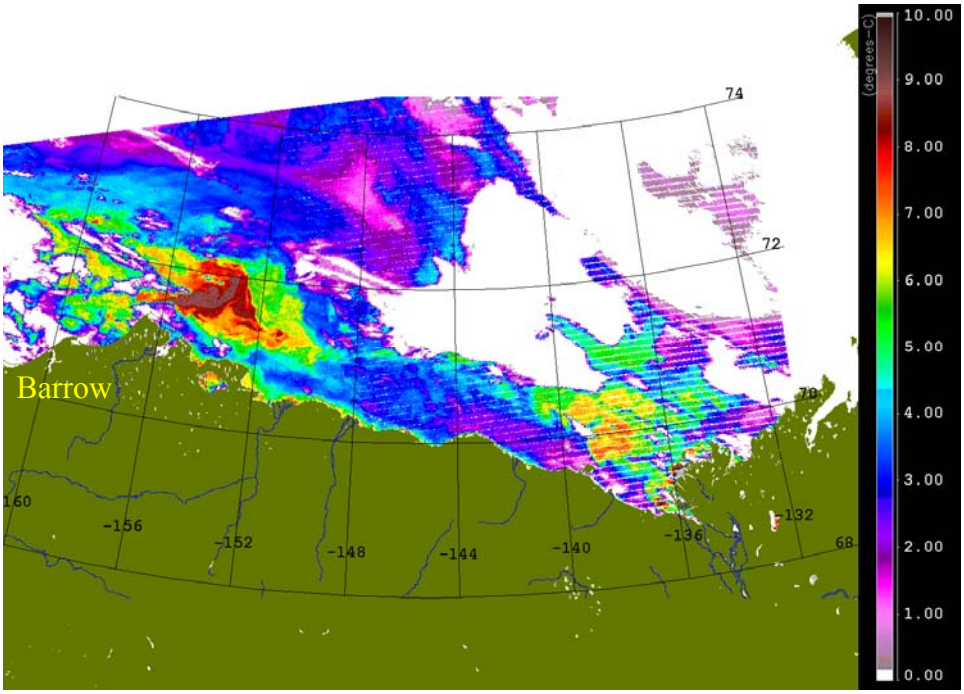

Figure 4.1.2. September 11, 2007 MODIS SST image of the ABS, showing spreading of warm Alaskan Coastal Water onto the shelf and slope north and east of Barrow. The relatively warm water in the eastern Beaufort Sea likely reflects remnants of the Mackenzie River plume.

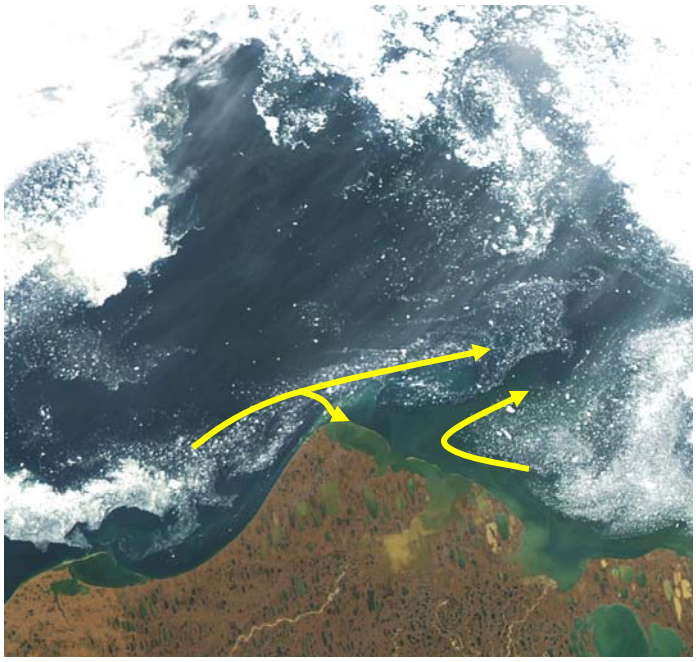

Figure 4.1.3. September 4, 2006 MODIS visible image suggesting bifurcation (split yellow arrow) of the outflow from Barrow Canyon as it rounds Pt. Barrow. Winds at the time were ~3.5 m s^{-1} from the south. MODIS image provide by NASA/GSFC, MODIS Rapid Response (courtesy S. Okkonen).

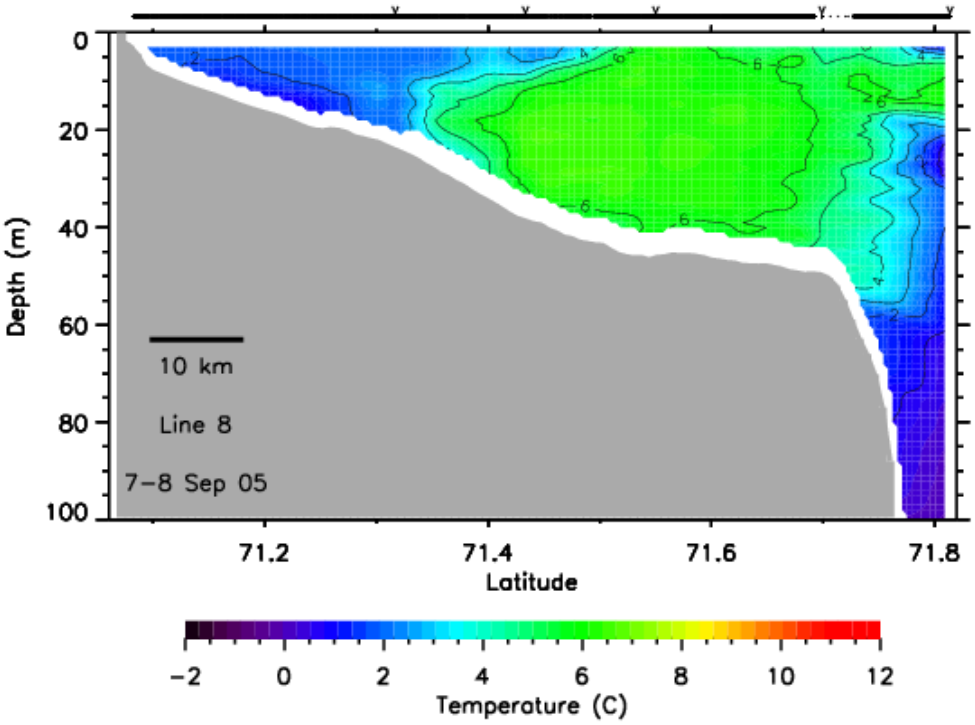

Figure 4.1.3. Cross-shelf temperature section ~50 km east of Barrow showing warm (>5°C) Alaska Coastal Water from the Chukchi Sea over the ABS shelf. The section was occupied under weak northward winds of ~2 m s^{-1} (courtesy S. Okkonen).

Ongoing work, supported by MMS-Coastal Marine Institute on simple process model studies of the landfast ice zone suggest that an inflow that mimics turning of the ACC along the western boundary of the ACW can establish along-shore pressure gradients beneath the landfast ice zone of the ABS and force water eastward (in the absence of any offshore wind-forcing). These results are illustrated in **Figures 4.1.4a-d**, which shows isopleths of sea level within 25 km of the coast for various values of the under-ice friction coefficient and landfast ice extent (*Kasper and Weingartner*, in prep.). Although the model is idealized and considers only an inflow along the western boundary (x=0), it suggests that in the absence of any additional forcing, the inflow could easily penetrate eastward for more than 100 km along the coast.

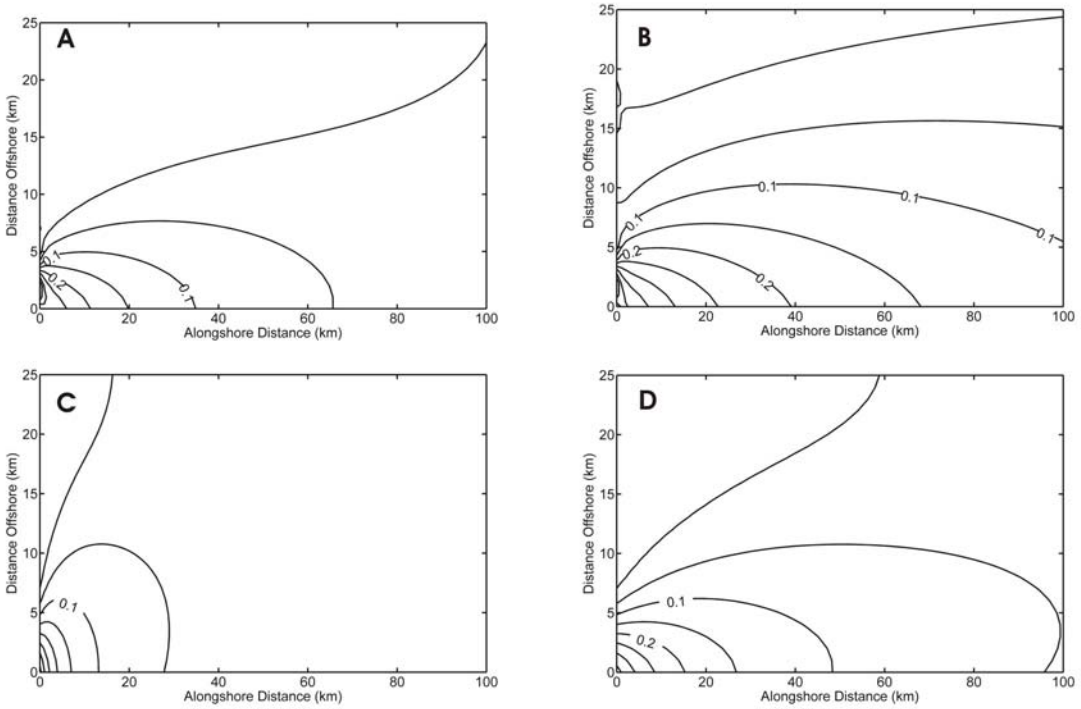

Figure 4.1.4. Panels A-D depict the steady-state cross- and along-shore sea level beneath the landfast ice zone along the ABS coast when forced by an inflow along the western boundary (left –hand side of each panel). The different sea-level distributions reflect differences in the magnitude of the under-ice friction coefficient and/or the extent of landfast ice (from *Kasper and Weingartner*, in prep.a). Unless otherwise stated the bottom and under-ice friction coefficient is 10^{-4} m s^{-1} and the landfast ice width is 26 km (A). B) landfast ice width = 60 km. C) the under-ice friction coefficient increases quadratically offshore within the landfast ice zone and is ~ 10^{-3} m s^{-3}. D) the under-ice friction coefficient increases linearly offshore within the landfast ice zone and is ~10^{-4} m s^{-3}.

Finally we note that prior to the availability of ADCP technology no over-winter moored measurements were obtained inshore of the ~50 m isobath. We have recently succeeded with the mooring design used in the NOPP program and other MMS-supported studies (*Weingartner et al.*, 2009) in being able to safely (at least reasonably so) deploy oceanographic instruments inshore of this depth.

Need for information

The circulation in the region of the junction between the Chukchi and Beaufort continental shelves is likely complex given the abrupt change in coastline orientation, change in shelf width between the Chukchi and Beaufort shelves, and the convergence of the mean westward wind-driven flow over the ABS with the mean northeastward flow along the eastern flank of Barrow Canyon. The nature of this junction will vary with the winds and ice environment. The regional circulation is such that contaminants introduced on either the Chukchi or Beaufort shelf will likely have a variety of fates. These include being advected from one shelf to the other, flushed offshore into the Arctic Ocean basin (see section 4.2), or perhaps accumulating within the vicinity of the western ABS due to flow convergence between the two shelves. The conditions under which these various scenarios occur are not well known. The region appears to be an especially important habitat for a variety of marine birds and mammals, especially bowhead whales that feed in the area in fall. The observations to date, while suggestive, have been limited due to weather and other operational constraints.

Study Goals

The goal of the recommended observations is to determine the structure of the seasonally-varying circulation in the western Beaufort Sea in response to changes in winds and ice cover. In particular, the observations are geared to determine the fate of the ACC as it flows past Pt. Barrow and they should determine how seasonal variations in wind velocity and ice cover affect the exchange of water between Barrow Canyon and the mid and inner shelf of the ABS.

Approach

We envision a 4-year field program conducted between Cape Halkett (western Harrison Bay) and Barrow (**Figure 4.1.5**). A fifth year is needed to complete analyses. The first year would be devoted to HFR site preparation activities. This includes obtaining necessary permits, presentation of the project to the villages of Nuiqsuit and Barrow, organizing logistical operations, and constructing the RPMs. In prior HFR deployments, we have spent as much as 8 – 12 months preparing and awaiting for receipt of permits from the relevant agencies. Moreover there are several options available for the logistical support of the HFR sites. These may include boat, air, and/or snow-machine transport. Included amongst these is possible USCG support of these sites, which may be the most cost effective. After exploring these various options, we concluded that support assets are constantly changing on the North Slope and that it would be premature to choose and budget for an approach that may not be in existence, if and when MMS decides to pursue this recommended study. *We have therefore budgeted for boat support of the remote HFR sites at Cape Simpson and Cape Halkett, with helicopter support for service visits and winter securitization at Cape Halkett and fixed-wing aircraft for the same at Cape Simpson*.

In the second year we would deploy 3 LongRange HFRs (range ~170 km) at Barrow, Cape Simpson and Cape Halkett. The coverage would extend from western Harrison Bay to Barrow Canyon and across the continental slope. The goals of the first year HFR deployments are to: 1) characterize the regional surface water circulation and 2) guide the location of year-round subsurface moorings in the second year. The HFR sites are chosen to optimize both sampling and logistics. However, each site would require an RPM (the Barrow site is located at the tip of Point Barrow where there is no shoreside power). The Cape Simpson site is currently unoccupied although in recent years it supported oil exploration activities. It has a gravel

runway amenable to fixed wing aircraft or helo and easy access to the beach from the airstrip or by boat. The Cape Halkett site is the least accessible and here the HFR+PRM deployment would have to involve boat and/or helicopter from Oliktok Point or the Colville River delta.

The subsurface moorings on the 15 m isobath are located inshore of the landfast ice zone in winter, whereas the moorings on the 35 m isobaths are located mid-shelf and offshore of the landfast ice where water from the Chukchi shelf flows eastward on the western ABS at least occasionally (e.g., the 35 m isobath is centered at the location of the warm Chukchi water in **Figure 4.1.3)**. Both of these moorings could be deployed from a small vessel, such as the *R/V Annika Marie*, ported in Prudhoe Bay. The moorings would be bottom-mounted ADCPs with SeaCat temperature/conductivity and pressure recorders included. In addition to examining the along-shore penetration of Chukchi shelf water, the array's focus on the middle and inner shelf will permit examining along-shore differences in the circulation in this region in winter. Hydrographic (CTD) mapping would be conducted during the mooring deployment and recovery phases as well. The hydrography could be accomplished in several different ways:

1. CTD sampling would occur from the mooring deployment vessel (a single seasonal survey);

2. If the mid- and inner shelf moorings are deployed in the same year as the offshore oceanic boundary study then the larger vessel could conduct another shelf survey when it is in the area, or;

3. by a 1 – 2 month deployment of a glider during the mooring operations. At the end of the mission the glider would be commanded to return to Barrow or to Prudhoe Bay for recovery by a small vessel.

Of all the options, the last provides the most extensive spatial and temporal hydrographic coverage.

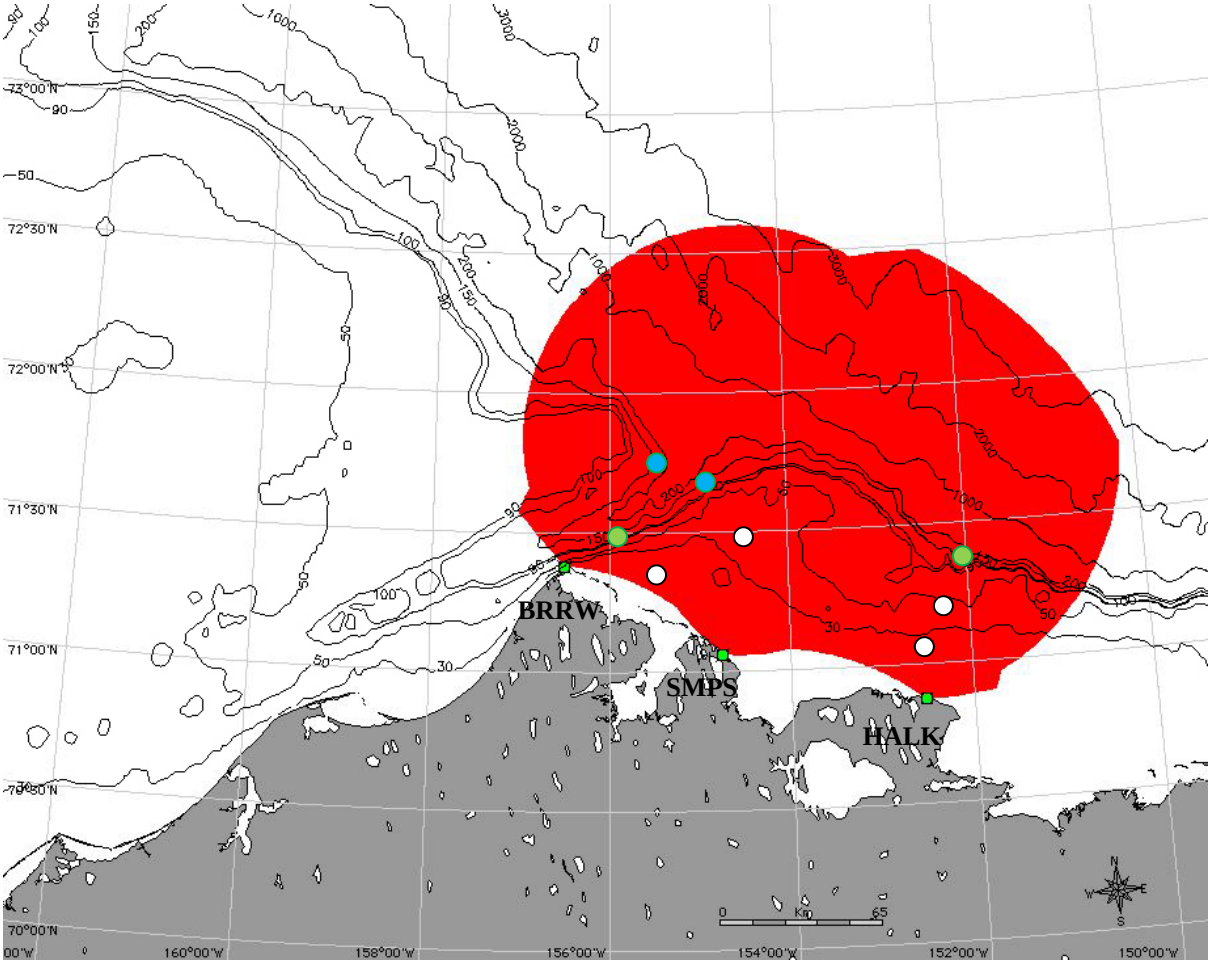

Figure 4.1.5. Bathymetric map of the western ABS showing location of HFR sites at Barrow(BRRW), Cape Simpson (SMPS), and Cape Halkett (HALK) and the red defines the nominal HFR radar mask. White circles denote the tentative location of bottom-mounted moorings on the 15 and 35 m isobaths. The green circles are moorings that comprise a portion of the oceanic boundary study and the blue circles are the approximate location of the JAMSTEC moorings at the mouth of Barrow Canyon.

Ideally, the western boundary study would coincide with the oceanic boundary studies discussed in the next section. By so doing, two of the mooring sites that comprise the oceanic boundary work (green circles, **Figure 4.1.4**) would be within the HFR mask as well as the JAMSTEC moorings at the mouth of Barrow Canyon (blue circles). Moreover, the combined moored array would permit a closer examination of along-shore differences in the shelf and shelfbreak circulation.

Budget (approximate costs)

YEAR 1. Construction of the RPMs, purchase of HFRs, obtaining permits, and planning logistics. (January – December)

**Personnel*
Senior Personnel (1 man-month) $18,000

Technical Personnel (12 man-months)	$96,000
**Travel*	
Fairbanks-Barrow; Fairbanks-Nuiqsuit, Fairbanks-Anchorage; lodging in all places	$10,000
**Contractual Services:*	
Permitting fees	$3,000
HughesNet communication costs	$3,600
Commodities	
Misc. field supplies for HFR site support	$20,000
Hughesnet satellite communications systems	$1,500
Laptop computer (w/ software)	$5,000
Equipment	
3 Remote Power Modules ((RPMs)	$390,000
3 CODAR LongRange HFRs	$430,000
*OVERHEAD (50% indirect costs)	$68,500
Total YEAR 1:	**$1,044,500**

YEAR 2. Establish HFR sites, HFR sampling, partial HFR site demobilization for winter, equipment purchases for YEAR 3 (January – December)

**Personnel*	
Senior Personnel (1 man-month)	$18,000
Technical Personnel (12 man-months, includes mob/demob & site visits pay)	$96,000
Analysis Personnel (12 man-months)	$96,000
**Travel:*	
Fairbanks-Deadhorse, Fairbanks-Barrow, vehicle rental; lodging	$30,000
**Contractual Services*	
Shipping (Fairbanks-Barrow and Deadhorse)	$25,000
Vessel support for deployments at Capes Halkett and Simpson (16 days, includes mob, food and fuel, crew)	$119,000
Barrow Arctic Science Consortium (Barrow site)	$40,000
Helicopter support for periodic site visits and demobilization (Deadhorse-Cape Halkett; 40 hours at $3100/hr)	$124,000
Fixed-wing support (Deadhorse-Cape Simpson; 50 hours at $1000/hr)	$50,000
HughesNet communication costs	$3,400
**Commodities*	
Laptop computer (w/ software)	$5,000

Equipment
SBE-25 CTD with transmissometer $33,000
4 oceanographic moorings
(mooring hardware, acoustic releases, ADCPs, SeaCats) $240,000

*OVERHEAD (50% indirect costs) $321,200
Total YEAR 2: $1,182,600

YEAR 3. Deploy moorings, operate HFR sites, and hydrography

**Personnel*
Senior Personnel (2 man-months) $36,000
Technical Personnel (12 man-months) $96,000Analysis Personnel(12 man-months) $96,000

**Travel:*
Fairbanks-Deadhorse, Fairbanks-Barrow, vehicle rental; lodging $30,000

**Contractual Services*
Shipping $3,000
CTD post-calibration $1,000
Vessel support (for HFR activation at Capes Halkett and Simpson, mooring deployments and CTD survey (16 days, includes mob, food and fuel, crew) $119,000
Barrow Arctic Science Consortium (Barrow site) $40,000
Helicopter support for periodic site visits and demobilization (Deadhorse-Cape Halkett; 40 hours at $3100/hr) $124,000
Fixed-wing support (Deadhorse-Cape Simpson; $50 hours at $1000/hr) $50,000
HughesNet communication costs $3,400

**Commodities*
Miscellaneous field gear and hardware $10,000
HFR and RPM replacement parts $30,000

*OVERHEAD (50% indirect costs) $337,200
Total YEAR 3: $947,600

YEAR 4. Recover moorings, remove HFR sites, conduct hydrography
**Personnel*
Senior Personnel (2 man-months) $36,000Technical Personnel (8 man-months) $64,000
Analysis Personnel(12 man-months) $96,000

**Travel:*
Fairbanks-Deadhorse, Fairbanks-Barrow, vehicle rental; lodging $15,000

**Contractual Services*
Shipping $25,000

Post-calibrations	$10,000
Vessel support for HFR de-activation at Capes Halkett and Simpson, mooring recoveries and CTD survey (20 days)	$149,000
Barrow Arctic Science Consortium (Barrow site)	$15,000
**Commodities*	
*OVERHEAD (50% indirect costs)	$337,200
Total YEAR 4:	**$615,000**

YEAR 5. Complete analyses and reporting

**Personnel*	
Senior Personnel (3 man-months)	$54,000
Analysis Personnel (6 man-months)	$48,000
**Travel:*	
Fairbanks-Anchorage	$2,000
**Contractual Services*	
Publication costs	$5,000
**Commodities*	
*OVERHEAD (50% indirect costs):	$54,500
Total YEAR 4:	**$163,500**
TOTAL PROJECT COST:	**$3,789,700**

4.2 THE OCEANIC BOUNDARY: Shelf-basin exchange via wind and eddies

Statement of the Problem

It is now firmly established that a shelfbreak current carrying Pacific-origin water exists at the edge of the ABS. The current is very narrow (order 10-15 km) and, in the absence of wind-forcing, flows to the east towards the Canadian Beaufort Sea (**Figure 4.2.1**). One of the important aspects of this current is that it dynamically links the conditions on the shelf with those in the interior basin (as well as upstream, see Section 4.1). The reason for this is that the shelfbreak current is highly variable in time, and, as a result, represents a very "leaky" boundary. In the absence of external forcing the current is dynamically unstable and forms eddies (*Spall et al.,* 2008). This leads to an exchange of mass and properties across the shelf edge, whereby shelf water is fluxed offshore and ambient basin water is fluxed onto the shelf. There are different types of eddies depending on the time of year, including anti-cyclonic, cyclonic, warm-core, cold-core, surface-intensified, and mid-depth intensified.

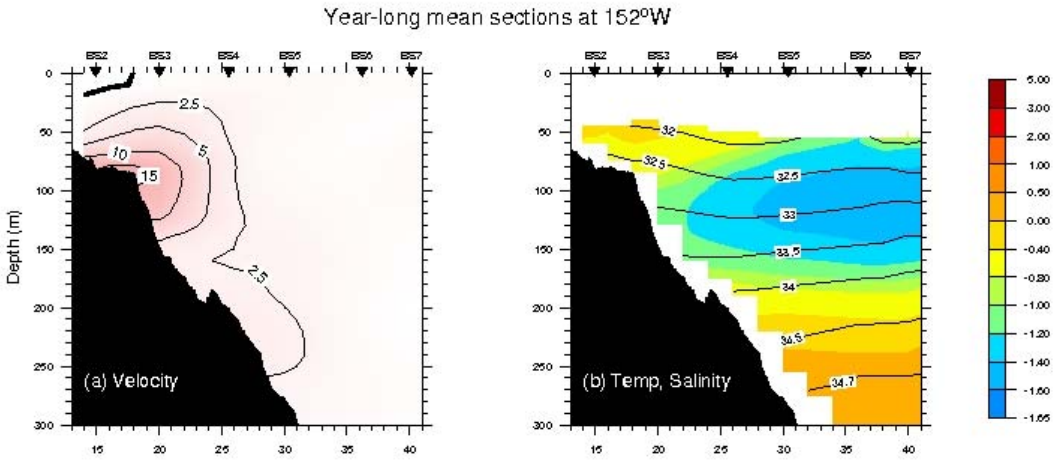

Figure 4.2.1. Year-long vertical sections across the shelfbreak of the ABS at 152°W. (a) Alongstream velocity (cm s^{-1}, where positive is along 125°T). (b) Potential temperature (color, °C) with salinity (contours) overlaid. The means were computed over the time period 2 August 2002 – 31 July 2003 (from *Nikolopoulos et al.,* 2009).

When the wind blows, the circulation at the edge of the ABS changes drastically. The two primary types of storms that influence the ABS are Arctic-born cyclones and Pacific-born Aleutian lows (**Figure 4.2.2**). The former results in westerly winds along the ABS, which accelerates the shelfbreak jet and leads to downwelling (near-bottom offshore flow from the shelf to the basin). The latter causes easterly winds which weaken or reverse the shelfbreak jet and results in upwelling (near-bottom flow onto the shelf from offshore). An upwelling example is shown in **Figure 4.2.3** (to be compared to the normal state of the current in **Figure 4.2.1**). For this particular storm, the shelfbreak jet reversed and flowed westward at > 1 m s^{-1}, and warm and salty Atlantic water—normally found near 200 m on the continental slope—was advected onto the shelf. Aleutian lows are most prevalent in late-autumn and winter, while polar cyclones are

most common in early-fall. However, both types of storms can occur during any month of the year. Based on mooring array data collected over the two-year period 2002-3, the shelfbreak jet is influenced by wind roughly 50% of the time.

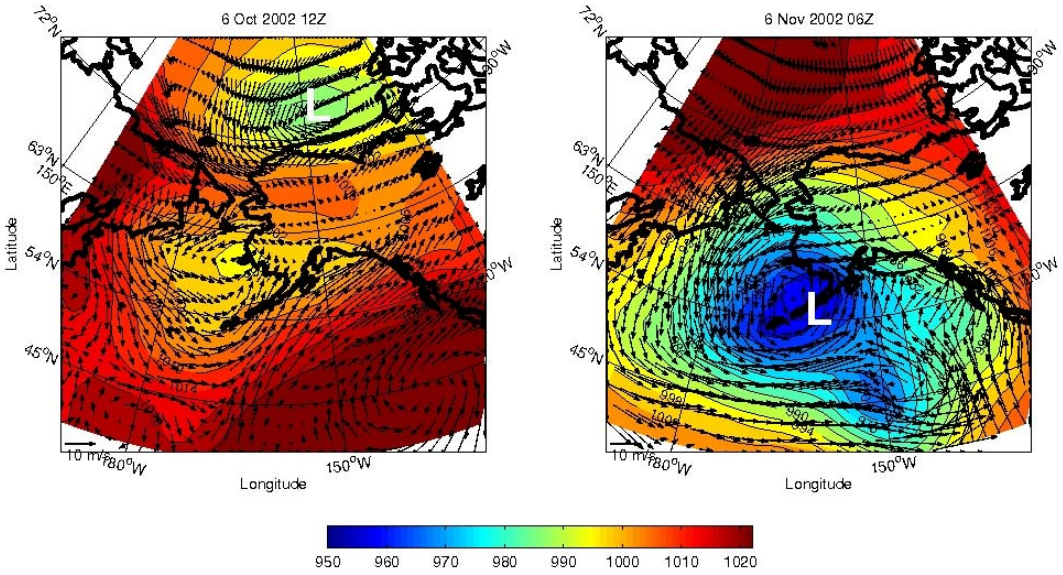

Figure 4.2.2. (left panel) Example of a polar cyclone resulting in westerly winds along the ABS. (right panel) Example of an Aleutian low that causes easterly winds along the ABS. In both plots the sea-level pressure (mb) is overlaid by the 10m wind vectors (m s^{-1}), from the NCEP reanalysis. The L denotes the center of the storm.

While it is known that eddy formation and wind-driven fluctuations result in shelf-basin exchange, the precise mechanisms (dynamics) and amount of exchange are not well understood or quantified. The following issues remain to be addressed.

Regarding wind-driven exchange:

(1) To what extent is the upwelling/downwelling on the ABS a local (two-dimensional) versus non-local (three dimensional) process? Answering this is essential for determining where the water comes from and where it goes to (for example, downwelled water will likely follow a very different path towards the basin in the three-dimensional case). Answering this question will also tell us if the ABS is impacted by remote storms.

(2) How does the presence of pack-ice and/or landfast ice impact the amplitude of the wind-driven upwelling/downwelling? Landfast ice is known on occasion to extend far offshore the Alaskan coast (beyond the shelfbreak, *Mahoney et al*., 2007). This will change the oceanographic response to wind-forcing, but in ways that are presently unknown. Recently it has been determined that when the concentration of pack-ice nears 100%, the extent of upwelling on the ABS shelfbreak diminishes (*Pickart et al.,* 2009). However, it is not obvious how the response varies for concentrations less than 100%. More work is needed to quantify the role of sea ice in modulating upwelling and downwelling. This is especially important in light of the possibility of reduced ice cover in the future and a

longer open-water period. Furthermore, it is predicted that the frequency and strength of polar cyclones will increase in a warmer climate.

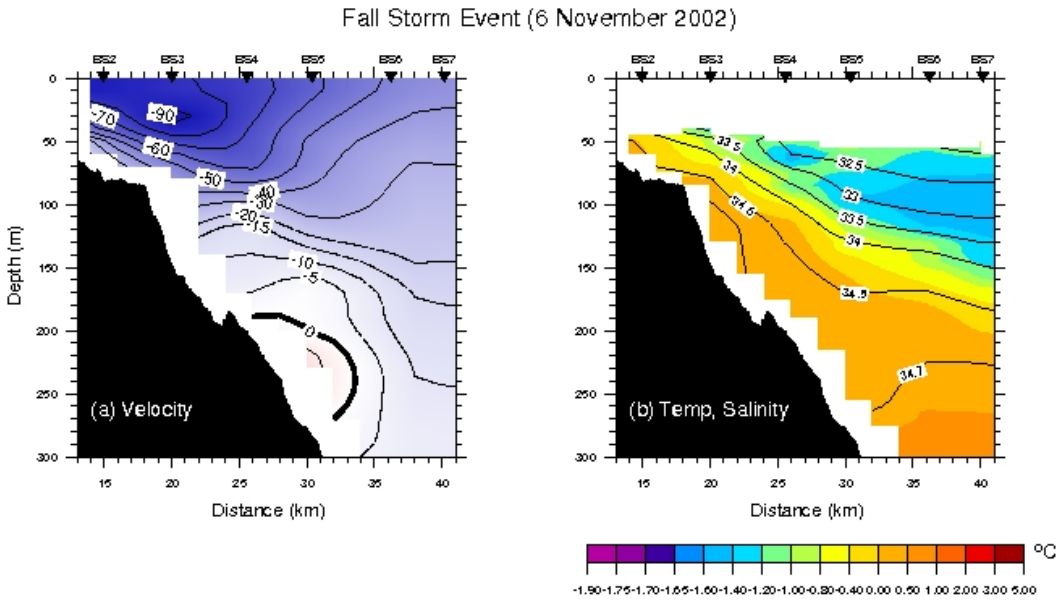

Figure 4.2.3. (a) Alongstream velocity (cm s^{-1}, where positive is along 125°T) and (b) potential temperature (color) overlaid by salinity (contours) at the height of an upwelling storm.

What is the magnitude of the cross-stream fluxes of mass, heat, salt, momentum, and other tracers due to upwelling and downwelling storms? Answering this will help us quantify the impact of storms on the property budgets of the ABS, both for an individual event and in an integrated sense over the course of the year.

Regarding eddy-driven exchange:

(1) What is the frequency of eddy formation over the course of the year and the relative contributions of the different types of eddies? Answering this question requires determining the stability characteristics of the different seasonal configurations of the shelfbreak jet. It has already been determined that the springtime configuration of the jet is unstable and readily forms eddies (*Spall et al*., 2008), but there are other (very different) forms of the current throughout the remainder of the year. Determining the alongstream variation of the jet will also shed light on this issue.

(2) What are the net fluxes of properties due to eddy formation? This can be addressed using a statistical approach at various locations along the ABS. Models have suggested that as much as 50% of the water carried by the jet is expelled into the interior basin (*Spall et al.,* 2008), but, if the transport of jet remains the roughly same, then an equal amount of water must be fluxed onto the shelf from offshore during eddy formation.

In addition to being an important site for exchange between the shelf and basin, the ABS shelfbreak is, at least seasonally, an important migratory corridor and habitat for marine mammals. During spring, three species of cetaceans (bowheads, belugas, and gray whales) migrate from the Bering Sea to the Chukchi/Beaufort Seas in search of prey, returning south again in the fall. These are the only cetaceans to inhabit the western Arctic in significant numbers. Based on 10-years of aerial surveys (*Moore et al*., 2000), habitat selection of these mammals species-specific and varies seasonally. In particular, during autumn the bowheads move onshore and swim westward along the shelf, with belugas strongly associated with the slope of the western Beaufort Sea (**Figure 4.2.4**). Moreover, it is likely that the shelfbreak current plays a fundamental role in the patterns and availability of prey. For example, large aggregations of bowheads have been observed near areas of upwelling during the summer season (*Bradstreet et al.,* 1987), and groups of whales have been spotted in regions of warm eddies (*Moore and Clarke*, 1992). This is perhaps not surprising in light of the elevated concentrations of nutrients, fluorescence, and zooplankton in the shelfbreak jet. The summer-to-fall habitat transition of the bowheads and belugas may be related to the synoptic and seasonal changes in the structure of the boundary current.

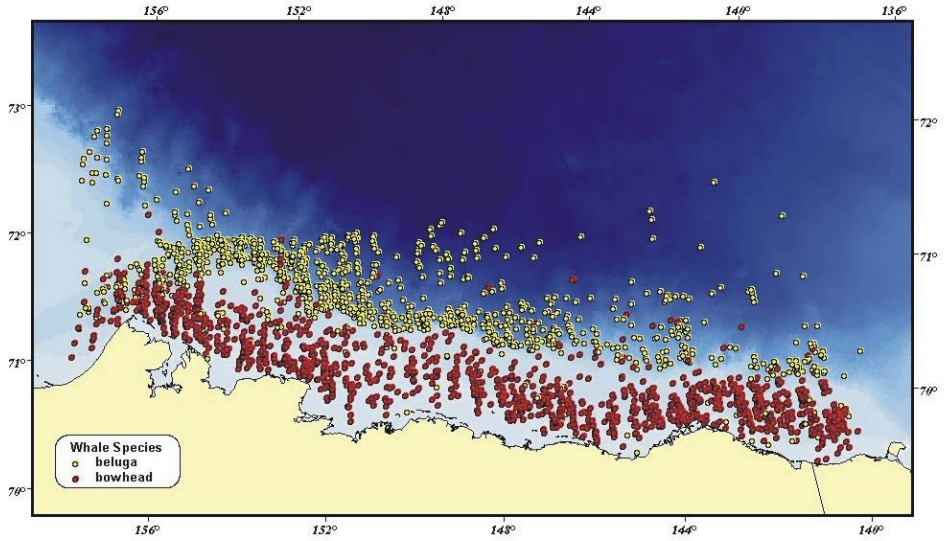

Figure 4.2.4. Historical distributions of beluga and bowhead whales in late summer and fall in the Alaskan Beaufort Sea (*Moore et al.,* 2000).

Review of previous work

The existence of the shelfbreak jet along the ABS was only recently established (*Pickart*, 2004; *Pickart et al.,* 2005; *Nikolopoulos et al*., 2009). Part of the reason for this is that the current is so narrow it escaped detection by typical shipboard measurements and sparsely-spaced moorings. It wasn't until the western Arctic Shelf-Basin Interactions (SBI) experiment in 2002-3 that a finely-spaced mooring array was deployed across the ABS shelfbreak (at 152°W). Hence, much of what we know about the shelfbreak jet stems from the analysis of the SBI data. The basic properties of the current are as follows. In the mean the jet transports approximately 0.15 Sv eastward (although this is highly variable in time, both seasonally and on short timescales). Averaged over the year the jet is bottom-intensified (**Figure 4.2.1**), but it has distinct seasonal configurations

(**Figure 4.2.5**). In spring the current advects cold and dense winter-transformed Pacific water and is bottom-intensified (**Figure 4.2.5, top panel**). In summer and early-fall the current is surface-intensified and carries warm and buoyant Alaskan Coastal Water (**Figure 4.2.5, middle panel**). At this time of the year the shelfbreak jet is essentially the eastward continuation of the Alaskan Coastal Current beyond Pt. Barrow. Note that even though the current is strongest at the surface, it is still trapped to the shelfbreak. In fall and winter the current becomes bottom intensified again (**Figure 4.2.5, bottom panel**), but there are significant differences from the springtime configuration. Notably, in winter there is warm water on the outer shelf, which is the result of many upwelling events. Also note the deep extension of the current between 200-300m. This enhanced eastward flow at depth is the result of the three-dimensional spin-down process after the upwelling storms subside (*Pickart et al.,* 2010).

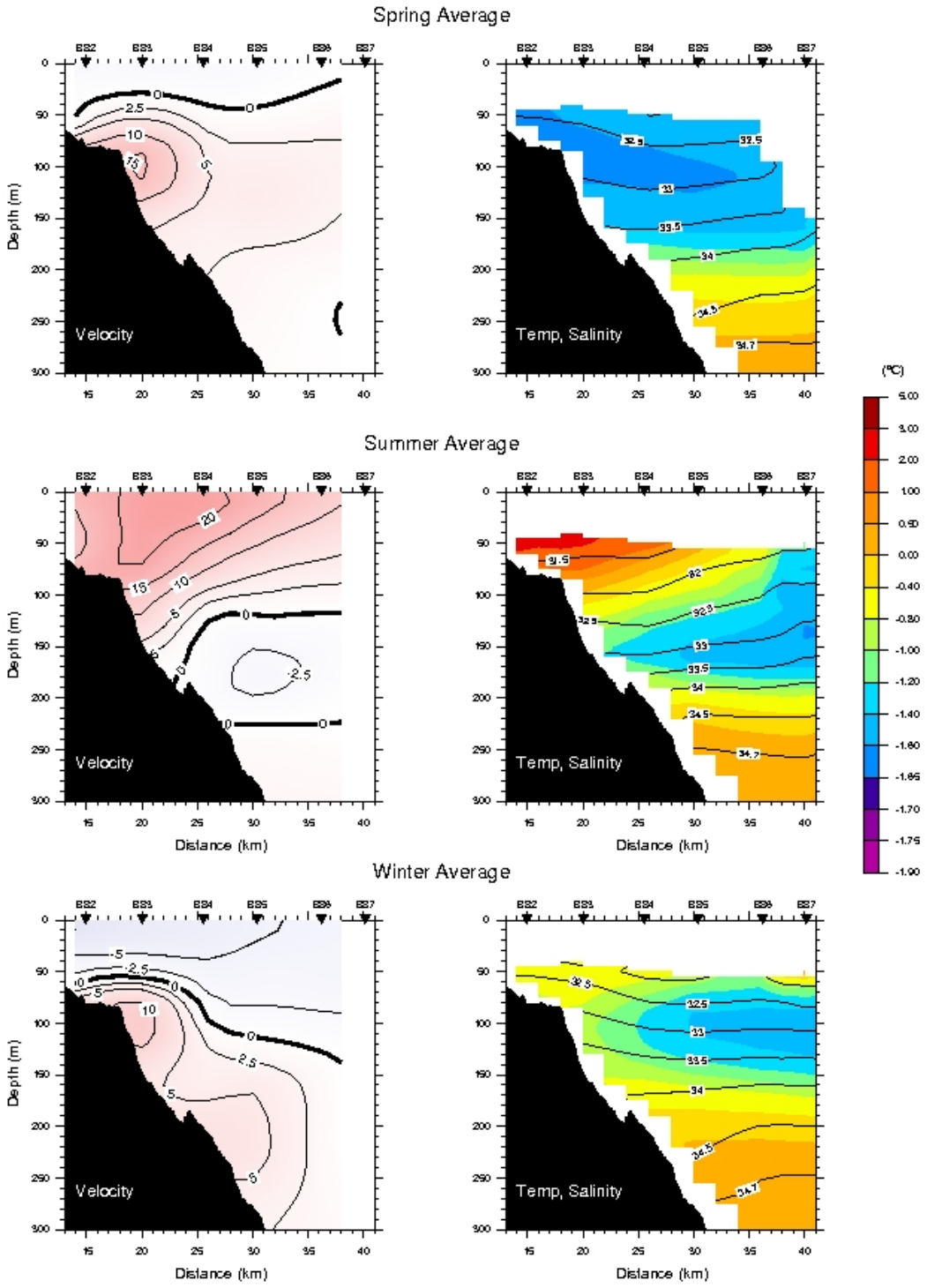

Figure 4.2.5. Composite seasonal averages of the shelfbreak jet. The left-hand panels are alongstream velocity (cm s^{-1}) and the right-hand panels are potential temperature (color) overlaid by salinity (contours).

While the seasonally-averaged configurations of the shelfbreak jet are "well behaved", synoptically the current is highly variable and can be significantly distorted. As discussed above, during upwelling storms the current reverses to the west and brings warm and salty Atlantic Water onto the shelf (*Nikolopoulos et al.*, 2009; see also **Figure 4.2.3**). The secondary (cross-stream) circulation during these storms is strong as well. This is shown in **Figure 4.2.6**, which displays the cross-stream velocity during the height of one such storm (the same storm depicted in **Figure 4.2.3**). The amplitude of the Ekman circulation is nearly 25 cm s^{-1} at the outer shelf, and the flow is not confined to the surface and bottom boundary layers but extends throughout the water column.

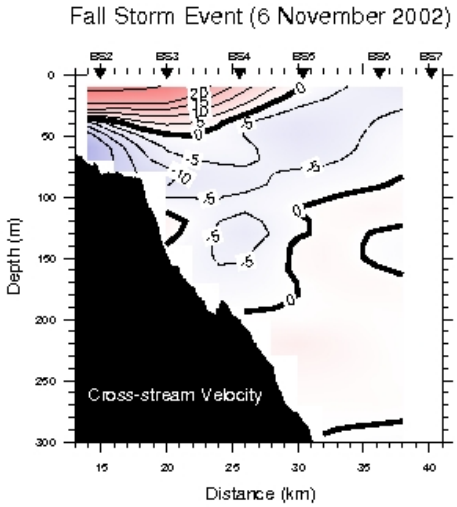

Figure 4.2.6. Cross-stream velocity (cm s^{-1}) at the height of the same upwelling storm shown in **Figure 4.2.3**. Positive flow is offshore.

As mentioned above, *Spall et al.* (2008) have analyzed the springtime configuration of the shelfbreak jet and have determined that, in the absence of wind, it is baroclinically unstable (a similar analysis remains to be done for the other configurations of the jet). **Figure 4.2.7** shows the distribution of Ertel potential vorticity (left hand panel) during the spring season, in the absence of storms. In particular, it is a composite average of the potential vorticity (PV) of the jet during the time period from April-June with the wind events removed. Near 100m depth note that the PV varies from low values to high values progressing offshore. By contrast, near 190m depth the PV transitions from high values near the slope to lower values offshore. This change in sign of the cross-stream PV gradient is a necessary condition for baroclinic instability of the current. The right hand panel of **Figure 4.2.7** shows the baroclinic energy conversion term from mean to eddy potential energy for the same time period, which shows strong energy conversion (enhanced near 150m) into the fluctuations (e.g., eddies). As discussed in *Spall et al.* (2008), this energy conversion results in rapid formation of eddies of the type observed offshore of the ABS shelfbreak.

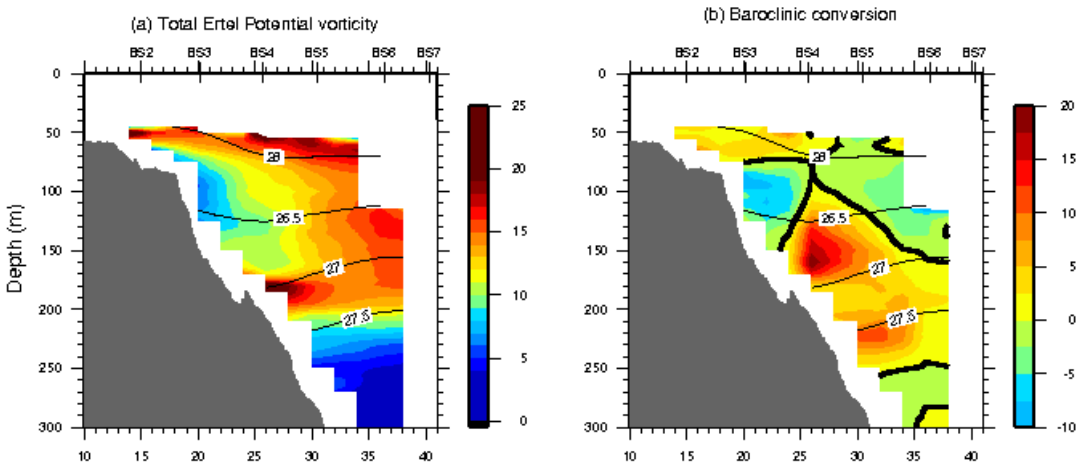

Figure 4.2.7. (a) Vertical section of Ertel potential vorticity ([(m s]$^{-11}$) for the springtime configuration of the shelfbreak jet when there are no storms (from *Spall et al.*, 2008). (b) Vertical section of baroclinic energy conversion (m^2 s^{-3} x 10^{-8}) for the same time period as in (a). Positive values mean conversion from mean to eddy potential energy.

Need for information

The data collected to date, largely from a single field program (the SBI experiment in 2002-3) suggests that the oceanic boundary of the ABS is quite permeable throughout the year. This has huge ramifications for the mass, heat, salt, and property budgets of the ABS, as well as the residence time of parcels on the shelf. In the absence of wind, the shelfbreak current is unstable and forms eddies leading to cross-stream exchange. During easterly and westerly wind events the shelfbreak jet is enhanced or reversed, and there are significant secondary flows; this also results in shelf-basin exchange. There are many aspects of these processes that remain poorly understood and whose ramifications remain uncertain. Such aspects include determining the remote vs. local response to storms, the role of sea ice in modulating the response, the magnitude of the wind-driven fluxes, the frequency and type of eddy formation, and the eddy-flux of properties in the absence of wind. Finally, we need to understand the atmospheric forcing better, including the role of sea-ice vs. open water on the wind field over the ABS, and the impact of the Brooks Mountain Range on local flow distortion (e.g. *Dickey*, 1961; *Kozo and Robe*, 1986; *Pickart et al*., 2010).

Study Goals

We suggest that fieldwork be conducted along the ABS shelfbreak in order to determine the three-dimensional processes responsible for wind-forced and eddy-driven shelf-basin exchange, and to estimate the magnitude of the fluxes. The observations should allow us to:

1. Determine what portion of the wind-driven response of the ABS is due to local winds versus propagation of signals from the west along the shelf edge wave guide. This is critical in order to understand the timing of the response and the fate of the upwelled and downwelled waters.

2. Assess the impact of pack-ice and landfast ice on the nature and amplitude of the upwelling/downwelling.
3. Determine the stability characteristics of the shelfbreak jet and document the frequency of eddy formation.
4. Quantify the cross-stream fluxes of mass, heat, salt, and momentum at several locations along the ABS in order to help gauge the degree of permeability of the oceanic boundary.

Meeting these objectives will enhance our understanding of the mechanisms and timing by which water and properties are exchanged across the ABS shelfbreak, and the impact that this transfer has on the stratification, circulation, and residence time of the shelf.

Approach

We recommend that a series of four moorings be deployed along the length of the ABS shelfbreak, from Barrow Canyon to roughly 144°W (blue squares in **Figure 4.2.8**). It is imperative that the moorings sample the full water column from the seafloor to the underside of the ice, measuring hydrographic properties, water velocity, sea ice properties, and bottom pressure. The placement of moorings in **Figure 4.2.8** is motivated in part by the previous SBI fieldwork and the modeling results of *Pickart et al.* (2010). This configuration should be sufficient to sort out the propagating versus local components of the wind-driven response, and determine if the western ABS is fundamentally different from the eastern ABS in this regard. We note that the 5th mooring in **Figure 4.2.8** (green square), while considered part of the array, is provided at no-cost to the program. This mooring (located at 152°W) is part of the Arctic Observing Network (AON) funded by the National Science Foundation.

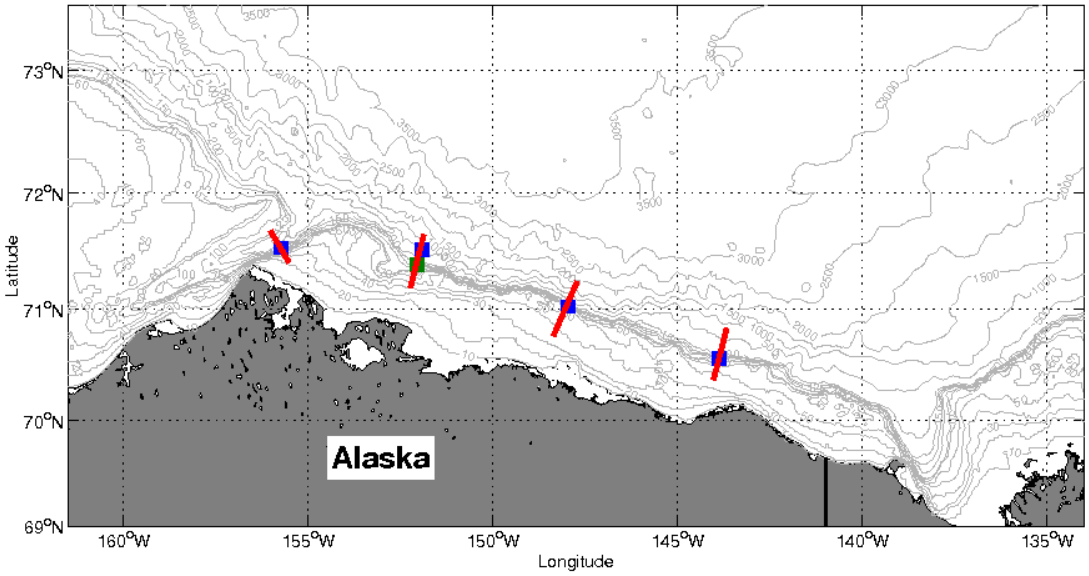

Figure 4.2.8. Proposed fieldwork for the oceanic boundary of the ABS. The moorings are denoted by squares. The blue squares represent the 4 moorings proposed here, and the green square marks the currently funded AON mooring. The red lines are the proposed CTD sections. The black line denotes the US-Canada land border.

Each mooring will contain the following components: (1) A tandem of two hydrographic profilers will sample the full water column. A McLane Moored Profiler (MMP) will measure from the seafloor to the depth of the top float (40m), and an Arctic Winch profiler will sample from the top float to the underside of the ice (see Section 2.5 for a description of the Arctic Winch). Together, these instruments will provide vertical profiles of temperature, salinity, dissolved oxygen, turbidity, and pH at 2m resolution. Present power constraints are such that the MMP can sample up to 12 times per day, and the Arctic Winch once per day. (2) An upward-facing Workhorse 300 KHz ADCP will be located on the top float, and an upward-facing Longranger 75 KHz will be situated near the bottom of the mooring. This configuration provides vertical profiles of water velocity at a resolution of approximately 5m, every hour. The Workhorse ADCP will also measure the ice velocity. (3) An upward-looking sonar on the top float will provide a timeseries of ice thickness once per hour. (4) A bottom pressure gauge will be mounted at the base of the mooring to provide information about the mass field. (5) Finally, two SeaBird MicroCats will be included on the mooring (one on the top float and one beneath the bottom stop of the MMP) to provide calibration information for the moored profilers.

This configuration of instruments has been used successfully in the past in the ABS. The timeseries returned from the array in **Figure 4.2.8** will allow us to meet the objectives discussed above, providing a first-ever three-dimensional view of the ABS shelfbreak. The array will deployed for 1 year, as there are strong seasonal variations in the atmospheric forcing and upstream conditions. During the deployment cruise, CTD sections will be occupied at each mooring site (red lines in **Figure 4.2.8**). These are required to optimally place the moorings in the center of the shelfbreak current (the CTD data provide useful calibration information as well).

The total length of the program is 3.5 years, starting in January. In the first half-year the moorings will be fabricated and the instruments prepared. The array will be in the water from year 0.5 to year 1.5. From year 1.5-2.5 the data will be calibrated and processed, and standard products will be constructed. During this time the pertinent satellite ice concentration data and meteorological fields will be assembled and put into useable form. The bulk of the scientific analysis will take place in year 2.5-3.5. The mooring deployment and recovery cruises will be 20 days in duration, with Dutch Harbor as the port.

There are several additions that would enhance this program. These include (i) A modeling study of the type presented in *Pickart et al.* (2010). This is a semi-idealized numerical simulation to help flesh out the underlying physics and better interpret the observations. (ii) Investigation of the high-resolution meteorological ETA model fields in the ABS region. This NCEP forecast model has 12 km resolution which captures the flow distortion due to the Brooks Range. (iii) Adding 3 additional moorings to the 152^{o}W location in order to fully resolve the shelfbreak jet. The value of such cross-stream resolution was demonstrated during the SBI experiment, but there were significant shortcomings in that program. Most notably, the Arctic Winch technology did not yet exist; hence the upper part of the water column was not measured. This left significant holes in the interpretation of the data. Budgets for these additional program components can be provided upon request.

Budget (approximate costs)

YEAR 1. Mooring preparation and deployments, hydrography cruise planning,

**Personnel*	
Senior Personnel (2 man-month)	
Technical Personnel (18 man-months)	
TOTAL	$252,355
**Travel*	
Massachusetts-Alaska for cruise planning and cruises	$46,260
Commodities	
Misc. supplies for moorings	$100,000
Equipment	
3 Arctic Winches	$360,000
300 kHz Workhorse ADCP	$52,600
75 kHz Workhorse ADCP	$105,000
ASL Upward looking Sonar	$129,600
Seabird bottom pressure recorder	$45,600
Seabird MicroCats	$27,260
*OVERHEAD (50% indirect costs) $214,270	
Total YEAR 1:	**$1,372,285**

YEAR 2. Mooring recovery, CTD collection, data analyses

**Personnel*	
Senior Personnel (2 man-month)	
Technical Personnel (14 man-months)	
TOTAL	$225,882
**Travel*	
Massachusetts-Alaska for cruise planning and cruises	$49,867
**Contractual Services and Commodities*	
Cruise supplies	$3,374
Calibrations	$23,490
*OVERHEAD	$190,950
Total YEAR 2:	**$493,563**

YEAR 3. Data analyses meetings

**Personnel*

Senior Personnel (3 man-month)	
Technical Personnel (9 man-months)	
TOTAL	$152,016
**Travel*	
Massachusetts-Alaska for cruise planning and cruises	$7,476
*OVERHEAD	$132,589
Total YEAR 3:	**$292,581**

YEAR 4. Data analyses, meetings, publication costs

**Personnel*	
Senior Personnel (3 man-month)	
Technical Personnel 1 man-months)	
TOTAL	$73,584
**Travel*	
Massachusetts-Alaska for technical meetings	$8,092
**Contractual Services*	
Publication costs (reports and journals)	$10,000
*OVERHEAD	$64,181
Total YEAR 4:	**$156,207**
Estimated Total Project Cost:	**$2,314,636**

4.3. THE EASTERN BOUNDARY: exchange with the Mackenzie Beaufort Shelf.

Statement of the Problem

The eastern boundary of the ABS is influenced by westward spreading of shelf and slope waters from the Mackenzie Beaufort Sea shelf. The Mackenzie shelf is subject to the massive (~12,000 m^3 s^{-1} on annual average) discharge from the Mackenzie River (**Figure 4.3.1**). This discharge is strongly seasonal with the peak in early June being ~35,000 m^3 s^{-1} before gradually dwindling to ~5,000 m^3 s^{-1} through late fall and winter. However, the winter discharge is not negligible, but isof the same magnitude as the peak Colville River discharge in summer (**Figure 4.4.1**). In addition, the Colville and the other arctic rivers that empty directly onto the ABS shelf cease flowing from November through May whereas the Mackenzie maintains a steady discharge.

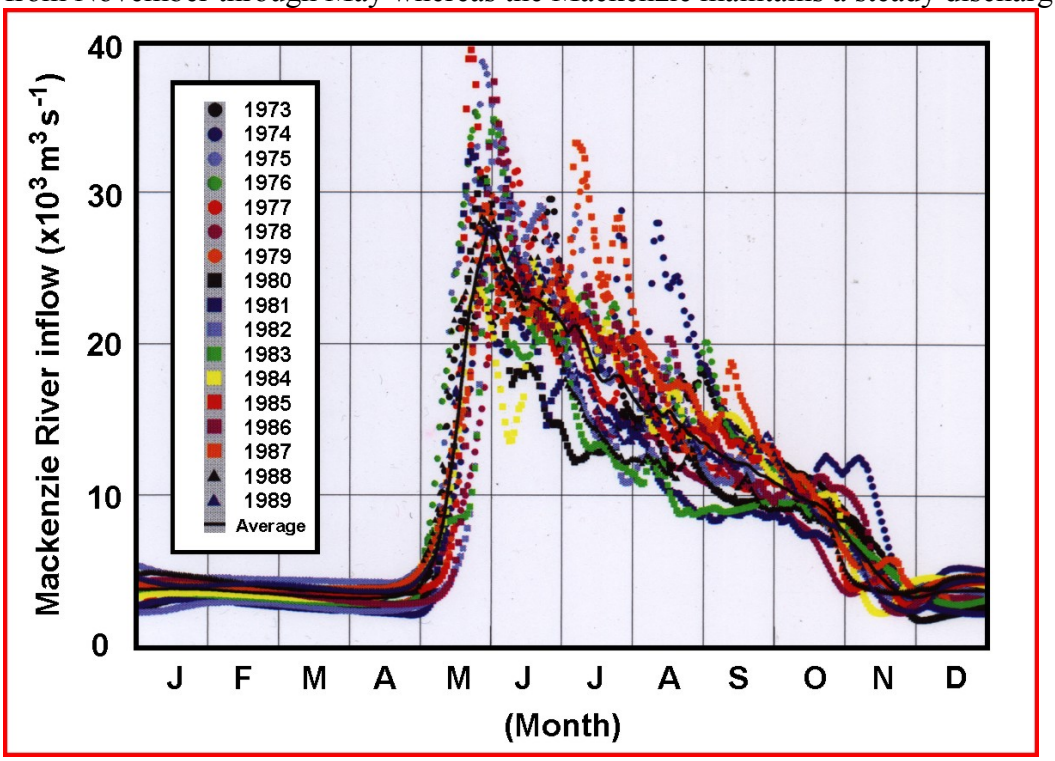

Figure 4.3.1. Daily (symbols) and mean daily (solid black curve) Mackenzie River discharge, 1973-1989. (Figure courtesy of R. Macdonald.)

In summer, the Mackenzie River discharge establishes a broad (>80 km), thin (~10 m), warm, dilute plume that results in a strongly stratified shelf (**Figure 4.3.2**). The strong stratification inhibits vertical mixing by winds. Under the influence of the prevailing northeasterly winds the plume drifts westward (**Figure 4.3.3**) and may substantially influence the retreat of sea ice over the eastern ABS shelf and slope. Indeed, a review of satellite imagery indicates that summer ice retreat over the ABS shelf first begins along the eastern boundary due to the apparent influence of the plume. Since this retreat involves both the the landfast and pack ice, the eastern ABS shelf will respond differently to wind-forcing than the ice-covered regions farther west. The influence of the Mackenzie shelf is not only confined to summer. For example, *Weingartner et al.* (2009) show that westward winds associated with fall storms are often sufficiently strong to carry Mackenzie shelf water along the entire extent of the ABS.

It is not known if any Mackenzie plume waters spread westward in winter beneath the landfast ice. *Macdonald and Carmack* (1991) suggest that most of the winter river discharge is ponded inshore of the stamukhi zone. Nevertheless the edge of the landfast ice is porous and could deliver winter discharge onto the shelf.

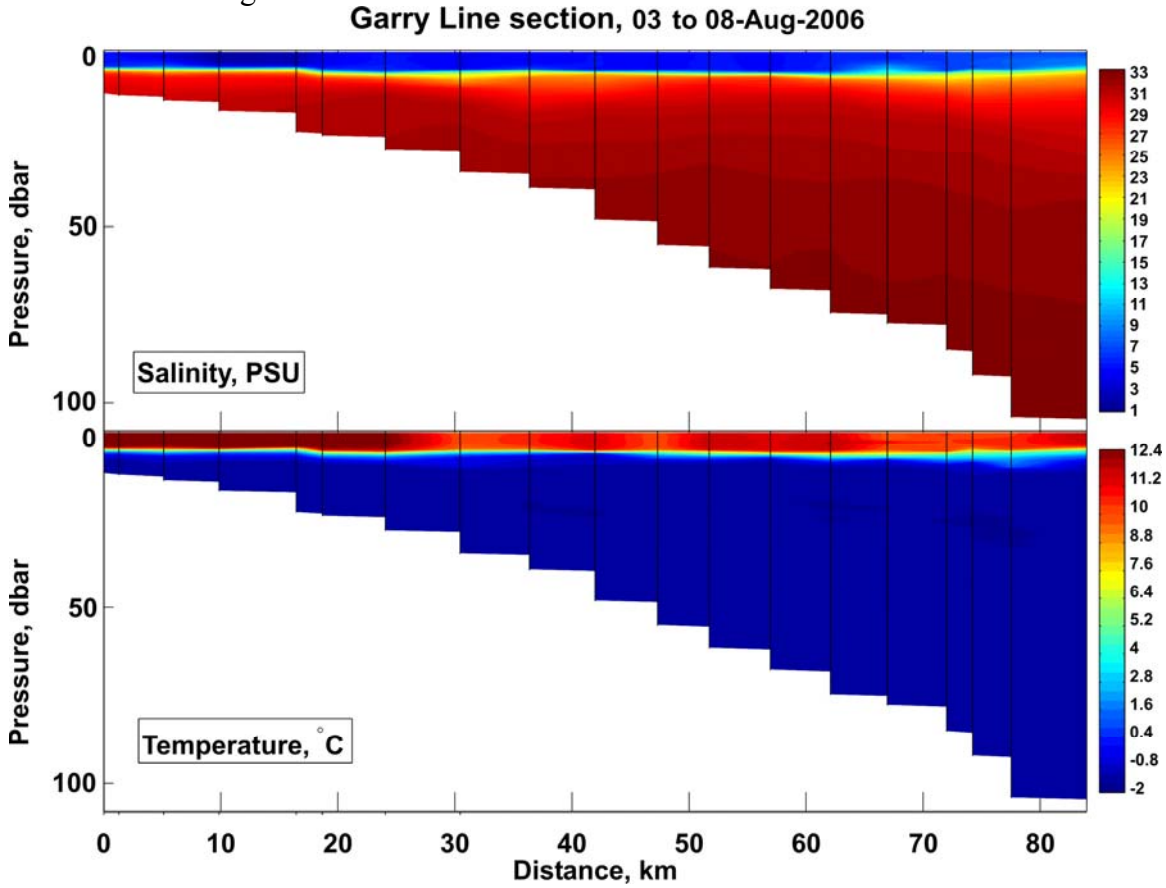

Figure 4.3.2. Cross-shelf distribution of salinity (upper) and temperature (lower) over the Mackenzie shelf in August 2008. (Courtesy of W. Williams).

Although the plume is modified due to lateral and vertical entrainment as it spreads, it remains strongly stratified, implying that the eastern ABS shelf and slope may be more strongly stratified than the western and central ABS (*Aagaard,* 1984; *Macdonald et al*., 1999), especially in summer and fall. Consequently, the wind-forced response (including upwelling and downwelling) of the eastern ABS shelf and shelfbreak are likely different from the responses over the central and western ABS. We also expect that the lateral boundaries of the plume are enveloped by strong, shallow fronts in which strong, but shallow, current jets are embedded. These fronts are prone to instabilities that generate meanders and eddies (as suggested in **Figure 4.3.3**), which could induce cross-plume (and cross-shelf) dispersion.

The eastern boundary of the ABS shelf is also close to Mackenzie Canyon, which is a prominent upwelling region (*Kulikov et al.,* 1998, *Williams et al.,* 2006). That upwelling, forced by wind and influenced by topography, is important in bringing slope waters onto the Beaufort shelf. It is also thought to impact biological production by transporting nutrient-rich waters (*Williams et al.,* 2006) which subsequently drift westward under the influence of the winds (**Figure 4.3.4**).

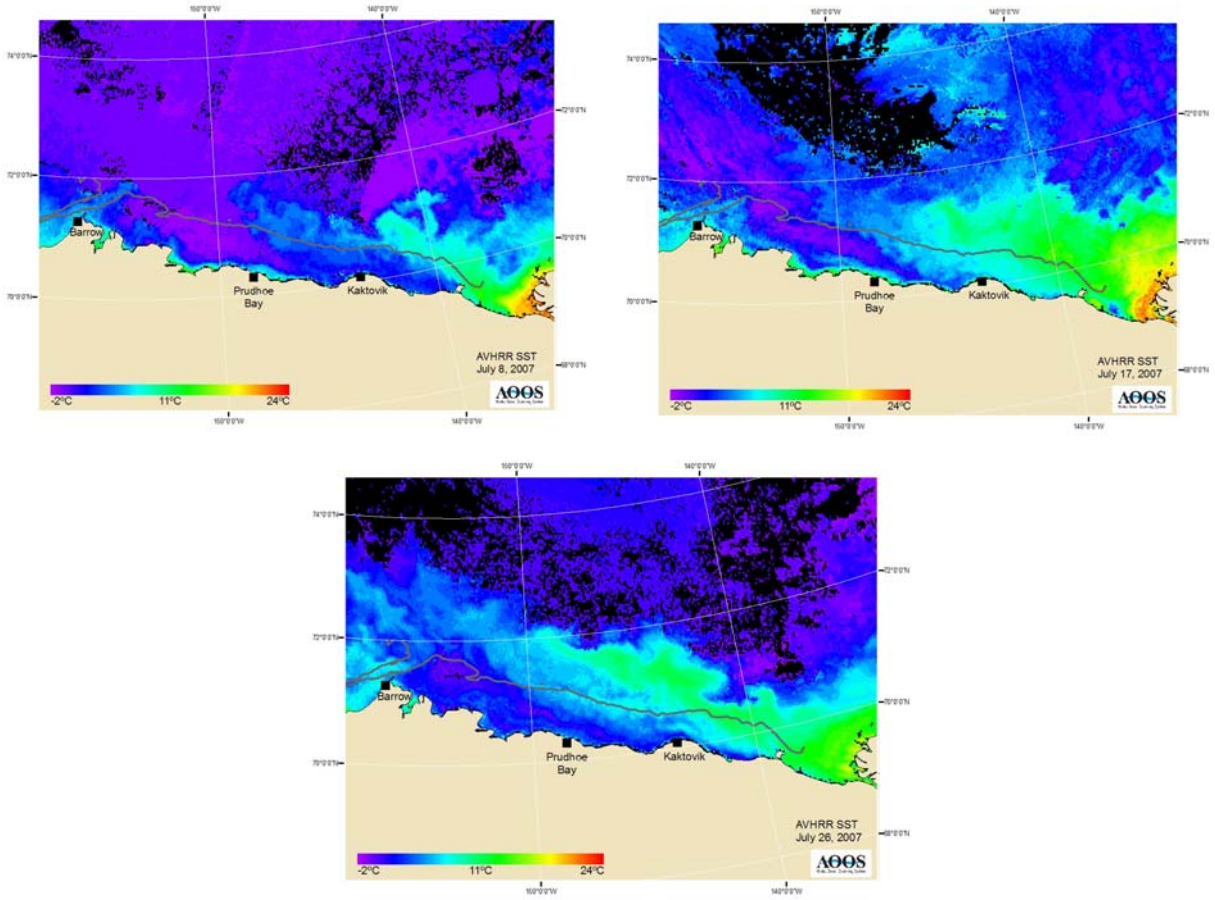

Figure 4.3.3. An series of satellite infrared images from the ABS and Mackenzie shelf showing the westward spreading of Mackenzie shelf waters in July 2007. Black areas are clouds, blue is ice, and yellow and orange denote the spreading plume.

It appears that the head of the Mackenzie Canyon and the region west of Herschel Island are important bowhead foraging areas in fall (**Figure 4.3.5;** *Moore et al, 2000*; *Harwood et al*., in press). However, bowheads feed primarily on copepods in the eastern ABS (*Lowry et al.,* 2004), whereas bowheads feeding in the western ABS mainly consume euphausiids (*Ashjian et al.* 2010).

Finally, the fate of the eastward flowing shelfbreak jet (section 4.2) is unclear. **Figure 4.3.6** is a composite of mean currents within 10 m of the bottom in the Chukchi Sea and at about 100 m depth along the Beaufort shelfbreak. (Note that **Figure 4.3.6** depicts the mean *subsurface* circulation and so differs from **Figure 4.1.3**, which illustrates the inferred *surface* circulation around Barrow under relatively weak southerly winds.) The vector distribution suggests that the ABS jet extends eastward to at least 145^{o}W whereas the flow along the Mackenzie shelfbreak is westward. If this is the case then the along shelfbreak flow is clearly convergent. Hence the continuity of the shelfbreak flow is uncertain based on existing measurements. (Some caution should be exercised in interpreting this figure because the data used in the compilation were collected in different years and the location of the moorings on the Mackenzie shelfbreak may not captured the eastward flow. However, the simple model discussed by *Spall et al.,* (2008)

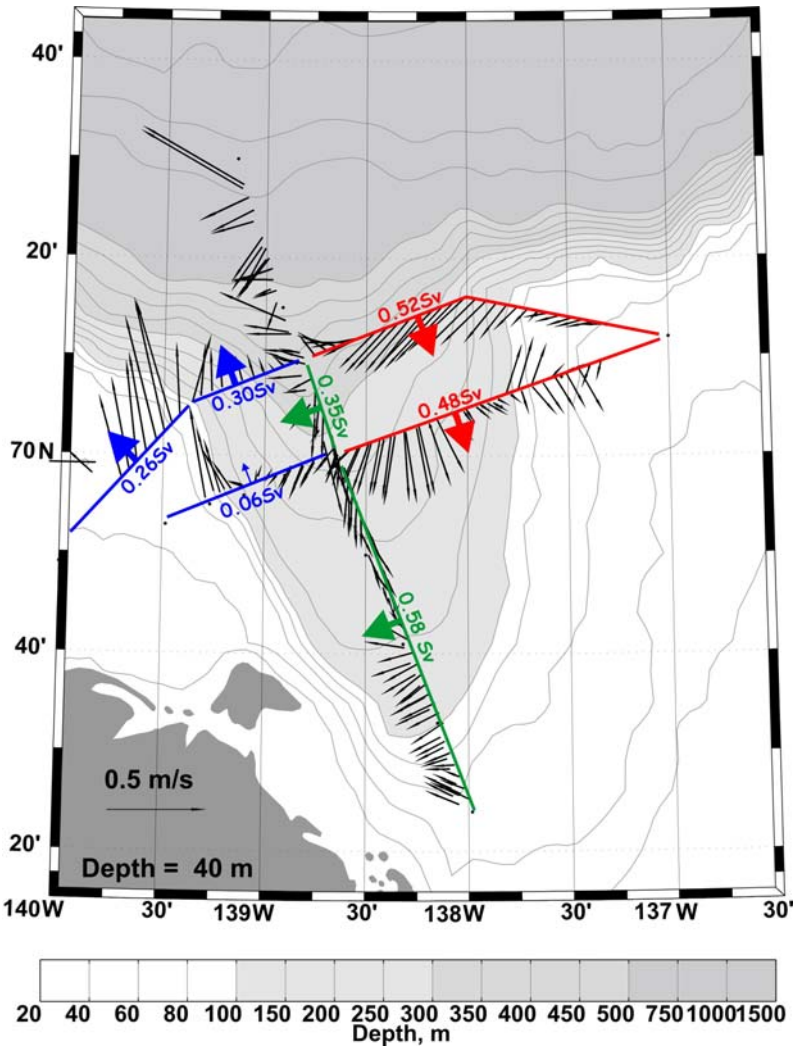

Figure 4.3.4. Vectors (and transports) obtained from a vessel-mounted ADCP survey over Mackenzie Canyon in the eastern Beaufort shelf. Note the inflow along the eastern flank of the canyon, westward flow at the head of the canyon and northwestward flow along the west side of the canyon. This upwelling flow event advected slope waters from ~200 m depth into the canyon. (From *Williams et al.*, 2006).

suggests that the wind distribution over the Beaufort Gyre could, in fact, give rise to along-shore changes in the shelfbreak flow field, including a reversal in the eastern Beaufort.) If in fact the shelfbreak flow is convergent, then much of the mass contained in this current must be expelled laterally (most likely into the basin). The convergence must also be associated with a dramatic alteration in the mean vorticity structure of the shelfbreak and slope, so that cross-shelf exchanges in the eastern ABS may be quite different than those to the west.

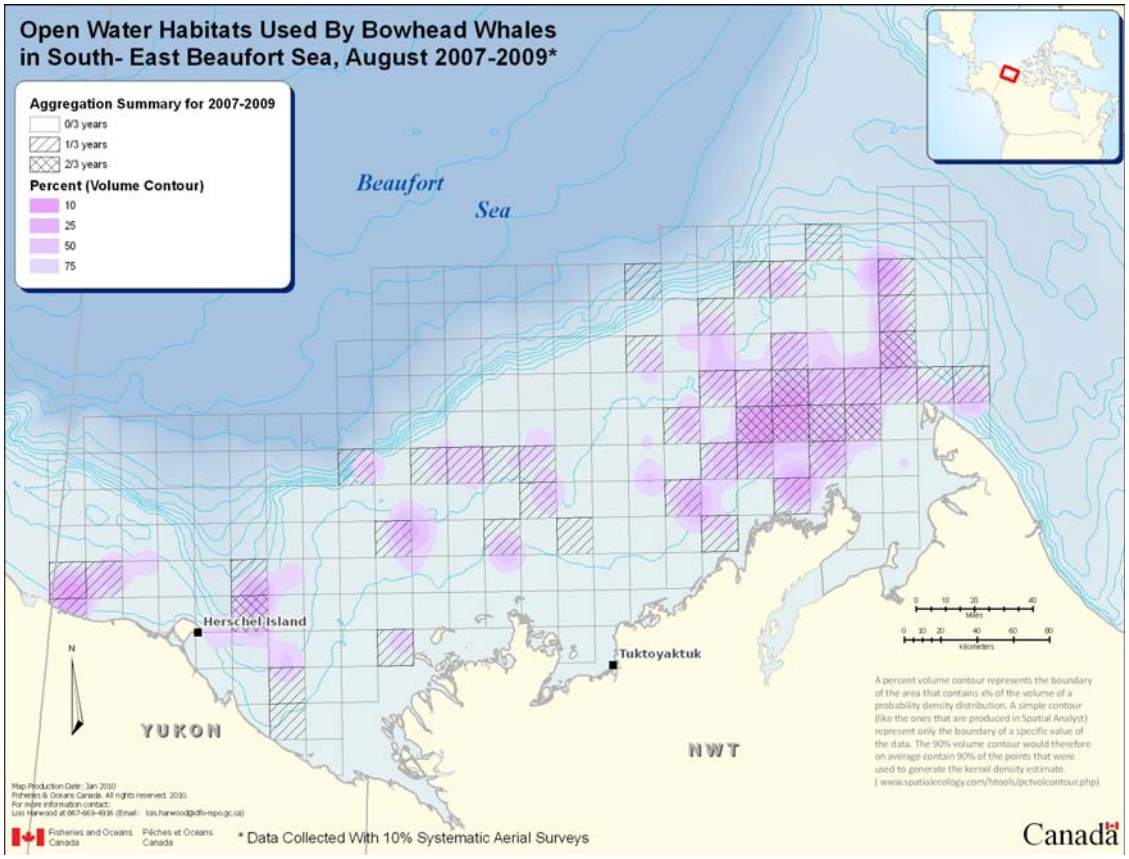

Figure 4.3.5. The distribution of bowhead whales over the Mackenzie Beaufort shelf in August 2007-2009. (From *Harwood et al*., in press)

Review of previous work

The authors are aware of no recent work in this region other than that described above.

Need for information

The eastern ABS shelf and shelfbreak appear to be quite different from the western and central ABS due to the influence of dilute Mackenzie shelf waters (including the Mackenzie plume), upwelling in Mackenzie Canyon, and possible convergence in the shelfbreak flow field. Hence, the eastern ABS may be mechanistically different in terms of its response to both along- and cross-shelf exchanges. However, there is a comparative dearth of information from the eastern ABS. Consequently, we are not in a position to outline a detailed set of circulation studies at this time. These may in fact be warranted in the future, but recommendations on where and how best to make such measurements should be discussed after completing a preliminary survey of the eastern ABS. We thus recommend that preliminary surveys be conducted to guide the development of future studies.

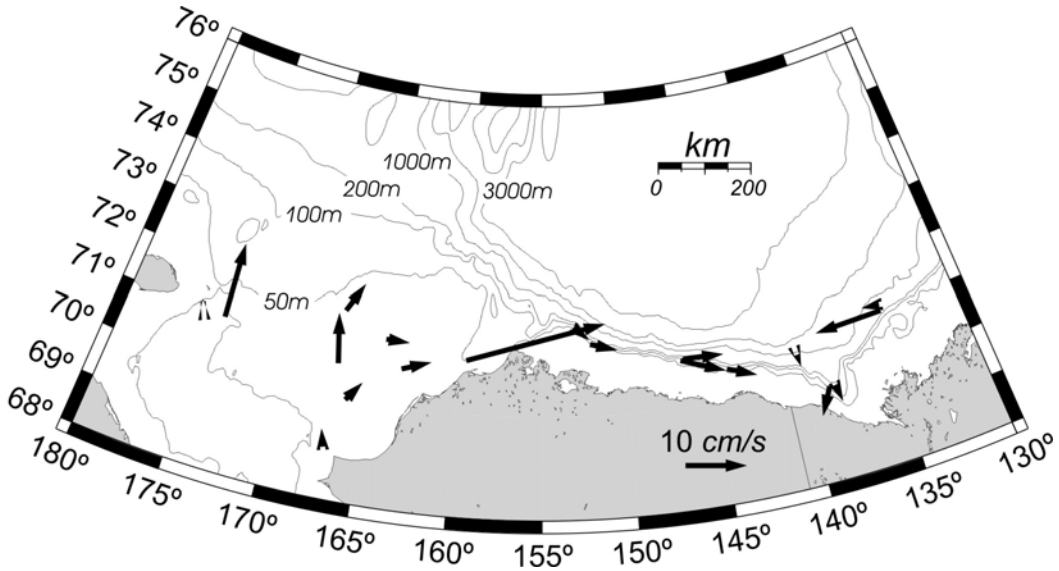

Figure 4.3.6. Composite record-length mean currents from current meters ~10 m above bottom in the Chukchi Sea and at ~100 m depth along the Beaufort Sea shelfbreak (from *Weingartner,* 2006).

Study Goals

The preliminary surveys should assess:

1. The hydrographic and velocity structure of the shelfbreak and slope;
2. The hydrographic structure of the inner and outer shelf in summer, and;
3. a geochemical survey to determine if Mackenzie plume water penetrates westward on the inner shelf in winter.

Data from the first two objectives would be used for comparison with hydrographic data from elsewhere on the ABS. In aggregate, the results would guide future studies and provide a better basis for determining how these should be conducted.

Approach

Although the first two objectives should be attempted coincidentally, logistics may not permit doing so. Over the next three years the NSF-funded Arctic Observing Network (AON) program will have a vessel operating in the Beaufort Sea (Chief Scientist, Pickart) upon which eastern ABS boundary sampling may be possible. Alternately, the CGC *Sir Wilfrid Laurier* transits through the area in summer and returns in mid-fall. The return trip would permit CTD sampling at that time (*Carmack,* pers. comm.). These relatively deep-draft vessels are required for the outer shelf and slope sampling and they could sample inshore to about the 30 m isobath. A smaller vessel, working in August, could sample inshore and to the shelfbreak, but cannot work in these waters after early September. The third goal can be achieved as a separate program and its logistics are unique. At this time it seems possible to combine the inshore work from a small vessel, with the AON-supported offshore work, if this an eastern boundary survey is conducted , then we urge this approach. However, we feel that the goals of the preliminary survey will not suffer greatly if uncoordinated.

The first goal consists of adding three additional shelfbreak transects to the oceanic boundary survey (Section 4.2 and **Figure 4.2.8**). Those additional transects along with the two easternmost transects of **Figure 4.2.8** are shown in **Figure 4.3.7**. The transects include a section along ~141°W, a dogleg section across the western and eastern walls of Mackenzie Canyon and a third section along 136°W. These high resolution CTD sections would determine how the shelfbreak hydrographic structure changes moving eastward and if the eastward-flowing shelfbreak jet disintegrates somewhere along the eastern boundary of the ABS. The sampling here should also include geochemical samples for $\delta^{18}O$ and barium (Ba) following *Macdonald et al.* (1999) since this combination, along with salinity, provides an unambiguous matrix that allows discriminating the dilute Mackenzie plume from dilute sea ice melt water. (Note that the sampling for $\delta^{18}O$ and Ba is straightforward since the analyses require only about 10 ml for each measurement and no special shipboard handling is required.). The first goal budget assumes time is available on the AON cruise, but we indicate the approximate costs if carried out on the *Laurier.*

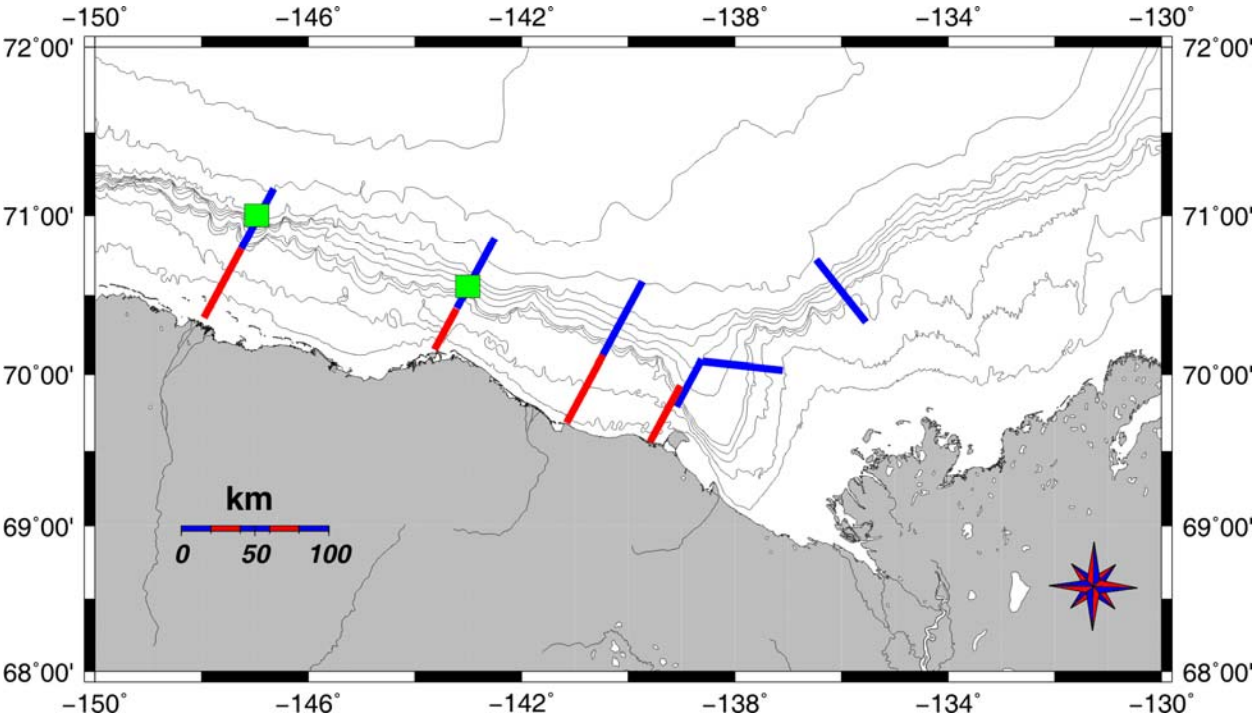

Figure 4.3.7. CTD/geochemical sampling transects in the eastern ABS. Blue transects are the shefbreak/slope transects and include those along about 147 and 143°Wshown in **Figure 4.2.8**. The red transects are the inshore extension of the offshore transects. Green squares are mooring locations discussed in Section 4.2.

The second goal would be addressed by an August ship survey that includes a CTD, water sampling (for $\delta^{18}O$ and Ba), and the deployment of satellite-tracked drifters. This survey would begin north of Herschel Island along the western wall of Mackenzie Canyon (where satellite imagery suggests that the Mackenzie plume is flowing northwestward). Sixteen satellite-tracked CODE-type drifters (drogued at 1 m) would be deployed along this transect. The drifters record temperature (and can be equipped with conductivity sensors for salinity) with GPS positions

determined half-hourly. Drifter data is downloaded daily via Service ARGOS, and available in near realtime via a website. (An example of this approach in a Bering Sea study is at: http://mather.sfos.uaf.edu/drifters/AYKSSIdrifters/index.html.). Our prior experience is that these expendable drifters would easily function through October unless crushed by ice.

Additional transects would extend from the coast offshore to about the 80 m isobath and tie into the offshore transects. Each transect (including roundtrip travel time along the transect) would require about 12 hours and include stations spaced at 4 km intervals. Geochemical sampling would occur at every other station and be limited to surface, mid-depth, and bottom. The results should indicate the proportion of Mackenzie River water over the shelf in the eastern ABS and, in conjunction with other data from the western and central ABS would allow determining the magnitude of along-shelf differences in hydrographic structure over the ABS. The budget for the second goal assumes an August survey that extends across the shelf and is uncoordinated with the outer shelf work.

The approach for the third goal consists of bi-weekly sampling offshore of Kaktovik through winter (after the landfast ice has set up). We suggest that the residents of Kaktovik conduct this sampling and that it include obtaining a vertical CTD profile between the 10 – 15 m isobaths along with surface and bottom water sampled for Ba and $\delta^{18}O$. The sampling is simple and straightforward and would simply determine the presence or absence of Mackenzie River water in winter as far west as Kaktovik.

Budget (approximate costs)

GOAL 1. The costs for the CTD processing and analyses are included in the budget for the oceanic boundary (section 4.2) and this budget assumes shiptime costs are absorbed by the NSF-AON project. Additional costs are for the collection and analyses of the Ba and $\delta^{18}O$.

**Personnel*	
Senior Personnel (1 man-month)	$18,000
**Contractual Services:*	
$\delta^{18}O$ analyses (400)	$12,500
Barium analyses (500)	$12,500
Shipping	$500
Commodities	
Sampling vials (1,000)	$1,000
*OVERHEAD (50% indirect costs)	$22,500
Total GOAL 1:	$67,000

If conducted from the *Sir Wilfrid Laurier* we suggest that 4 days of shiptime be budgeted at $28000/day.

GOAL 2. August CTD and geochemical sampling on eastern ABS

**Personnel*	
Senior Personnel (2 man-month)	$36,000
Technical Personnel(3 man-months, includes mob/demob & field pay)	$24,000
Analysis man-months(2 man-months)	$26,000
**Travel:*	
Anchorage-Deadhorse, lodging in Deadhorse	$3,800
**Contractual Services*	
Shipping	$4,500
Miscellaneous field gear and hardware	$5,000
Service ARGOS satellite communication fees	$12,000
$\delta^{18}O$ analyses (400)	$12,500
Barium analyses (400)	$12,500
Charter vessel (16 days, includes mob, food and fuel, crew)	$118,380
CTD post-calibration	$1,000
Commodities	
Sampling vials (1000)	$1,000
16 satellite-tracked drifters	$84,000
Satellite imagery	$7,500
Laptop computer (w/ software)	$2,500
Publication costs	$3,000
Equipment	
SBE-25 CTD with transmissometer and 6-place Rosette Sampler:	$49,000
Winch with conducting wire	$9,500
*OVERHEAD (50% indirect costs):	$176,800
Total GOAL2:	$589,000

GOAL 3. Winter-weekly CTD and geochemical sampling from Kaktovik

**Personnel*	
Senior Personnel (1 man-month)	$18,000
Technical Personnel(1 man-month)	$8,000
Local hire (for sampling; 3 man-months)	$32,000
**Travel:*	
Anchorage-Kaktovik, lodging in Deadhorse	$2,800
**Contractual Services*	
Shipping	$1,000
Miscellaneous field gear and hardware	$7,500
$\delta^{18}O$ analyses	$1,000

Barium analyses	$1,000
Snow-machine rental and fuel costs ($250/day x 21)	$15,750
CTD post-calibration	$1,000
Commodities	
Sampling vials	$150
Ice augurs and spare bits	$2,000
Laptop computer (w/ software)	$2,500
1.7 l Niskin bottles (3 @ $500)	$1,500
Publication costs $1,000	
Equipment	
SBE-19 portable CTD	$17,000
*OVERHEAD (50% indirect costs):	$47,575
Total GOAL 2:	$159,800

4.4. THE COASTAL BOUNDARY: under-ice river plumes.

Statement of the Problem

Coastal freshwater discharge from North Slope rivers affects the circulation and stratification of the inner shelf (at least) during spring breakup and throughout the summer (and possibly early fall). However the structure and dynamics of river outflow plumes are poorly understood on the ABS. While studies conducted on mid-latitude shelves have shed considerable light on the behavior of buoyant discharge plumes in these settings, the applicability of these studies to the ABS remains unclear for four primary reasons. First, North Slope rivers release nearly 90% of their annual discharge over a two week period during the spring freshet(as exemplified by the Colville River discharge in **Figure 4.4.1**), in sharp contrast to the more slowly varying discharges characteristic of temperate regions. Hence the results of steady state models of

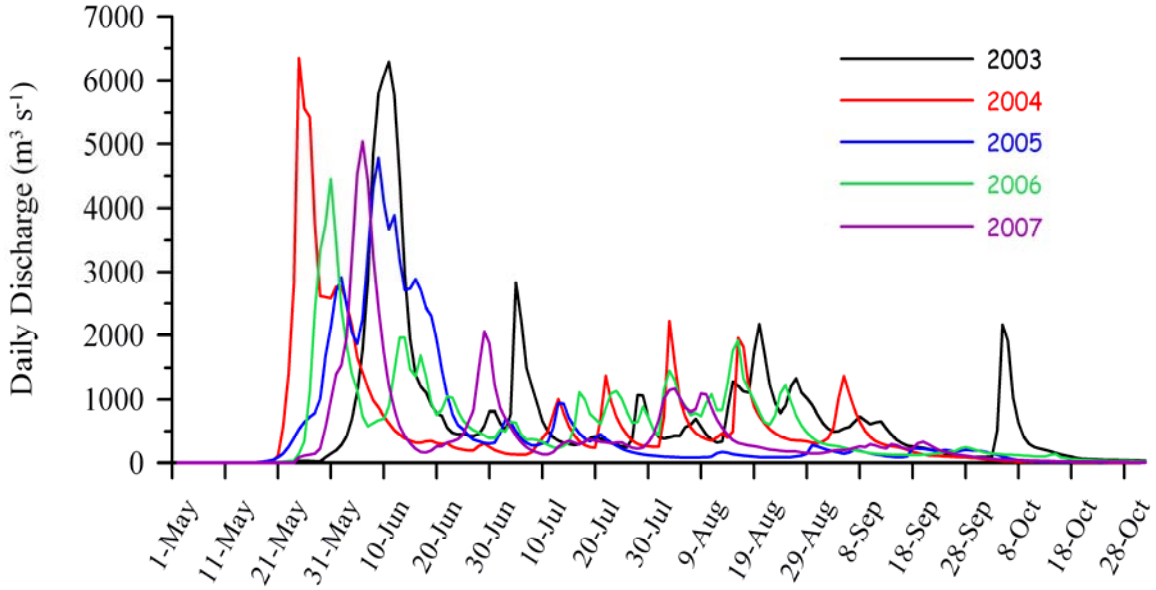

Figure 4.4.1. 2003-2007 annual discharge cycles for the Colville River (data from USGS).

plume behavior on temperate shelves may not apply in the ABS. Second, the plumes formed by the outflow of North Slope rivers spread seaward beneath landfast ice. Consequently the plume's dynamics will be influenced by frictional coupling to the bottom of the landfast ice. How this frictional coupling affects the plume's motion is unknown. Third, the buoyant plume is spreading into an ambient shelf whose stratification is rapidly changing due to ice melt. As evident in **Figure 4.4.2**, the time scale of the spring freshet (~10 days) is only slightly shorter than the time scale associated with decay of the landfast ice along the coast (~20 days). Fourth, the landfast ice insulates the plume from the direct action of the surface wind stress and tides in the ABS are feeble (~2 cm s^{-1}) so that wind-induced Ekman transport and the turbulent energy for mixing are both negligible. Consequently the plume is highly stratified (**Figure 4.4.3**), and may be frictionally decoupled from shelf waters beneath the plume.

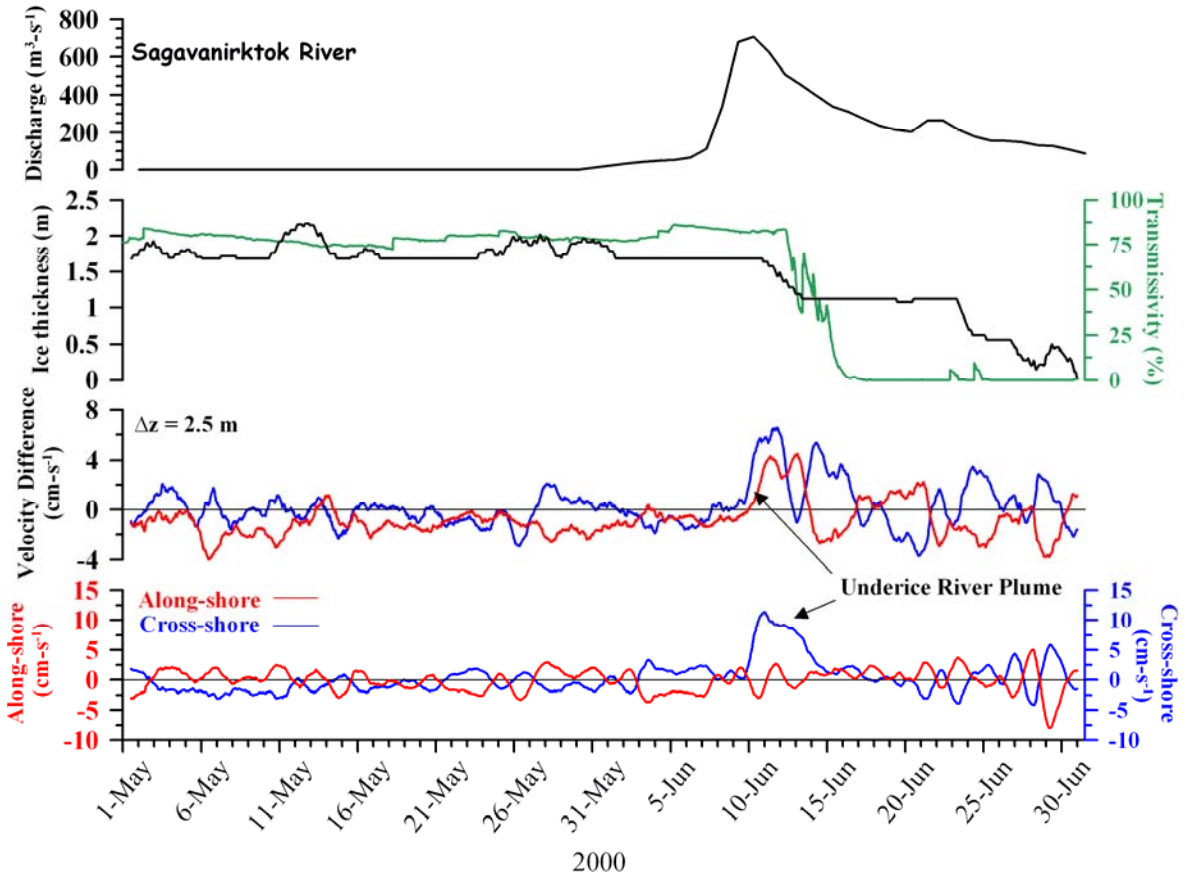

Figure 4.4.2. May through June time series of (from top to bottom) Sagavanirktok River discharge, ice thickness (black), transmissivity (green), cross- and along-shore velocity shear, and cross- and along-shore velocities. Along-shore (cross-shore) components are red (blue).

We also note that during the spring freshet, river waters have high suspended sediment concentrations. *Trefry* (2009) suggests that ~80% annual flux of total suspended sediments, particulate organic carbon (and associated metals) and ~50% of the annual riverine influx of dissolved organic carbon and trace metals is associated with the freshet. Hence the fates of these materials are intimately linked to dispersal of the under-ice plume. Much of the particulate material appears to settle out beneath the plume and then be re-suspended in fall by storms and freezing.

Review of previous work

Aside from the work summarized above we are aware of only one suite of studies that examined under ice river plumes. *Ingram* (1981) and *Ingram and Larouche* (1987) reported on observations from the Great Whale River Plume in Hudson Bay and *Li and Ingram* (2007) addressed mixing within this non-rotating plume as it spread beneath the ice. The observations indicated that under-ice river plumes spread over 500–2000 km^2 in horizontal area, compared to 50 km^2 in open water (for a similar discharge). They also found that the under-ice plumes are 2-3 times thicker in the vertical compared to plumes formed from similar discharges in open water.

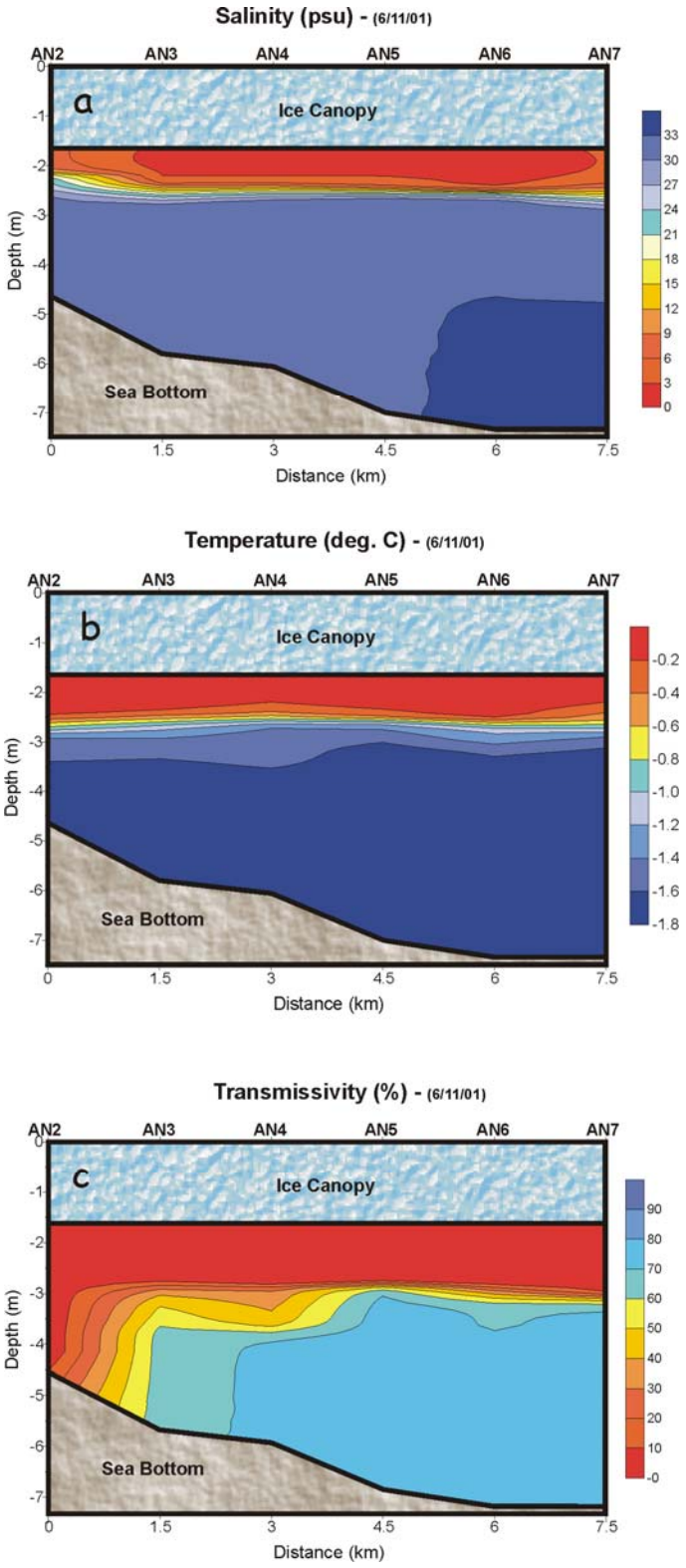

Figure 4.4.3. Cross-shore sections of salinity (top), temperature (middle), and transmissivity (bottom) across Stefansson Sound on June 11, 2001 (from *Weingartner et al.*, 2009).

Li and Ingram theoretically examined aspects of the plume with a 2-D model and ascribed some of these differences to frictional coupling with the ice and to tidal processes. However, their model did not include the Coriolis influence and it is doubtful that the tidal processes so prominent in Hudson Bay play a role in the ABS.

Weingartner et al. (2009) found that the largest cross-shore velocities observed during the October through June landfast ice season were associated with the under-ice river plume. Typical under-ice cross-shore velocities were 1-2 cm s^{-1} ice except when an under-ice river plume was present. However, when an under-ice river plume was present the cross-shelf velocities increased to about ~10 cm s^{-1} and remained at that level until the ice broke free from the coast and started to freely drift. This suggests that river waters and their associated burden may be dispersed broadly over the inner shelf. However, their current measurements were made from a bottom-mounted ADCP so that side lobe contamination from the ice-water interface likely obstructed measurements from within much of the under-ice plume. *Weingartner et al.* (2009) computed the offshore spreading scale (derived by *Yankovsky and Chapman* [1995] under steady-state, inviscid conditions) to the Kuparuk discharge during the spring freshet and estimated that the offshore extent of the plume would be ~25 km. They estimated that the propagation speed of the plume should allow it to attain this distance within ~2 days. On the other hand, Trefry (pers. comm.) did not detect Kuparuk River water beneath the landfast ice beyond about ~15 km offshore, although his survey was limited in scope and duration. *Kasper and Weingartner* (in prep. b) use idealized numerical models that include frictional coupling between the landfast ice and an under-ice river plume to show that the *Yankovsky and Chapman* [1995] spreading scale does not hold for under-ice plumes. The effects of ice-ocean friction are illustrated in **Figure 4.4.4** for a pulsed discharge of 6000 m^3 s^{-1} (similar to the Colville River discharge) without ice (Panel A), with the landfast ice edge 26 km offshore (Panel B), and the landfast ice edge 80 km offshore (Panel C). The model results indicate that under ice plumes spread much further offshore when ice is present than when absent.

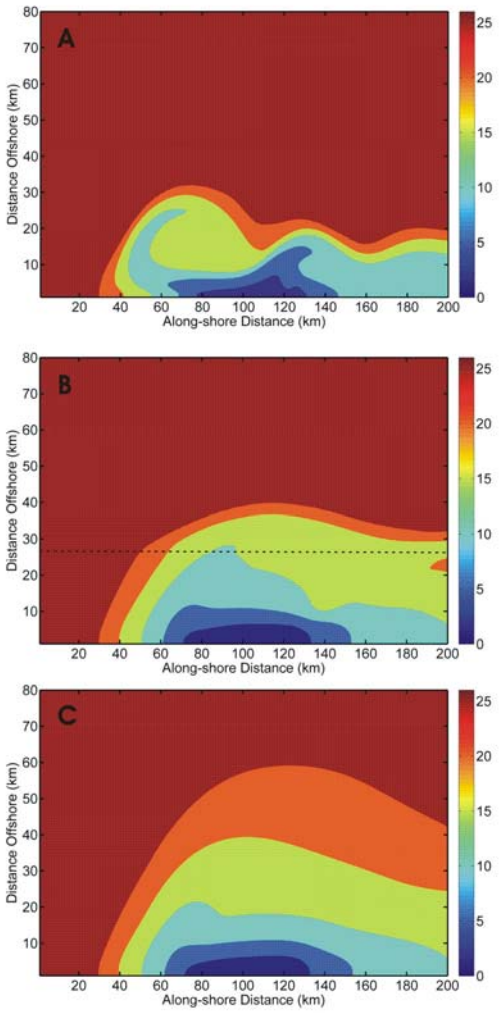

Figure 4.4.4. (A) Density anomaly, Δρ (ρ-1000, kg m $^{-3}$), at the surface after thirty days (no ice cover). (B) Δρ at the surface after thirty days for an ice cover that covers the area inshore of the 20 m isobath. The ice edge is marked by the dashed line ~26 km from the coast. (C) Δρ at the surface after thirty days for an ice cover that covers the entire domain.

Need for information

The characteristics of under-ice plumes in the ABS are poorly known both theoretically and observationally. However, the plumes represent an important element in the seasonal cycle of this shelf since they affect the transport of water and dissolved and suspended materials, which may influence the ecosystem on the inner shelf (*Dunton et al*., 2006) and the dispersal of contaminants. For example, under-ice plumes are a potential vehicle for discharged oil (whether spilled at sea or carried into the ocean by rivers). In addition to floating, the oil blobs may bond to particulate material and thus settle out along the path of the plume only to be re-suspended and then transported by currents later in the season or incorporated into the landfast ice during freeze-up. Since remnants of these plumes extend into summer they also affect the stratification and thus the response to wind-forcing on the inner shelf. That response is asymmetric being strongly sheared under westward (upwelling-favorable) winds and weakly sheared under

eastward (downwelling favorable) winds. Numerical models of the ABS must properly simulate the seasonal evolution of stratification in order to reflect properly the circulation on this shelf.

Study Goals

We suggest observations be conducted to determine the three-dimensional and time varying structure of under-ice plumes on the ABS. Ideally the observations should determine the:

1. velocity structure across and within the plume;
2. offshore and lateral spreading of the plume;
3. the changes in time of the temperature, salinity, and suspended materials over the water column within the region influenced by the plume and offshore of the plume.

In aggregate these objectives will determine how an impulsively initiated under-ice river plume will propagate over the inner shelf beneath the landfast ice and into a receiving fluid whose stratification is likely changing concurrently.

Approach

We recommend that the field work be focused offshore of the Colville River beyond the barrier islands. The Colville River, which is routinely gauged, is the largest river draining Alaska's North Slope and its offshore waters are relatively unimpeded by barrier islands. Access to the field site is achieved at Oliktok Point and logistical support may be available from an offshore artificial island. The field work consists of both through-ice current meter moorings (suspended beneath the ice) and a CTD grid (**Figure 4.4.5)** over a ~60 x ~40 km. The moorings would be deployed along a single transect within the middle of the grid beginning near the 10 m isobath and extending offshore to about the 30 m isobath. Each mooring would consist of a 1200 or 600 kHz instrument (depending upon total water depth) operating in pulse-coherent mode (Water mode 12 on Teledyne [RDI] ADCPs) to acquire data useful for measuring both slowly-varying currents and turbulence within and across the plume. Within a few meters of the mooring we would install a string of 2 - 3 SeaCats (depending upon water depth) equipped with temperature, salinity, pressure, and transmissivity. At least one SeaCat would be deployed close to the bottom of the ice (within the plume) and the other (1 or 2) would be beneath the anticipated plume depth. The SeaCat string would be supplemented with a string of ~25 HOBO thermistor strings. These relatively cheap thermistors would allow vertical resolution of the temperature distribution across the plume. Based on the temperature structure in **Figure 4.4.3**, we suggest placing thermistors about 25 cm apart across the upper 4 - 5 m of the water column and 1 – 2 m apart below 5 m.

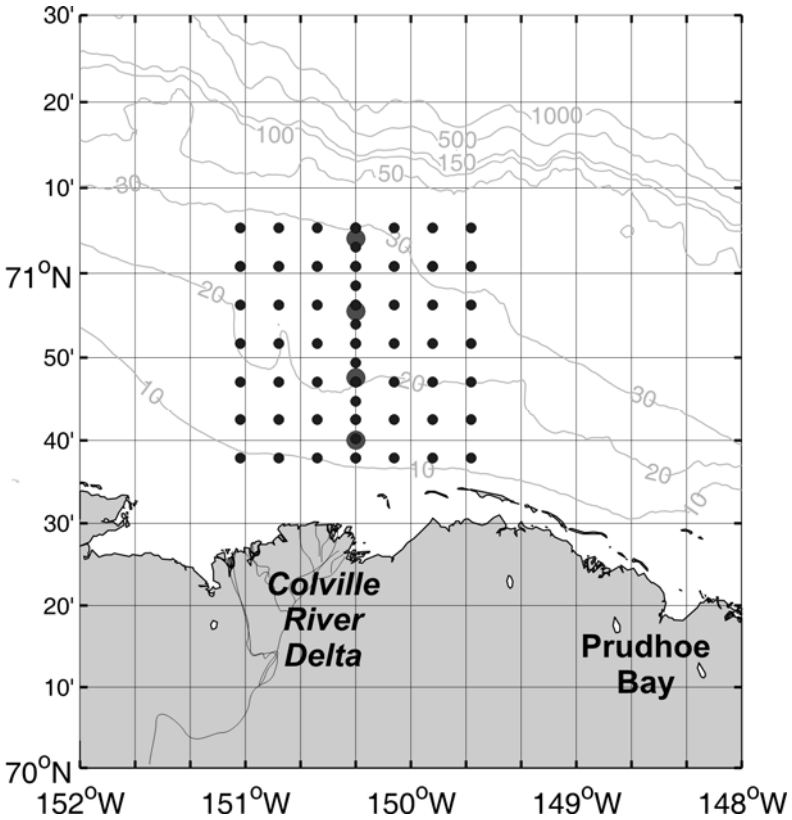

Figure 4.4.5. Example sampling grid for downward-looking through-ice moorings (large solid circles) and CTD grid (smaller circles) offshore of the Colville River Delta.

We suggest a two-year field program. In Year 1, we would occupy the CTD grid once shortly after river breakup. (CTD sampling would be timed with the discharge, which is available in realtime from USGS and/or from ConocoPhillips). The results from the Year 1 survey will refine the Year 2 locations of the moorings and CTD stations. In Year 2, we would deploy the moorings in late April/early May (before river breakup) with recovery occurring in late June (after peak discharge but before the landfast ice breaks up). At the time of mooring deployment, we would conduct a broad scale CTD survey in order to determine the temperature and salinity structure of the shelf prior to breakup. We anticipate relatively uniform temperature-salinity conditions in late April so this CTD survey may be fairly broad and occupy a subset of the regular CTD grid. (From a modeling perspective, the pre- breakup conditions would constitute the initial conditions of the inner shelf.) We would then occupy the more extensive CTD grid constructed from the Year 1 results. CTD sampling along the mooring transect would occur every couple of days, with other stations sampled less frequently.

Sampling options:

1. The through-ice ADCPs will not be able to sample to within 25 cm of the underside of the ice. If MMS desires velocity measurements closer to the ice a current meter (for example Nortek Acoustic Doppler Velocimeter) capable of making point measurements could be added to the sampling scheme. This option would add about $25000 to the total project cost.
2. MMS may want to consider combining airborne electromagnetic (AEM) sea-ice thickness measurements (Section 4.5) with the under-ice survey. The AEM has the

capability of detecting under-ice plume extent and so could map both the horizontal (but not vertical) extent of the plume as well as ice thickness. By combining the AEM survey with the CTD sampling, ground-truthing of the AEM could be obtained.

3. Although not strictly within the provenance of the workshop discussion, results obtained since that meeting suggest that the landfast ice may be a vehicle by which oiled sediments can be transported over the ABS shelf. As discussed by *Eicken et al.* (2005) and *Weingartner et al.* (2009) considerable sediment is incorporated into the landfast ice, particularly during freeze-up. The sediment may then be transported by the landfast ice during break-up or released, in place, to the seabed upon melting. Since sediments can adsorb oil and oil appears to migrate into the ice matrix, the drift and decay of landfast ice provides a means by which oiled material may be re-distributed over the ABS. The recommended under-ice plume study could accommodate an additional effort to examine the fate of landfast ice (and its attendant sediment load) at breakup. The additional work involves sampling (via ice cores) the landfast ice for sediment content during the early May and June CTD surveys. This would provide an estimate of the total sediment load within the landfast ice in the survey region. During the June survey, the field party would deploy satellite-tracked drifters on the ice during the CTD survey. The drifters would begin transmitting upon deployment on the ice and continue transmitting once the ice melted and the drifters were released into the water. We recommend using ~15 drifters in such a study. In addition, we would include a remote sensing component to assess ice concentration and retreat. Remote sensing data (AVHRR, MODIS) would also allow for upscaling of these measurements to the regional scale, building on past work demonstrating the utility of visible-range and near-infrared satellite imagery in mapping sediment-laden ice extent (*Huck et al.,* 2007). The costs for this project are provided below. This effort would be conducted in Year 2 of the under-ice-plume survey.

Budget (approximate costs)

Year 1 (October 1 – September 30)	
**Personnel*	
Sr Personnel(1 man-month)	$18,000
Technical Personnel	
(5 man-months, includes mob/demob & field pay)	$40,000
Local guide/polar bear guard (1 man month)	$11,000
Analysis man-months(1 man-months)	$13,000
**Travel:*	
Anchorage-Deadhorse, P/U rental, lodging in Deadhorse	$6,000
Field camp (if oil industry support is not available)	$6,000
**Contractual Services:*	
Snow machine rental: (3 @ $120/day x 10)	$3,600
Shipping/storage fees	$5,000
CTD Calibration	$2,000
Permits	$1,000
Commodities	
Toboggans, misc. hand tools, safety gear, etc.	$17,000
Equipment	
SBE-25 CTD with transmissometer or equivalent	$33,000
*OVERHEAD (50% indirect costs)	$59,400
Year 1 Total:	**$211,200**

Year 2 (October 1 – September 30)	
**Personnel*	
Sr Personnel (1.5 man-months)	$27,000
Technical Personnel (12 man-months)	$96,000
Analysis man-months (2.5 man-months)	$32,500
Local guide/polar bear guard (2 man month)	$22,000
**Travel:*	
Anchorage-Deadhorse, P/U rental, lodging in Deadhorse	$15,000
Field camp (if oil industry support is not available)	$20,000
**Contractual Services*	
Snow machine rental: (4 @ $120/day x 40)	$19,200
Shipping/storage fees	$10,000
CTD Calibration	$1,000
Permits	$1,000
**Commodities*	
Ice drill (steam)	$3,000
Misc. field gear, mooring hardware	$10,000
600 HOBO thermistors$6,000	
Equipment	
4 600 kHz Teledyne ADCPs	$100,000
10 SeaBird Seacats with transmissometer	$90,000
*OVERHEAD (50% indirect costs):	$131,400
Year 2 Total:	**$584,400**
Year 3 (October 1 – September 30)	
**Personnel*	
Sr Personnel(2 man-months) $36,000	
Analysis man-months(8 man-months)	$104,000
**Travel:*	
Fairbanks-Anchorage (4 days per diem)	$2,000
National Meeting (5 days per diem) $5,000	
**Contractual Services*	
Publication costs	$5,000
*OVERHEAD (50% indirect costs): **Year 3 Total:**	**$228,000**
Total 3-year cost:	**$977,20**

Additional costs associated with the tracking of landfast ice through breakup.

**Personnel*	
Sr Personnel (0.5 man-months)	$9,000
Technical Personnel (3 man-months)	$24,000
Analytical Personnel (2.5 man months)	$32,500
**Travel:*	
Anchorage-Deadhorse, lodging in Deadhorse	$3,800
**Contractual Services*	
Service ARGOS satellite communication fees	$35,000
Shipping/storage fees	$1,000
Miscellaneous field gear and hardware	$5,000
**Commodities*	
10 satellite-tracked drifters	$30,000
Satellite imagery	$7,500
*OVERHEAD (50% indirect costs)	$73,900
Total:	$221,700

4.5. THE SEA ICE BOUNDARY: thickness and under-ice topography

Statement of the Problem

Substantial, large-scale reductions have been observed in Arctic sea ice extent over the past two decades (**Figure 4.5.1**). Direct observations are required to track ice variability and provide data to improve models and understand the ocean circulation in ice-covered waters.

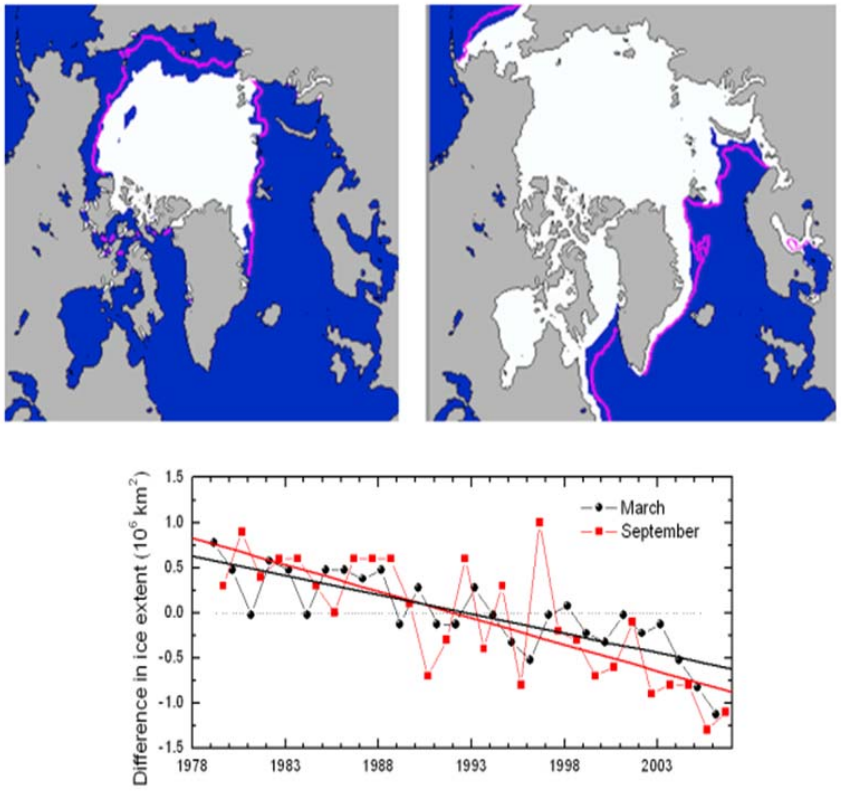

Figure 4.5.1 Sea ice extent in September and March 2006 (shown in white). The magenta lines indicate the median minimum and maximum extent of the ice cover for the period 1979-2000. The March 2006 maximum was a record minimum for the period 1979-2006 (Courtesy of National Snow and Ice Data Center, NSIDC). Bottom panel shows time series of the difference in ice extent in March (maximum) and September (minimum) from the mean values for the time period 1979-2006. Based on a least squares linear regression, the rate of decrease in March and September was 2.5% per decade and 8.9% per decade, respectively.

Results based on passive microwave satellite data (*Fowler et al.*, 2004; *Rigor and Wallace,* 2004) suggest that since 1983 the oldest ice in the Arctic is being lost due to an increase in sea-ice melt as well as exported through Fram Strait. If the old ice is indeed being lost, then changes in ice thickness distribution can be expected to be significant. *Maslanik et al.* (2007) merged ice thicknesses computed from the ICESat satellite to produce a proxy ice thickness data set from 1982 to the present that clearly shows the persistent loss of perennial ice cover over this period of time indicating that the oldest and thickest ice is being lost from the central Arctic ice pack

(**Figure 4.5.2**). Much of the oldest ice has already disappeared and 58% of the multi-year ice now consists of 2 and 3-year ice compared with 35% in the mid-1980s.

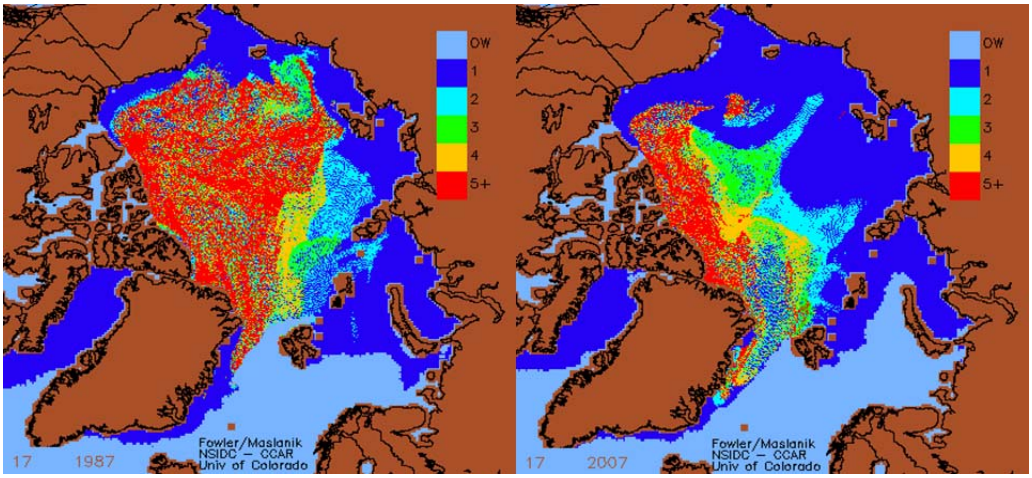

Figure 4.5.2. Left. 1987 ice age inferred from satellite tracking Right:. 2007 ice age inferred from satellite tracking. (Maslanik, pers. comm.)

Long-term observations over all seasons are needed because thermodynamic processes tend to dominate the annual cycle while dynamic processes dominate interannual cycles (*Walsh et al*., 1985).

Studies of the ABS could benefit from being constrained by knowledge of the sea ice thickness distribution. Satellite measurements that quantify the sea ice thickness distribution could help in this regard, but this is no longer possible with the loss of ICESat.

If model forecasts are true, and present trends continue, less sea ice may cause shifts in the shelf circulation and its response to winds, and freezing and thawing. This in turn could lead to changes in the migration patterns of marine mammals, as well as the productivity of fish stocks and other trophic levels in the marine food chain. The ABS ice thickness in particular is critical for identifying the formation and decay rates of fast ice because this ice has historically protected the Alaska coast from erosion. Coastlines unprotected by ice suffer from extensive and rapid erosion as experienced at Shishmaref and other Alaskan villages. Direct measurements of thickness at the kilometer and smaller scale are critical to understand the dynamics of the coastal zone and inner shelf, to develop oil spill response scenarios, and for marine navigation.

While changing sea ice cover has been reasonably well-documented over the basin very little is known about the changes in the seasonal ice characteristics (particularly thickness) of the ABS shelf. Analysis of ice conditions has by necessity been mostly on a large, coarse scale, and most of the discussion has centered on findings obtained from passive microwave satellite data. Such data is typically analyzed on a 25 km grid, and is not suited for inner shelf studies (due to land contamination effects in the data) or during the summer at ice concentrations below 50% (due to signatures changing with meltwater accumulation at the ice surface).

The western Arctic (East Siberian, Chukchi and Beaufort Seas) has seen some of the most significant sea ice changes and is poised to experience increased economic activities. This

includes plans for offshore oil and gas development, increased shipping along existing transport pathways and potential expansion of tourism, fisheries and other traffic northward through Bering Strait.

Review of previous and current work

The mean ice draft in a sector offshore Alaska decreased 1.5m from the mid-1980s to the early 1990s (*Tucker et al.,* 2001) and is postulated to be related to the strength of the Beaufort Gyre and Arctic Oscillation (AO) and NAO indices (*Proshutinsky and Johnson*, 1997; *Thompson and Wallace* 1998). However, no long-term trend from 1950 to the present day in ice flux from the Arctic through Fram Strait has been found, based upon air pressure differences across Fram Strait (*Vinje*, 2001), although the 1950s and 1990s appear to be the most variable in the record. Vinje suggests that the increase in ice export through Fram Strait in the 1990s accounts for the decreasing ice thickness in the Arctic Ocean. They show that the North Atlantic Oscillation (NAO: the air pressure difference between Iceland and Portugal) correlates with ice thinning and thickening over the 50 year record. It would be useful to have a pan-arctic record of thickness to compare with pressure records to further test this idea and supplement regional studies of the ABS.

Modeling indicates that sea ice thickness will change more quickly than sea-ice extent (*Dick*, 2001). Under-ice measurements from submarines indicate a 40% decline in thickness in the central Arctic Ocean (*Rothrock et al.*, 1999, *Rothrock and Zhang*, 2005). We can see this dramatic change by comparing the satellite derived sea ice age (*Fowler et al*., 2004) from April 2007 with that from 1987 (**Figure 4.5.3**).

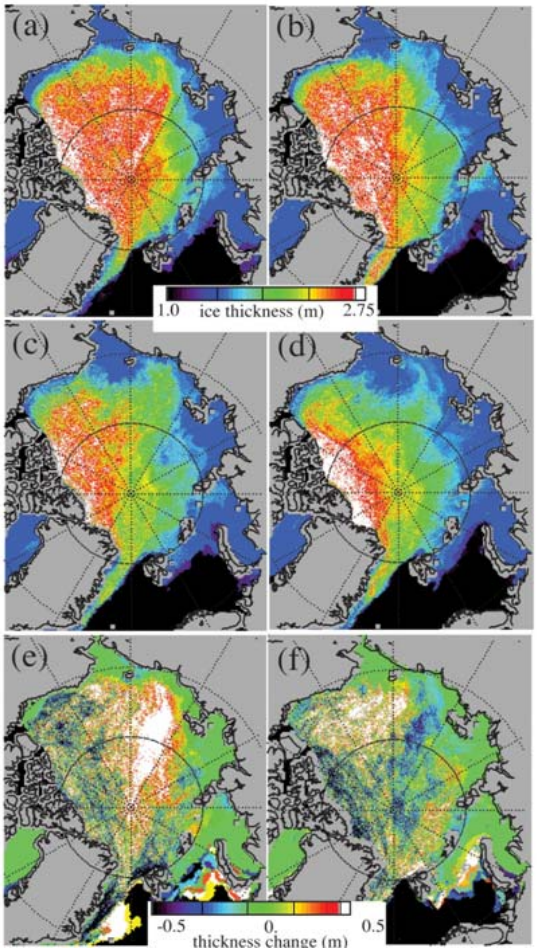

Figure 4.5.3. Mean spring ice thickness for 1982-1987 (a), 1988-1995 (b), 1996-2000 (c), and 2001-2007 (d). Mean 1982-1987 thickness minus mean 1993-1996 thickness (e) mean1993-1996 thickness minus mean 2001-2007 thickness (f).

Submarine data show extremely rapid sea ice thinning. *Rothrock et al.* (1999, 2003) analyzed the SCICEX cruises of 1993, 1996, and 1997 and compared these with autumn data from 1958, 1960, 1962, 1970, and 1976 to find that the mean ice thickness decreased by 1.3 m compared to data acquired during the 1958-1976 period. The thinning continued through the 1990s and contributed to the overall reduction in ice thickness of 0.1m y^{-1}. *Rothrock et al*. (1999) suggested two explanations for the observations: wind variations that could have exported more ice to the Atlantic, and/or less ice growth or more ice melt.

However, the locations of the submarine observations were biased toward such thinning. *Holloway and Sou* (2002) sampled their model at the submarine locations and found a 45% reduction in ice thickness, but a total ice volume loss of 12%, with 9% due to increased ice export, and 3% due to less growth or more melt. Holloway and Sou's results suggest that the cause of the ice thickness reduction is redistribution within the Arctic. Simulations by *Rothrock and Zhang* (2005) indicate that thinning was greatest over level ice while ridged ice exhibited thinning due to melt. The mechanisms by which ice mass is being depleted bear directly on the question of whether the ice pack is responding to a large-scale pervasive warming trend or to

more regionally-limited variations in atmospheric circulation (e.g., via effects on ice transport). These uncertainties regarding the true nature of ice mass loss suggest the need for direct measurements of ice thickness to assess change.

The coastal zone

One of the implications of ice redistribution is that much of the mass might be present within areas of heavily ridged and rafted ice cover. *Hibler et al.* (1974) noted this possibility, and described the importance of interannual sampling over areas of heavily ridged and rubbled ice including the coastal zone. One assessment of the need for sea ice measurements acknowledges that only two locations in the Beaufort Sea are routinely observed, that there is a need for thickness measurements at the km scale, and that the orientation and rates of formation of sea ice ridges in the ABS (and elsewhere) are unknown (*Hutchings and Bitz*, 2005). The earliest work on the ABS is from *Tucker et al.*, 1979 who showed large geographic and temporal variability in ridging intensity. However the data they acquired were heavily averaged and lacked horizontal resolution. We attempted to secure these data to examine the fine scale variations, but they are no longer available.

A review of 36 years of ice charts from the ice-covered Beaufort continental shelf shows little evidence of any trend in areal coverage although there is a small thinning trend of 0.07 m/decade based on analysis of a 12-year draft record of pack ice (*Melling et al.,* 2005). They emphasize that the knowledge of pack-ice thickness lags far behind our understanding of concentration and extent. However, ice thickness directly bears on the meachnical properties, and hence the dynamics of sea ice.

Discussions of Arctic ice thickness often begin with reference to the map derived from ice-profiling sonar draft data from the deep Arctic basin (*Bourke and Garrett*, 1987), however thickness is virtually unknown in the coastal zone seasonal ice predominates (*Melling et al.,* 2005). The development of ice-profiling sonars (ULS) in the late 1980s made possible a continuous record of point observations from the southern Beaufort Sea from 1990 (*Melling and Riedel,* 2004). How such point observations of draft from ULS compare with airborne EM thickness measurements is not known. Analysis of ice draft from ULS moored on the continental shelf of the Beaufort Sea in winter of 1990 characterized the mixture of first year and multi-year ice as having a mean draft of 3 m and ice keels with drafts up to 27 m (*Melling and Riedel,* 1995). Whether these characteristics are typical across the broader ABS continental shelf remains essentially unknown.

The Alaskan Beaufort coastal zone is ice-covered for 9 months with both drifting pack and "immobile" landfast ice that extends 20-40 km offshore. Detailed reviews of the relation between landfast ice formation and decay with bathymetry and atmospheric forcing are described by *Mahoney et al.* (2007a,b). There are times when it extends across the shelf. A schematic of the ice from the coast to offshore is shown in **Figure 4.5.4**. The duration of this ice determines the seasonal navigation window for the nearshore region. The historical variability of the navigable window (offshore of Prudhoe Bay) is large (**Figure 4.5.5**)

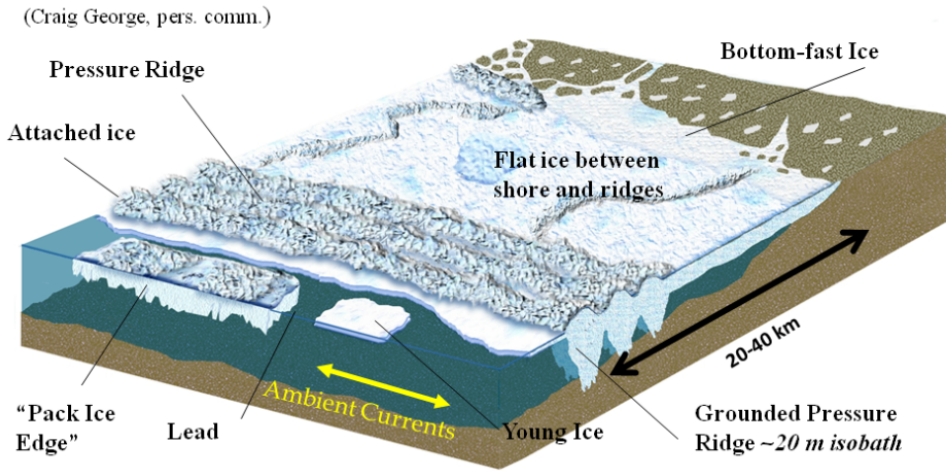

Figure 4.5.4. Schematic of sea ice from the coast to beyond the 20m isobath, a distance here of 20-40 km. (Courtesy of C. George.)

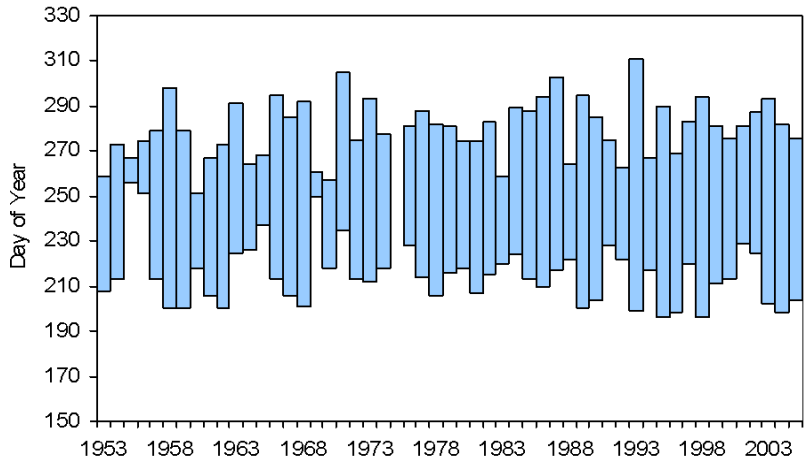

Figure 4.5.5 Opening and closing dates for navigation to Prudhoe Bay. The duration varies from 0 days (1975) to 112 days (1993). Courtesy of Drobot and Proshutinsky.

Ice thickness variability across the shelf near Prudhoe Bay is suggested by the ~45 km long ICESat-derived surface topography section in **Figure 4.5.6**. (Although useful during its lifetime, ICESat coverage was limited and it is no longer available due to the demise of the onboard laser. Moreover, the ICESat sensor was only turned on intermittently in order to conserve power, hence there are few transits of the ABS.) Sea ice thickness should now be acquired at much finer scales and closer to the coast using airborne electromagnetic measurements. Both satellite and EM measurements demonstrate an ice field with topography/thickness that is variable in both time and space. This variability implies that the surface stress distribution varies similarly with ice cover and thickness. These variations should affect the ocean circulation through frictional coupling and the blocking and channeling of flows.

Need for information

An observation program defined largely by the needs of established research and stakeholder communities is driven by a number of issues related to the seasonal and coastal ice cover in a changing Arctic. These issues include the following.

The seasonal evolution and decay of landfast ice is poorly known. Landfast ice forms rapidly in early to mid-October and upon formation incorporates substantial quantities of suspended sediment. The fate of this sediment-laden ice afterbreak–up, melting, and advection is poorly known. Oil and/or oil adsorbed onto sediment incorporated into the landfast ice matrix may be dispersed along quite different pathways than oil in water or at the ice-water interface. The under-ice topography may steer or channel flows, affect frictional coupling between the water and ice, and induce a pressure drag on the flow field acting essentially an energy sink.

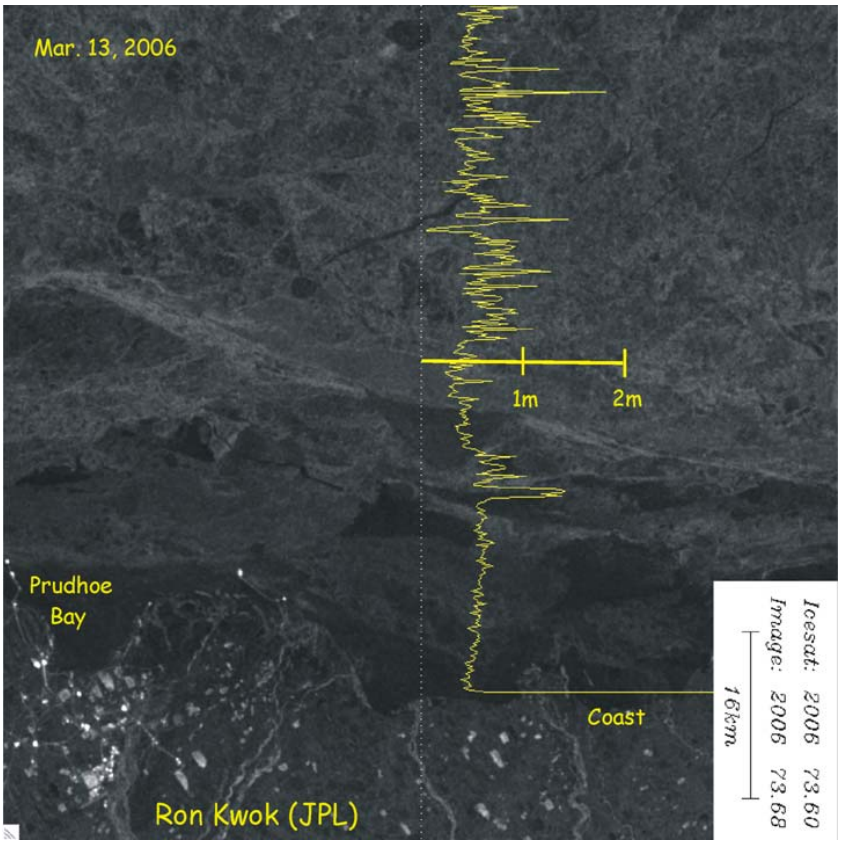

Figure 4.5.6. ICESat derived surface topography over 45km track (yellow line) over SAR sea ice imagery off Prudhoe Bay. Note transition from nearshore landfast ice to offshore packice

There appears to be little cross-shelf flow between the landfast and pack ice zones. Without detailed data, we assume that material suspended or dissolved in the water column will accumulate within the landfast ice zone throughout winter. This assumption needs to be tested since it bears on the dispersal of spills. Moreover, understanding pathways for the dispersal of under-ice plumes may depend strongly on the under-ice topography.

The under-ice topography of the landfast ice zone is almost completely unknown. At fine scales, sea ice thickness has been mapped using on-ice, sled-mounted EM sensors **(Figure 4.5.7).**

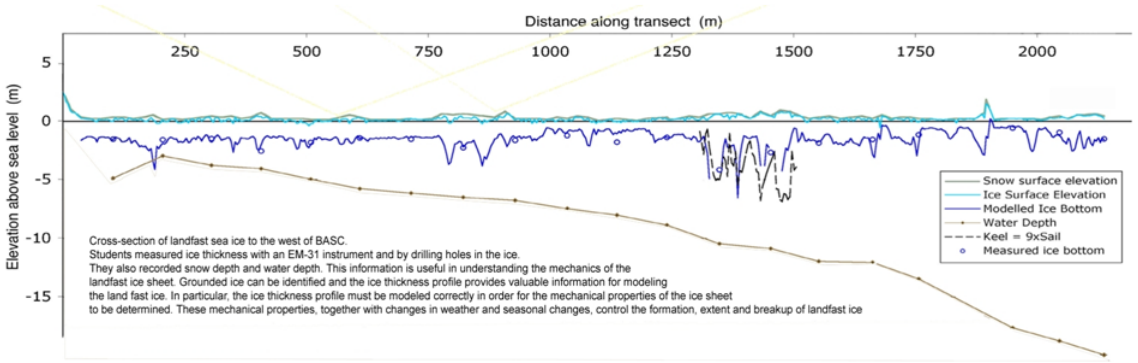

Figure 4.5.7. EM measured ice thickness along transect west of Barrow Arctic Science Consortium site. The EM-31 is dragged along the ice by walking or by snowmachine to provide high resolution thickness data.

The ice topography may be a key driver for ocean circulation and may physically trap or channel the flow. We have little idea of how the under-ice topography (or thickness) varies through time and space across the shelf, yet this is essential knowledge for engineering design purposes, to plan oil spill cleanup response, and to understand under-ice circulation. An example of airborne EM thickness transects across the shelf from a multi-year program (NSF SIZONET) is shown in **Figure 4.5.8.**

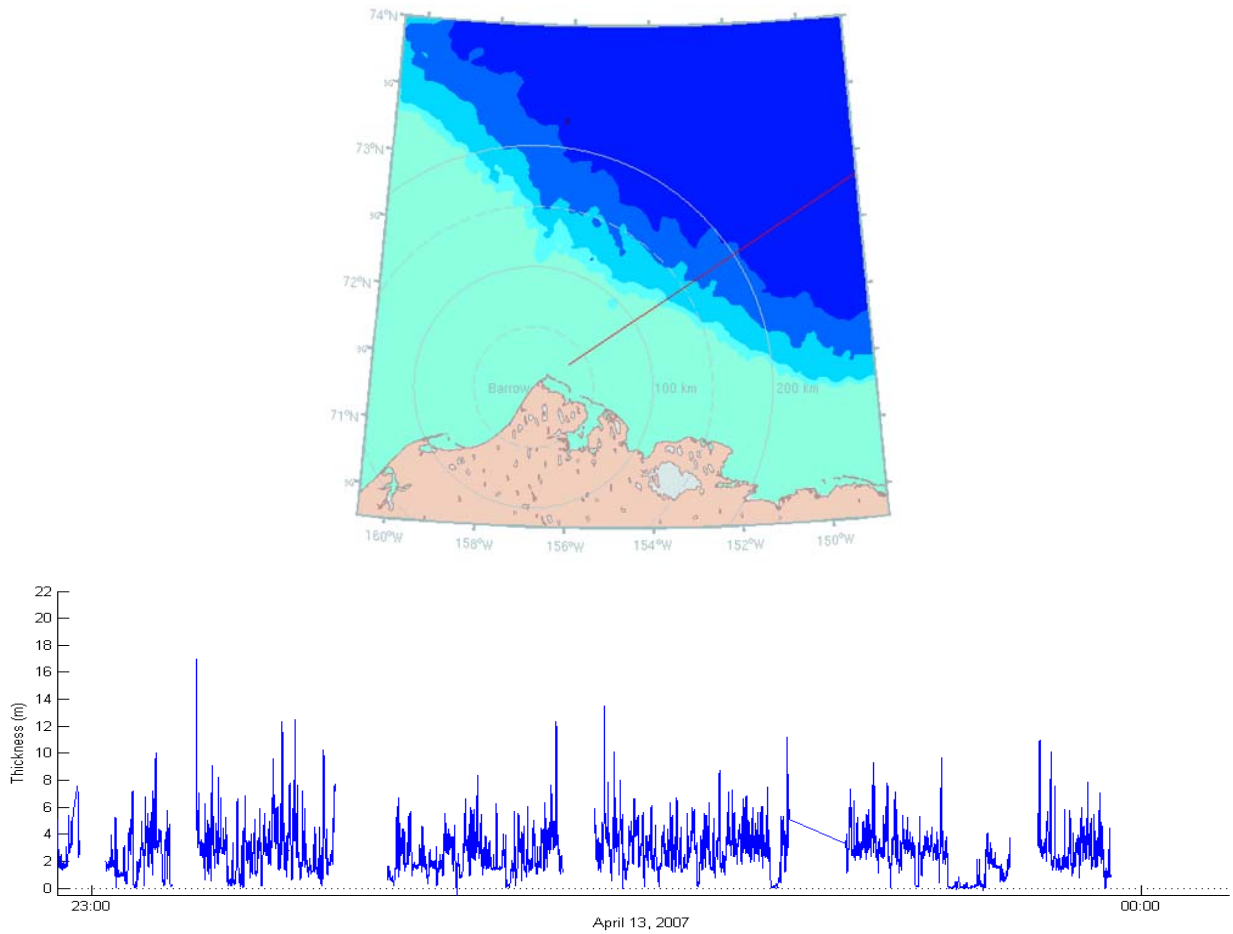

Figure 4.5.8. Flight line from Barrow, Alaska across the shelf for EM Bird sensor during NSF Sizonet program. Ice thickness (below, in blue) from April 13th, 2007. (PIs Eicken, Johnson, Perovich).

Limited measurements suggest that the cross-shore flow can be large when river plumes spread beneath the landfast sea ice during the brief period between river breakup and landfast ice breakup (~2 weeks). The cross-shelf flow can potentially carry material many kilometers offshore. Freshwater plumes may in fact be an important exception to the assumption of little cross-shelf flow discussed above. The airborne EM measurements recommended here would provide information useful to identifying where oil might collect in the event of an under-ice spill and may provide guidance on under-ice oil spill recovery approaches.

Study goals

Sea ice thickness measurements are needed:

1. In regions where seasonal sea ice forecasts are critical such as off Barrow and Prudhoe. Measurements should include sample lines across the shelf, provide existing models with thickness data, replacing the use of multiyear sea ice concentration as a proxy for ice thickness (*Drobot*, 2007) or modeled ice thickness (*Lindsey et al.,*

2007). In both cases, observations of thickness would almost certainly lead to better forecasts (*Drobot*, pers. comm.; *Rigor*, pers.comm.).

2. To provide sea ice roughness to evaluate the role of topography and roughness on channeling cross-shelf flow. This is to be coupled with oceanographic observations of flow under the ice and studies to quantify the role of sea ice in modulating upwelling and downwelling.
3. To statistically characterize in both time and space, the ice thickness distribution, ridging intensity, and ridge orientation.
4. To evaluate airborne EM work for detection and tracking of buoyant plumes. Current work indicates that airborne EM can detect buoyant plumes, but further work is needed (Holladay, pers.comm.). Roughness is also relevant to understanding the pathways of buoyant plumes.
5. For offshore mapping of sea ice thickness in areas frequented by marine mammals. The survivability of some Arctic mammals, including polar bears and seals, is tied to ice thickness and its evolution and decay. If we are to properly assess future changes in these species, additional information on ice thickness is needed. Such studies can be conducted simultaneously with many of the above suggested goals.
6. To address the new economic realities emerging, such as expanded oil and gas exploration and the possibility of economically-viable shipping (*Brigham and Ellis*, 2004). These activities are vulnerable to variations in ice thickness, and measurements would be useful to help these sectors plan their future activities.
7. To conduct routine ice tracking programs along the ABS because ice moves. Simply analyzing conditions at fixed locations may provide an incorrect view of the factors affecting the ice, especially for analyses that span multiple years. Ice velocities can be obtained using a two-dimensional cross-correlation technique applied to sequential SMMR (from 1982–1987), SSM/I (from 1987–present), AMSR (2002–present), and AVHRR (1982–present). Buoy trajectories (1982–present) can be used to create vectors, which can be merged with the satellite-derived vectors to create an interpolated daily dataset. A retrospective analysis could be completed from about 1982 onward. The ice velocity vectors are estimated by tracking displacements of features between sequences of daily composite images. Additional technical details are available in *Fowler et al.* (2004). One of the key strengths of this approach is the merging of multiple satellite and buoy observations which leads to greater accuracy and precision in ice tracking compared with other techniques based only on buoys or single satellite data. It also helps minimize errors during summer when microwave data are less useful. GPS units transmitting locations to satellite may also be useful to track specific, high interest ice floes.

The overarching goals are to map the thickness distribution, measure the gradients of sea ice thickness in the along- and cross-shore directions over the ABS, and assess whether thickness variations are isotropic or anisotropic using airborne EM sensor (flight distances are shown in **Figure 4.5.9**), and establish an ice-tracking program along the ABS. Thickness is the key unknown for the ice volume problem.

The recommended sea ice thickness measurements would be use to further establish the accuracy of airborne EM for broad-scale studies of sea ice thickness variability related to climate change. Repeat surveys or repeat long transects over key locations such as a “Barrow line” or “Prudhoe

line" will build a key time series data set of sea ice thickness (and other) measurements for future estimates of long-term variability and global climate change. These measurements will coordinate with other observations such as ice mass-balance buoys, ULS, and proposed UAV laser.

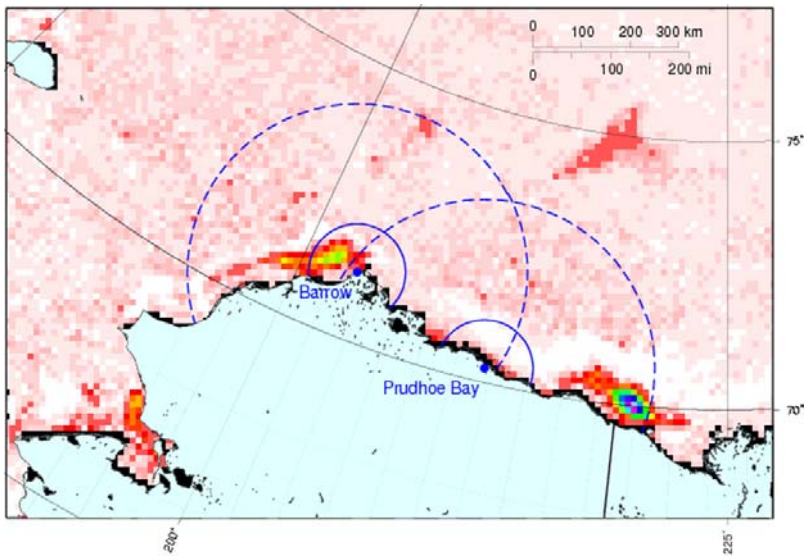

Figure 4.5.9. Helicopter flight distances from Barrow and Prudhoe Bay plotted over sea ice concentration from AMSRE.

Recommended budget (approximate) assuming quarterly sampling at one location. The below budget assumes work out of Barrow. Logistics costs of working from other sites may differ.

Year 1 (October 1 – September 30) – Organizational lead time is necessary to notify the PIC or BIRD vendor, arrange helicopter logistics, and organize field logistics. The program will acquire the sensor and complete initial training. In Barrow helicopter flights over sea ice during whaling season require permits and is accomplished through The Whaling Captains Association and the North Slope Borough. Other sites will require coordination with similar local entities.

**Personnel*	
Sr Personnel (2.0 man-months)	$39,000
Technical Personnel (6 man-months)	$48,000
**Travel:*	
Anchorage – Barrow, lodging, 2 trips for 2 people	$6,000
Anchorage to Montreal or other location for initial EM training	$5,000
Equipment	
EM PIC sensor (a 2007 Geosensors quotation for PIC, spare parts, calibration, and initial training on a BO105 was $150K. This estimate is adjusted 4% annually for price increase for 2010)	$169000

*OVERHEAD (50% indirect costs)	$49000
Year 1 Total:$316000	
Year 2 (October 1 – September 30)	
**Personnel*	
Sr Personnel (2.0 man-months)	$39000
Technical Personnel (12 man-months)	$108000
Analytical Personnel (12 man-months)	$108000
**Travel for quarterly sampling*	
Anchorage-Barrow, P/U rental, lodging for 2 for 9 days x 4 campaigns	$24000
**Contractual Services*	
(A Polar Field Services estimate for a 2010 sampling campaign with EM "Bird" out of Barrow is for 22 hours air support with 12 hours (4 days @ 3 hours) for weather at $3094 per hour.	
Flight costs (22 hrs x $3094 x 4 campaigns)	$424000
**Commodities*	
machine shop, shipping boxes, supplies, field gear	$20000
Equipment	
Computers, hard drives, backup	$8000
*OVERHEAD (50% indirect costs)	$139500
Year 1 Total: $776,500	
Years 3 and beyond (October 1 – September 30)	
**Personnel*	
Sr Personnel (2.0 man-months)	$41,000
Technical Personnel (12 man-months)	$75,000
Analytical Personnel (12 man-months)	$75,000
**Travel for quarterly sampling*	
Anchorage-Barrow, P/U rental, lodging for 2 for 9 days x 4 campaigns	$25,000
**Commodities*	
machine shop, shipping boxes, supplies, field gear	$5,000
Equipment	
Computers, hard drives, backup	$3,000
* *Subtotal*$224,000	
*OVERHEAD (50% indirect costs)	$112,000
**Contractual Services*	
(A Polar Field Services estimate for a 2010 sampling campaign with EM "Bird"out of Barrow is for 22 hours air support with 12 hours	

(4 days @ 3 hours) for weather at $3094 per hour.
Flight costs $441,000

Years 2 and beyond Total: $777,000

5.0 POTENTIAL COLLABORATIONS

While explicit collaborations cannot be established at this time, we believe that a firm intent from MMS to pursue one or more of the studies outlined above would lead to a number of collaborations. There is precedent for this as exemplified by two of the programs discussed in Section 3.0 including the NOPP program in the central ABS and the ongoing MMS-oil industry collaboration in the Chukchi Sea involved industry partnerships. In the recent past, oil companies with offshore oil interests expressed interest in the sea ice thickness measurements and had committed funds on a proposal that was unfortunately declined. As discussed in Section 3.0, JAMSTEC has had long-standing interests in the Barrow Canyon area and they have expressed a desire to collaborate by sharing logistics or, at the very least, by sharing data. Our discussions with Canadian scientists at the Institute of Ocean Sciences (within Canada's Department of Fisheries and Oceanography) indicate that the Canadian government would collaborate on eastern boundary studies that bridge the boundary. We also have an ongoing dialog with Chinese researchers concerning joint research in the Beaufort/Chukchi Sea. While these talks are still preliminary, the Chinese have done research cruises in the Chukchi Sea in the past and have expressed interest in returning in the future and working collaboratively with American scientists. Korea has a new icebreaker and will initiate a decade-long program in the Chukchi/Beaufort seas starting in summer 2010. They are amenable to joint projects and have expressed a willingness to carry out collaborative work from their vessel (including making berths available for foreign investigators).

Collaborations, either in sharing sampling platforms, sampling approaches, and/or data are of mutual benefit, and we expect that these can and will be established for most of the programs presented in this report. We emphasize that the potential collaborators must have sufficient lead time to appropriately budget, allocate sampling resources, and discuss, comment, and shape the proposed research. We believe that a prudent way to proceed is to allot two years lead time (e.g., before the first field season) to work with potential collaborators so that they can plan and budget accordingly. Establishing these connections may require some preliminary funding for MMS personnel and/or PIs to co-ordinate the effort.

6.0. SUMMARY

The physical oceanographic studies recommended in this report would provide an improved understanding of the how the various boundaries influence the time-varying circulation and thermohaline setting of the ABS. We contend (and the consensus of the 2003 workshop attendees) that these influences result in considerable along- and cross-shelf variability, although to date this variability has not been adequately described. Indeed, the water property distributions from the central ABS (**Figure 3.0.2**) are a striking example of how these influences are manifested on this shelf. Circulation models of the ABS must realistically incorporate these influences if they are to be used as an effective management tool.

Acquiring the observations necessary to delineate the various physical features and processes operating on the ABS is a challenge. However the assorted technologies reviewed herein have the capability to do so with unprecedented temporal and spatial resolution. Each of these has been applied successfully in mid-latitude settings and most have been used successfully in the Chukchi/Beaufort region. The data obtained from these sensors would lend themselves to a

careful evaluation of future modeling activities and provide a wealth of information useful for engineering purposes.

While the approach adopted in this report addressed studies pertinent to each boundary, it should be remembered that the boundaries operate in aggregate; forcing along one boundary may modify the response along another. As such, the optimal approach would be to address these collectively, although we recognize that there are practical limitations to this approach. If MMS decides to act on the recommended studies, the agency should consider combining aspects of several of the programs outlined. As one example, we suggest combining the western and oceanic boundary studies with elements of the sea-ice and eastern boundary studies. In particular, the moorings along the oceanic and western boundary would provide along- and cross-shelf coverage of this region. In addition, all of the western boundary shelf moorings and two of the four oceanic shelfbreak moorings would be within the proposed HFR radar mask, which provides synoptic coverage of the surface circulation over a broad area. Similarly, conducting ice thickness mapping over the western shelf while moorings are in place would complement the oceanographic measurements and aid in the interpretation of the current measurements. As a second example, we urge including the eastward extension of the shelfbreak CTD lines (shown in blue in **Figure 4.3.7**) with the oceanic boundary sampling as this would provide quasi-synoptic coverage of the entire oceanic boundary from Barrow Canyon to the Mackenzie shelf. Finally, the coastal boundary study in conjunction with a nearshore sea-ice thickness survey would be complementary in several respects. The ice thickness maps would discern the extent to which under-ice plumes are steered by the underice topography, while the CTD measurements could ground-truth the EM sensor's detection capability with respect to mapping under-ice plumes.

The concentration herein has been on physical oceanography of the Alaskan Beaufort Sea. However, the results of the recommended studies would enhance our understanding of the physical foundations of this marine ecosystem and are essential in identifying biologically sensitive areas. Clearly there are large benefits obtained by incorporating biological and chemical sampling on some of the recommended cruises and by the addition of biochemical sensors on some of the moorings. The studies outlined here will undoubtedly lead to external collaborations and we envision that the MMS-sponsored activities will leverage additional resources to be applied to the ABS.

7.0 ACKNOWLEDGEMENTS

This work benefited from useful discussions with Eddy Carmack, Seth Danielson, Hajo Eicken, Craig George, Chris Guay, Stefan Hendricks, Rob Macdonald, Sue Moore, Rob Rember, Mike Spall, Stephen Okkonen, Bill Williams, and Peter Winsor.

8.0 REFERENCES

Ashjian, C. A., S. R. Braund, R. G. Campbell, J. C. George, J. Kruse, W. Maslowski, S. E. Moore, C. R. Nicolson, S. R. Okkonen, B. F. Sherr, E. B. Sherr, and Y. Spitz. *in press*. Climate Variability, Oceanography, Bowhead Whale Distribution, and Iñupiat Subsistence Whaling near Barrow, AK. *Arctic*.

Barrick, D. E., B. J. Lipa, and R. D. Crissman. 1985. Mapping surface currents with CODAR. *Sea Technology* 26: 43-48.

Bourke, R. H. and R. P. Garrett. 1987. Sea ice thickness distribution in the Arctic Ocean. *Cold Regions Science and Technology* 13: 259-280.

CODAR Ocean Sensors. 2003. SeaSonde® Radial Site Operating Theory. 14 p.

Corti, S., F.Molteni, and T.N. Palmer. 1999. Signature of recent climate change frequencies of natural atmospheric circulation regimes. *Nature* 398: 799-802.

D. M. Le Vine , M. Kao, R. W. Garvine, and T. Saunders. 1998. Remote Sensing of Ocean Salinity: Results from the Delaware Coastal Current Experiment. *Journal of Atmospheric and Oceanic Technology* 15: 1478-1484.

Dick, C. 2001. Arctic sea ice thickness. News from the AOSB. *AOSB Newsletter*.

Dickey, W. W. 1961. A study of a topographic effect on wind in the Arctic. *Journal of Meteorology* 18: 790-803.

Dickson, B. 1999. All change in the Arctic. *Nature* 397: 389-391.

Drobot, S. D. 2003. Long-range statistical forecasting of ice severity in the Beaufort/Chukchi Sea. *Weather and Forecasting* 18: 1161-1176.

Drobot, S. D., J.A. Maslanik, and C.F. Fowler. 2006. A long-range forecast of Arctic summer sea-ice minimum extent. *Geophysical Research Letters* 33: L10501, doi:10.1029/2006GL026216.

Dunton, K.H., T. Weingartner, and E.C. Carmack. 2006. The nearshore western Beaufort Sea ecosystem: Circulation and importance of terrestrial carbon in arctic coastal food webs, *Progress in Oceanography* 71: 362–378.

Eicken, H., R. Gradinger, A. Graves, A. Mahoney, Rigor I, and H. Melling. 2005. Sediment transport by sea ice in the Chukchi and Beaufort Seas: Increasing importance due to changing ice conditions? *Deep-Sea Research II* 52: 3281-3302.

Eriksen, C. C., T. J. Osse, R. D. Light, T. Wen, T. W.Lehman, P. L. Sabin, J. W. Ballard, and A. M. Chiodi. 2001. Seaglider: A Long-Range Autonomous Underwater Vehicle for Oceanographic Research. *IEEE .Journal of Oceanographic Engineering* 26:424-436.

Fowler, C., W. Emery, and J.A. Maslanik. 2003. Satellite derived arctic sea ice evolution Oct.

1978 to March 2003. *Transactions Geoscience and Remote Sensing Letters* 1: 71-74.

Harwood, L. A., J. Auld, A. Joynt, and S. E. Moore. *in press*. Distribution of bowhead whales in the SE Beaufort Sea during late summer, 2007-2009. *CSAS Research Document*.

Holloway, G., and T. Sou. 2002. Has Arctic sea ice rapidly thinned? *Journal of Climate* 15:: 1691-1701.

Hutchings, J, and C. Bitz. 2005. Sea ice mass budget of the Arctic (SIMBA) workshop: Bridging regional to global scales. *Report From NSF Sponsored Workshop Held at Applied Physics Laboratory, Univ. of Washington, Seattle, WA, Feb 28-Mar 2, 2005.*

Ingram, R. G. Characteristics of the Great Whale River Plume. 1981. *Journal of Geophysical Research* 86: 2017-2023.

Johnson, M., S. Gaffigan, E. Hunke, and R. Gerdes. 2007. A comparison of Arctic Ocean sea ice concentration among the coordinated AOMIP model experiments. *Journal of Geophysical Research* 112: C04S11, doi:101029-2006JC003690.

Kasper, J. and T. Weingartner. *in prep a*. The effect of landfast ice on a lateral inflow to a shelf sea.

Kasper, J. and T. Weingartner. *in prep b*. The spreading of a buoyant river plume beneath a landfast ice cover.

Klein, L. A. and C. T. Swift. 1977. An improved model for the dielectric constant of sea water at microwave frequencies. *IEEE Transactions on Antennas Propagation* AP-25104-111.

Kozo, T. L., and R.Q. Robe. 1986. Modeling winds and open-water buoy drift along the eastern Beaufort Se coast, including the effects of the Brooks Range. *Journal of Geophysical Research* 91: 13,011-13,032.

Kulikov, Y., E. Carmack, and R. Macdonald. 1998. Flow variability at the continental shelf break of the Mackenzie Shelf in the Beaufort Sea. *Journal of Geophysical* 103:12,725-12,741.

Lagerloef, G., F. R. Colomb, D. Le Vine, F. Wentz, S. Yueh, C. Ruf, J. Lilly, J. Gunn, Y. Chao, A. DeCharon, G. Feldman, and C. Swift. 2008. The Aquarius/SCA-D Mission: designed to meet the salinity remote challenge. *Oceanography* 21: 68-81.

Li, S. S., and R. G. Ingram. 2007. Isopycnal deepening of an under-ice river plume in coastal waters: Field observations and modeling. *Journal of Geophysical Research* 112: C07010, doi:10.1029/2006JC003883.

Lindsay, R. W., and J. Zhang. 2005. The Thinning of Arctic Sea Ice, 1988-2003: Have We Passed a Tipping Point? *Journal of Climate* 18: 4879-4894.

Logerwell, E., K. Rand, S. Parker-Stetter, J. Horne, T. Weingartner, and B. Bluhm. 2009. *Beaufort Sea Marine Fish Monitoring 2008: Pilot Survey and Test of Hypotheses*, OCS Study MMS 2008-062; 133 p.

Lowry, L., G. Sheffield, and J. C. George. 2004. Bowhead whale feeding in the Alaskan Beaufort Sea, based on stomach contents analyses. *Journal Cetacean Research & Management* 6: 215-23.

Macdonald, R. W., and E. C. Carmack. 1991. The role of large-scale under-ice topography in

separating estuary and ocean on an Arctic shelf. *Atmosphere-Ocean* 29: 37-53.

Macdonald, R. W., E. C. Carmack, F. A. McLaughlin, K. K. Falkner, and J. H. Swift. 1999. Connections among ice, runoff, and atmospheric forcing in the Beaufort Gyre. *Geophysical Research Letters* 26: 2223-2226.

Macdonald, R. W., and E. C. Carmack. 1991. The role of large-scale under-ice topography in separating estuary and ocean on an Arctic shelf. *Atmosphere-Ocean* 29 (1): 37-53.

Macdonald, R. W., E. C. Carmack, F. A. McLaughlin, K. K. Falkner, and J. H. Swift. 1999. Connections among ice, runoff, and atmospheric forcing in the Beaufort Gyre. *Geophysical Research Letters* 26: 2223-2226.

Mahoney, A., H. Eicken, A. G. Gaylord, and L. Shapiro. 2007a. Alaska landfast sea ice: Links with bathymetry and atmospheric circulation. *Journal of Geophysical Research* 112: C02001, doi:02010.01029/02006JC003559.

Mahoney, A., H. Eicken, and L. H. Shapiro. 2007b. How fast is landfast sea ice? A study of attachment and detachment of nearshore ice at Barrow, Alaska. *Cold Regions Science and Technology* 47: 233-255.

Manabe, S., and R. J. Stouffer. 1994. Multiple Century Response of a Coupled Ocean-Atmosphere Model to an Increase of Atmospheric Carbon Dioxide. *Journal of Climate* 7:5-23.

Maslanik, J. A., C. Fowler, J. Stroeve, S. Drobot, J. Zwally, D. Yi, and W. Emery. 2007. A younger, thinner Arctic ice cover: Increased potential for rapid, extensive sea ice loss. *Geophysical Research Letters* 34: L24501, doi:24510.21029/22007GL032043.

Melling, H., D. A. Riedel, and Z. Gedalof. 2005. Trends in the draft and extent of seasonal pack ice, Canadian Beaufort Sea. *Geophysical Research Letters* 32, L24501, doi:10.1029/2005GL024483.

Melling, H., and D. Riedel. 2004. Draft and movement of pack ice in the Beaufort Sea: A time-series presentation April 1990 August 1999. *Canadian Technical Report on Hydrographic and Oceanic Science* 238: 1-24.

Melling, H. and D. Riedel. 1995. The underside topography of sea ice over the continental shelf of the Beaufort Sea in the winter of 1990. *Journal of Geophysical Research* 100: 13641-13653.

Moore, S. E. 2000. Variability of Cetacean Distribution and Habitat selection in the Alaskan Arctic, Autumn, 1982 - 91. *Arctic* 48: 448-460.

Moore, S. E. D. P. DeMaster, and P. K. Dayton. 2000. Cetacean habitat selection in the Alaskan Arctic during summer and autumn. *Arctic* 53: 432-47.

Morison, J. H., K. Aagaard, and M. Steele. 2000. Recent Environmental Changes in the Arctic: A Review. *Arctic* 53: 359-371.

Moritz, R. E., C. M. Blitz, and E. J. Steig. 2002. Dynamics of recent climate change in the Arctic. *Science.* 297: 1497-1502.

Mysak, L. A. and D.K. Manak. 1989. Arctic sea-ice extent and anomalies. *Atmosphere-Oceans* 27: 376-405.

Nikolopoulos, A., R.S. Pickart, P.S. Fratantoni, K. Shimada, D.J. Torres, and E.P. Jones. 2009. The western Arctic boundary current at 152°W: Structure, variability, and transport. *Deep-Sea Research II* 56: 1164-1181.

Okkonen, S. R., C. J. Ashjian, R. G. Campbell, W. Maslowski, J. L. Clement-Kinney, and R. Potter. 2009. Intrusion of warm Bering/Chukchi waters onto the shelf in the western Beaufort Sea. *Journal of Geophysical Research* 114: C00A11, doi:10.1029/2008JC004870.

Parkinson, C. L., D.J. Cavalieri, P. Gloersen, H. J. Zwally, and J. C. Comiso. 1999. Arctic sea ice extents, areas, and trends, 1978-1996. *Journal of Geophysical Research* 104: 837-856.

Pickart, R. S. 2004. Shelfbreak circulation in the Alaskan Beaufort Sea: Mean structure and variability. *Journal of Geophysical Research* 109: C04024 10.1029/2003JC001912.

Pickart, R. S., G.W.K. Moore, D. J. Torres, P. S. Fratantoni, R. A. Goldsmith, and J. Yang. 2009. Upwelling on the continental slope of the Alaskan Beaufort Sea: Storms, ice, and oceanographic response. *Journal of Geophysical Research* 114: doi:10.1029/2008JC005009.

Pickart, R. S., M.A. Spall, G.W.K. Moore, T. J. Weingartner, R.A. Woodgate, K. Aagaard, and K. Shimada. *submitted*. Anatomy of an autumn upwelling event in the Alaskan Beaufort Sea, Part I: Atmospheric forcing and local versus non-local response. *Journal of Physical Oceanography*.

Pickart, R. S., T. J. Weingartner, S. Zimmermann, D. J. Torres, and L. J. Pratt. 2005. Flow of winter-transformed Pacific water into the western Arctic. *Deep-Sea Research II* 52: 3175-98.

Proshutinsky, A. Y., and M. Johnson. 1997. Two circulation regimes of the wind-driven Arctic Ocean. *Journal of Geophysical Research* 102: 12,493-12,514.

Richter-Menge, J, M. Hopkins, R.Lindsay, H. Melling, D. Perovich, I.Rigor, T. Tucker, A. Thorndike, and J. Zhang. 2001. Sea ice thickness: the great integrator. In Large scale observations: a SEARCH workshop.

Rigor, I. G., and J. M. Wallace. 2004. Variations in the age of Arctic sea-ice and summer sea-ice extent. *Geophysical Research Letters* 31: L09401, doi:10.1029/2004GL019492.

Rind, D., R. Healy, C. Parkinson, and D. Martinson. 1997. The role of sea ice in 2xCO2 climate model sensitivity: Part II: hemispheric dependencies. *Geophysical Research Letters* 24: 1491-1494.

Rothrock, D. A., and J. Zhang. 2005. Arctic Ocean sea ice volume: What explains its recent depletion? *Journal of Geophysical Research* 110: C01002, doi:10.1029/2004JC002282.

Rothrock, D. A., J. Zhang, and Y. Yu. 2003. The arctic ice thickness anomaly of the 1990s: A consistent view from observations and models. *Journal of Geophysical Research* 108: 3083, doi:10.1029/2001JC001208 .

Rothrock, D. A., Y.Yu, and G.A. Maykut. 1999. Thinning of the Arctic sea-ice cover. *Geophysical Research Letters* 26: 3469-3472.

Schofield, O., J. Kohut, D. Aragon, L. Creed, J. Graver, C. Haldeman, J. Kerfoot, H. Roarty, C. Jones, D Webb, and S. Glenn. 2007. Slocum Gliders: Robust and Ready. *Journal of Field Robotics* 24: 473-85.

Serreze, M. C, J.A.Maslanik, T.A. Scambos, F.Fetterer, J. Stroeve, K.Knowles, C.Fowler, S.Drobot, R. Barry, and T. Haran. 2003. A record minimum arctic sea ice extent and area in 2002. *Geophysical Research Letters* 30:1110, doi:10.1029/2002GL016406.

Serreze, M. C., J. E. Walsh, F. S. Chapin III, T. Osterkamp, M. Dyurgerov, V. Romanovsky, W. C. Oechel, J. Morison, T. Zhang, and R. G. Barry. 2000. Observational evidence of recent change in the northern high-latitude environment. *Climatic Change* 46: 159-207.

Spall, M. A. R.S. Pickart, P.S. Fratantoni, and A.J. Plueddemann. 2008. Western Arctic shelfbreak eddies: Formation and transport. *Journal of Physical Oceanography* 38: 1644-68

Thompson, D. W. J., and J. M. Wallace. 1998. The Arctic Oscillation signature in the wintertime geopotential height and temperature fields. *Geophysical Research Letters* 25: 1297-1300.

Trefry, J. R., R. D. Rember, R. P. Trocine, and J. S. Brown. 2004. *ANIMIDA Task 7: Partitioning of Potential Anthropogenic Chemicals between Dissolved and Particulate Phases in Arctic Rivers and the Coastal Beaufort Sea*, OCS Study MMS 2004-031, 86 p. U.S. Department of Interior, Minerals Management Service, Anchorage, Alaska.

Tucker III, W. B., W. F. Weeks, and M. Frank. 1979. Sea Ice ridging over the Alaskan continental shelf. *Journal of Geophysical Research* 84: 4885-4897.

Tucker, W. B., J. W. Weatherly, D.T. Eppler, L.D. Farmer, and D.L.Bentley. 2001. Evidence for rapid thinning of sea ice in the western Arctic Ocean at the end of the 1980s. *Geophysical Research Letters* 28: 2851-2854.

Vinje, T., 2001: Fram Strait ice fluxes and atmospheric circulation 1950-2000. *Journal of Climate,* 14: 3508-3517.

Williams, E. C. Carmack, K. Shimada, H. Melling, K. Aagaard, R. W. Macdonald, and R. G. Ingram. 2006. Joint effects of wind and ice motion in forcing upwelling in Mackenzie Trough, Beaufort Sea. *Continental Shelf Research* 26: 2352-66. doi: 10.1016/jcsr.2006.06.012.

Wadhams, P., J. P. Wilkinson, and S. D. McPhail. 2006. A new view of the underside of Arctic sea ice. *Geophysical Research Letters* 33: L04501, doi:10.1029/2005GL025131.

Walsh, J. E., W. E. Hibler III, and B. Ross. 1985. Numerical simulations of Northern Hemisphere sea ice variability. *Journal of Geophysical Research* 90: 4847-4865.

Wang, Y., M. L. Heron, A. Prytz, P. V. Ridd, C. R. Steinberg, and J. M. Hacker. 2007. Evaluation of a New Airborne Microwave Remote Sensing Radiometer by Measuring the Salinity Gradients Across the Shelf of the Great Barrier Reef Lagoon . *IEEE Transations on Geoscience and Remote Sensing* 45: 3701-9.

Weingartner, T., K. Aagaard, R. Woodgate, S. Danielson, Y. Sasaki, and D. Cavalieri. 2005. Circulation on the North Central Chukchi Sea Shelf. *Deep Sea Research, Part II* 52: 3150-3174.

Weingartner, T., K. Aagaard, R. Woodgate, S. Danielson, Y. Sasaki, and D. Cavalieri. 2005. Circulation on the North Central Chukchi Sea Shelf. *Deep Sea Research, Part II* 52: 3150-3174.

Weingartner, T. J. 2006. Circulation, thermohaline structure, and cross-slope transport in the Alaskan Beaufort Sea. OCS Study MMS 2006-031: 58 p.

Weingartner, T. J., D. J. Cavalieri, K. Aagaard, and Y. Sasaki. 1998. Circulation, dense water formation, and outflow on the northeast Chukchi shelf. *Journal of Geophysical Research* 103: 7647-7661.

Weingartner, T. J., S. L. Danielson, J. L. Kasper, and S. R. Okkonen. 2009. Circulation and water property variations in the nearshore Alaskan Beaufort Sea (1999-2007). *OCS Study MMS 2009-035* : 1-155.

Wilkin, J. L., and D. C. Chapman. 1990. Scattering of coastal-trapped waves by irregularities in coastline and topography. *Journal of Physical Oceanography* 20: 396-421.

———. 1987. Scattering of continental shelf waves at a discontinuity in shelf width. *Journal of Physical Oceanography* 17: 713-724.

Woodgate, R. A., K. Aagaard, and T. J. Weingartner. 2005. A year in the physical oceanography of the Chukchi Sea: Moored measurements from autumn 1990-91. *Deep Sea Research, Part II* 52: 3116-3149.

Yankovsky, A. E., and D. C. Chapman. 1997. A simple theory for the fate of buoyant coastal discharges. *Journal of Physical Oceanography* 27: 1386-401.